

PHOTOCHEMICAL AND THERMAL E/Z ISOMERIZATIONS
OF
SOME α,β -UNSATURATED IMINIUM SALTS

By

MARIANNE PANKRATZ, B.Sc.

A Thesis

Submitted to the School of Graduate Studies
in Partial Fulfilment of the Requirements
for the Degree
Doctor of Philosophy



McMaster University

E/Z ISOMERIZATIONS

OF

IMINIUM SALTS

DOCTOR OF PHILOSOPHY (1986)
(Chemistry)

MCMMASTER UNIVERSITY
Hamilton, Ontario

TITLE: Photochemical and Thermal E/Z Isomerizations of Some
 α,β -Unsaturated Iminium Salts

AUTHOR: Marianne Pankratz, B.Sc. (McMaster University)

SUPERVISOR: Professor R.F. Childs

NUMBER OF PAGES: xv, 189

ABSTRACT

Geometric isomerizations about the C=C and C=N bonds of a series of diaryl α,β -unsaturated iminium salts are investigated in this thesis. These isomerizations are important in several unsaturated iminium ions found in natural systems. The vision process relies on light absorption by the protein rhodopsin followed by Z/E isomerization. A similar reaction is used by certain bacteria to convert light energy into energy the organisms can use for cell functions.

A series of nine iminium salts, N-methyl-N-aryl-3-aryl-2-propenylidene iminium perchlorates, with various electron-withdrawing or electron-donating substituents on the aryl rings were synthesized and characterized. Three methods of isomerization of these molecules were examined--photochemical, electron transfer initiated, and thermal isomerization.

The electronic absorption and emission properties of these iminium salts, and the effect of the substituents on the regioselectivity of photoisomerization, led to some conclusions about the excited states involved in the isomerization. Although the molecules reach an initial excited state where the positive charge of the iminium group has migrated into the carbon framework of the molecule, the isomerization process is not governed by such an intermediate. It is

suggested that the state that governs photoisomerization has biradical character.

E/Z isomerization about the C=N bond of the unsubstituted iminium salt was accomplished by photoinitiated electron transfer from the donor, tris(2,2'-bipyridine)-ruthenium(II)dichloride, the first observation of this reaction.

The iminium salts crystallize as the E,E isomers, but undergo thermal isomerization in solution to produce a mixture of E and Z isomers about the C=N bond. In strong acid media, two mechanisms of isomerization were found. Electron-withdrawing substituted iminium salts isomerize by a nucleophile-catalyzed mechanism, and electron-donating substituents cause isomerization by protonation of the iminium salt.

To Helmut

ACKNOWLEDGEMENTS

I gratefully acknowledge the guidance and encouragement from my supervisor, Professor R.F. Childs, during my graduate studies. The other members of my supervisory committee, Professors J. Warkentin, W.J. Leigh, and M.J. McGlinchey are thanked for helpful suggestions.

Financial support in the form of scholarships from the Natural Sciences and Engineering Research Council and the E.L. Hooker Fund was appreciated.

Many people assisted during the course of my graduate work. The excellent technical assistance provided by B. Sayer, I. Thompson, and C. Schonfeld was greatly appreciated, as was the assistance by Professor J.J. McCullough in the cyclic voltammetry experiments.

I also wish to thank the members of my lab group, especially Carol Rogerson for practical advice, and Gary Shaw for proofreading parts of this manuscript.

The preparation of this manuscript was facilitated by the computer equipment kindly provided by Upper Canada Consultants.

Most of all I thank my parents, Franz and Eleonore Janzen, for their love, encouragement and their strong belief in the merits of education, and my husband, Helmut Pankratz, for his unfailing support during my studies.

TABLE OF CONTENTS

	Page
DESCRIPTIVE NOTE	ii
ABSTRACT	iii
ACKNOWLEDGEMENTS	vi
INTRODUCTION	
CHAPTER 1	1
I. Rhodopsin	3
Rhodopsin, Isorhodopsin and Bathorhodopsin	5
Photoisomerization of Rhodopsin	7
Regeneration of Rhodopsin	10
II. Bacteriorhodopsin	11
Photoisomerization of Bacteriorhodopsin	14
III. Effect of the Protein Environment	16
Structure of the Chromophore in Rhodopsin	17
Structure of the Chromophore in Bacteriorhodopsin	21
Effect of the Protein on Thermal Reactions	28
Effect of the Protein on Photochemical Isomerization	31

IV.	α,β Unsaturated Iminium Ions	33
	Absorption Studies	33
	Photochemical Isomerization	34
	Charge Delocalization in α,β Unsaturated Iminium Salts	37
V.	Longer Chain Iminium Ions	41
	Absorption Studies	41
	Photoisomerization	41
VI.	Photoisomerizations in Related Systems	41
VII.	Other Photoreactions	42
VIII.	Photoinduced Electron Transfer	44
IX.	Thermal Isomerization	47
RESULTS AND DISCUSSION		
CHAPTER 2	SYNTHESIS AND STRUCTURE	52
	I. Synthesis	52
	II. Geometric Isomerization	53
	Separation of C=N Isomers	63
	III. Structures of the E,E Iminium Salts	64
	Charge Distribution	64
	Solvent Effects	66
CHAPTER 3	PHOTOCHEMISTRY	67
	I. Absorption and Emission Studies	67
	Structure of the Excited State	71
	Lifetime of the Excited State	74
	Planar Excited States of Alkenes, Polyenes and Iminium Ions	75

II.	Photochemical E/Z Isomerization	80
	Quantum Yields	81
	Concentration Effects	83
	Effect of Dissolved Oxygen	83
	Medium Effects on Photochemistry	85
	Photostationary States	85
	Photoisomerization, Energy Surface	87
	Energy Barriers on Excited State Surfaces	92
	Electron Distribution of the Twisted State	95
	Regioselectivity in Photoisomerization	96
	Regioselectivity in Polyenes and Related Neutral Molecules	100
	Regioselectivity in Charged Molecules	104
	Effect of a Meta Substituent	105
III.	Intersystem Crossing	107
IV.	Internal Conversion	111
V.	Summary	112
CHAPTER 4	E/Z ISOMERIZATION BY PHOTOINITIATED ELECTRON TRANSFER	114
	I. Cyclic Voltammetry	114
	II. Electron Transfer in the Excited State	122
	Isomerization Initiated by Electron Transfer	122
III.	Summary	130

CHAPTER 5	THERMAL E/Z ISOMERIZATION	132
	I. Kinetic Measurements	133
	Substituent Effect	134
	Solvent Effect	134
	II. Mechanisms of Isomerization	136
	III. Summary	142
CHAPTER 6	EXPERIMENTAL METHODS	144
	I. Materials and Syntheses	144
	N-methyl, N-aryl-3-aryl-2-propenylidene iminium perchlorate	144
	p-methoxycinnamaldehyde, p-chlorocinnamaldehyde, p-methylcinnamaldehyde, m-methoxycinnamaldehyde	145
	N-methyl-p-chloroaniline	145
	II. Crystallization of E,E and Z,E Isomers	147
	III. Instrumental Techniques	147
	NMR spectra	147
	Absorption Spectra	149
	Fluorescence Spectra	149
	Infrared Spectra	150
	Cyclic Voltammetry	150
	Miscellaneous	151
	IV. Triplet-Triplet Energy Transfer Experiment	152
	V. Quantum Yield Measurements	152
	Optical Bench	152
	Actinometry	153

Quantum Yields	154
VI. Photostationary States	156
VII. Electron Transfer Experiments	160
Luminescence Quenching Experiments	160
NMR Experiments	160
VIII. Thermal Experiments	161
H ₂ O Measurements	161
Kinetic Measurements	162
Deuterium Incorporation	164
Super-Acid Solution of Iminium Salt 57	167
REFERENCES	168

LIST OF TABLES

		Page
Table 1-1	Some Spectroscopic Data for Rhodopsin, Bacteriorhodopsin, and the All-Trans Retinylidene Iminium Salt	18
Table 1-2	Absorption Maxima for Rhodopsin, Bacteriorhodopsin, and Retinylidene Iminium Salts in Various Solvents	25
Table 2-1	Physical Data for Iminium Salts 55-63	54
Table 2-2	Absorption Data for Iminium Salts 55-63	55
Table 2-3	^1H NMR Chemical Shift Data for Iminium Salts 55-63	56
Table 2-4	^{13}C NMR Chemical Shift Data	57
Table 2-5	^1H NMR Chemical Shift Data for Iminium Salts 64-72	61
Table 2-6	^1H NMR Chemical Shift Data for Iminium Salts 73-90	62
Table 3-1	Absorption Maxima as a Function of Substituent	73
Table 3-2	Quantum Yields of Photoisomerization	82
Table 3-3	Medium Effects on Photoisomerization Quantum Yields	84
Table 3-4	Photostationary State Compositions	86
Table 3-5	Absorption Maxima and Relative Quantum Yields of Photoisomerization of the para and meta methoxy iminium salts 59 and 95	106
Table 4-1	Reduction Potentials	118
Table 4-2	Variation of E_p with Scan Rate for Iminium Salt 57	120

Table 4-3	Quenching of tris(2,2'-bipyridine) ruthenium(II)dichloride, 97, Luminescence by Iminium Salts 55-60 in Acetonitrile	125
Table 4-4	Isomerization of Iminium Salt 60 on Irradiation of tris(2,2'-bipyridine) ruthenium(II)dichloride, 97	127
Table 5-1	Isomerization Rate Constants at 100°C in TFA and 0.01M H ₂ SO ₄ /TFA	135
Table 6-1	Physical and Spectroscopic Data for N-methyl, N-phenyl-3-(m-methoxyphenyl)-2-propenylidene iminium perchlorate, 95	146
Table 6-2	¹ H NMR Data for Iminium Salt 95	146
Table 6-3	Raw Quantum Yield Data for the Iminium Salts 55-59 in Trifluoroacetic Acid	157
Table 6-4	Raw Quantum Yield Data for Iminium Salts 60-63 in Trifluoroacetic Acid	158
Table 6-5	Raw Quantum Yield Data for Iminium Salts 59 and 60 in Various Solvents	159
Table 6-6	Raw Rate Data for the Isomerization of Iminium Salt 58 to 67 in TFA at 100°C	165
Table 6-7	Approximate Rate Constants for the Isomerizations of Iminium Salts 55-63 in TFA-d ₄ at 100°C	166

LIST OF FIGURES

		Page
Figure 1-1	Charge Distribution in the Ground States of Model Compounds of Retinylidene Iminium Salts	20
Figure 1-2	Charge Environment of Bacteriorhodopsin	22
Figure 1-3	Absorption Maxima of Dihydroretinylidene Iminium Salts	27
Figure 1-4	Charge Environment of Rhodopsin	28
Figure 1-5	Effect of Non-Conjugated Charged Groups on Absorption Maxima of Rhodopsin and Bacteriorhodopsin Models	29
Figure 1-6	Bond Lengths of Some Iminium Salts	40
Figure 2-1	Vinyl Region of the ^1H NMR Spectra of N-methyl, N-phenyl-3-(p-methoxyphenyl)-2-propenylidene iminium perchlorate, 59, in TFA (A) E,E isomer (B) Z,E isomer in a thermally produced mixture, and (C) E,Z and Z,Z isomers in an irradiated mixture	60
Figure 2-2	^{13}C NMR spectra of N-methyl, N-phenyl-3-(p-chlorophenyl)-2-propenylidene iminium perchlorate, 56 (A) TFA solution, and (B) solid state	65
Figure 3-1	Absorption Spectrum of N-methyl, N-phenyl-3-phenyl-2-propenylidene iminium perchlorate, 57, in TFA	69
Figure 3-2	Photoisomerization Regioselectivity in Some Polyenes	102
Figure 3-3	Photoisomerization Regioselectivity in Some Polyenals	103
Figure 4-1	Cyclic Voltammogram of N-methyl, N-phenyl-3-(p-chlorophenyl)-2-propenylidene iminium perchlorate, 56 (A) background (B) iminium salt	115

- Figure 4-2 Cyclic Voltammogram of N-methyl,
N-(p-nitrophenyl)-3-phenyl-2-propenylidene
iminium perchlorate, 60 119
- Figure 5-1 Hammett correlations for the rate constants
for isomerization of iminium salts with
substituents on the C₃ aryl ring, 55-59,
in TFA (___) and 55, 57, 59 in
H₂SO₄/TFA(---). 138
- Figure 5-2 Hammett correlations for the rate constants
of isomerization of iminium salts with
substituents on the N-aryl ring, 57, 60-63,
in TFA(___) and H₂SO₄/TFA(---). 138

INTRODUCTION

CHAPTER 1

Vision, the process whereby light reflected from objects around us is translated into images, is currently being studied from both chemical and biochemical perspectives. Organic molecules called rhodopsins act as the visible light absorbing pigments, and are located in cells in the retina of the eye.^{1,2,3,4} The human eye contains cone cells and rod cells. The cone cells are responsible for vision in bright light, and can distinguish colours by absorbing light of one of three parts of the visible spectrum: blue, green or red light. The rod cells are responsible for vision in low light levels, and cannot distinguish colours. All species of animal that can see contain visual pigments that are similar to the human pigments, however most animals have only one type of visual pigment and do not see in colour. Since animal retinas are easier to obtain than human ones, our understanding of the visual process comes from studies of animal rhodopsins, especially cattle rhodopsin.

When rhodopsin absorbs light, a reaction sequence is initiated that causes changes to the membrane in which the pigment is located, and eventually leads to a nerve impulse that is sent to the brain. There are approximately thirty million rhodopsin molecules in one rod cell in the eye. These cells are very sensitive to light, but also adaptable, as they

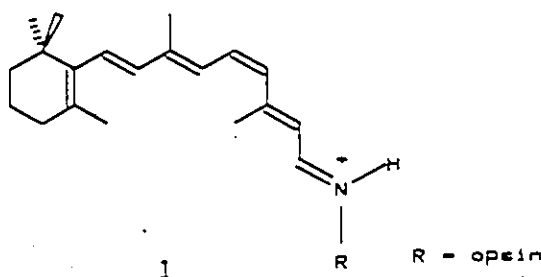
can detect as low as a few photons to as high as 10^6 photons of light per second. Each photon absorbed triggers a series of enzyme reactions that ends with hydrolysis of cyclic guanosine monophosphate (GMP) in the cell. Amplification of the original absorption event is responsible for the high sensitivity, in that one photon absorbed causes up to 10^4 molecules of cyclic GMP to be hydrolysed.

In the absence of light, an electrical current passes through the cell, generated by a sodium ion flow. Light absorption causes this current to decrease, possibly through the action of a transmitter that links the enzymic reactions with the changes in the membrane that stop sodium ions from passing through the cell wall. The change in electrical current causes a nerve impulse to be sent to the brain, where interpretation and creation of an image takes place.

Pigments that are similar to rhodopsin are found in at least two other organisms. These light-absorbing molecules are used not for vision, but for converting light energy into energy the organism can use for cell functions. Bacteriorhodopsin is one of four such proteins found in the surface membranes of a strain of bacteria called Halobacteria. Light absorption by the protein leads to the synthesis of adenosine triphosphate (ATP), an energy storage system of living cells.^{4,5} A green algae species, Chlamydomonas, moves in response to light, also because of a light absorbing pigment.³

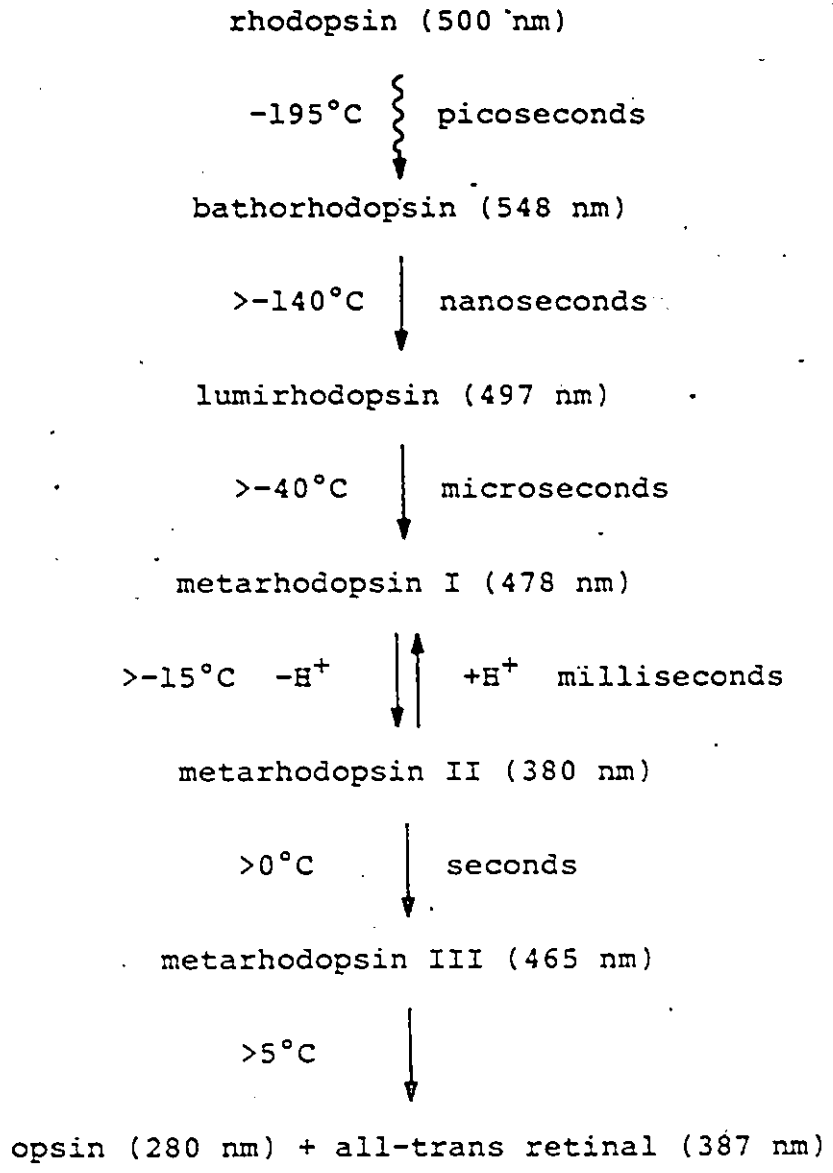
I. Rhodopsin

The chromophore of rhodopsin, 1, is one geometric isomer of retinal, 11-cis retinal, and is common to all animals. It forms an iminium bond with a lysine amino acid of the apoprotein, opsin.



Rhodopsin in human rod cells is red-coloured. The protein backbone does not absorb light in the visible region, so the long wavelength absorption band of rhodopsin, the one that is responsible for its colour, is caused by light absorption of the chromophore only. The opsin chain surrounds the chromophore, and exerts an influence on its absorption spectrum. Although each species of animal has the same chromophore, each has a different opsin, and the absorption maxima of the rhodopsins are also different, ranging from 440 to 600 nm.⁶

Light absorption by rhodopsin initiates a reaction cycle, Scheme 1-1. The intermediates were initially identified by their absorption maxima and have since been characterized by other spectroscopic techniques. The first intermediate, bathorhodopsin, absorbs light at longer wavelengths than does rhodopsin. Photocalorimetry studies have found that batho-



Scheme 1-1 The Photocycle of Bovine Rhodopsin

rhodopsin is 35 kcal/mole higher in energy than rhodopsin.⁷ This excess energy is used to form the remaining intermediates of the cycle, and to initiate the molecular changes that are translated into cellular processes and subsequent enzyme reactions. The way in which this is done is not yet understood.

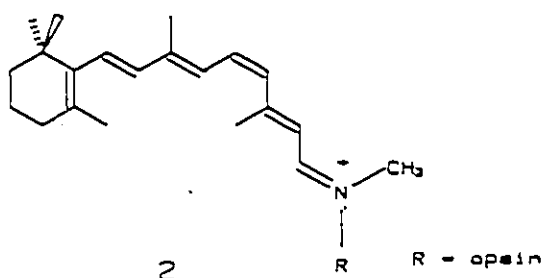
At the end of the cycle the chromophore, now in the all-trans configuration, separates from the protein by a hydrolysis reaction. In some species, such as squid⁸ and blowfly⁹ and some synthetic analogues of rhodopsin³, the final hydrolysis step does not occur. Instead, rhodopsin is regenerated directly from metarhodopsin.

Rhodopsin, Isorhodopsin, and Bathorhodopsin

Thermal reactions are essentially stopped at 77K, and light absorption by rhodopsin results in the formation of a photoequilibrium containing rhodopsin, bathorhodopsin and isorhodopsin.

The retinal chromophore of rhodopsin has an 11-cis C=C bond and is bound to a lysine residue of the protein by a C=N linkage, 1. It is generally agreed that the nitrogen of the C=N bond is protonated, as shown by vibrational spectroscopy experiments.¹⁰⁻¹⁴ The absorption maxima of aldehydes are not greatly affected by imine formation, but protonation of the nitrogen of an imine is known to shift its absorption maximum to longer wavelengths. Protonation of the imine linkage between retinal and opsin is thought to be responsible for part of the large difference between the absorption maximum

of retinal (380 nm) and that of rhodopsin (500 nm).^{2,15,16} A rhodopsin analogue has been synthesized where the iminium proton is replaced by a methyl group, 2.¹⁷ This molecule absorbs at 520 nm, close to the 500 nm absorption maximum of the natural pigment, providing further evidence that the pigment contains a protonated imine bond.



The configuration about the C=N bond of rhodopsin was found to be trans, by resonance Raman spectroscopy.^{14,18}

Isorhodopsin is observed in the photomixture only at low temperatures, not under physiological conditions. It can also be artificially formed by adding 9-cis retinal to opsin suspensions. The 9-cis retinal is attached to opsin by a trans, protonated C=N bond.¹⁴

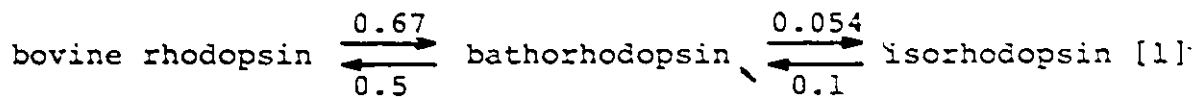
Bathorhodopsin is thought to have a twisted all-trans geometry¹⁰, with a protonated, trans C=N bond¹⁴, from resonance Raman spectra. It appears that bathorhodopsin may not be a unique species at 77K, as bathorhodopsin formed from isorhodopsin has a slightly different λ_{\max} than that formed from rhodopsin (542 nm and 546 nm respectively).¹⁹

When the photoequilibrium is established at $\leq 20\text{K}$, a species absorbing at 430 nm, hypsorhodopsin, was shown to be

present in the photomixture, by spectral subtraction techniques.²⁰⁻²² It is not certain whether hypsorhodopsin is formed in parallel to bathorhodopsin or is a precursor.²³⁻²⁵ Resonance Raman and FTIR spectra indicate that this species has a protonated C=N bond and a twisted all-trans form, but is different from bathorhodopsin.^{26,13} Theoretical calculations of the structure suggest that hypsorhodopsin is more twisted than bathorhodopsin.²⁷

Photoisomerization of Rhodopsin

The photoreaction of rhodopsin is characterized by its high efficiency. Quantum yields for the photoreaction were found to be species dependent, as demonstrated by the values in Equation 1 for bovine rhodopsin and in Equation 2 for squid rhodopsin.²⁸ The quantum yields are independent of irradiating wavelength, and do not change when D₂O is used instead of H₂O as solvent.

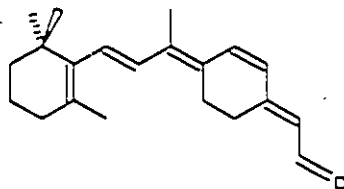


The reaction is thought to be a singlet state process. The only radiative pathway observed for deactivation of the excited state is fluorescence, and this is very weak. At room temperature the quantum yield for fluorescence is 1.2 (+0.5)

$\times 10^{-5}$.²⁹ This implies that the process that competes with fluorescence in the excited state could occur within about 0.1 ps. Picosecond absorption spectroscopy studies have shown that bathorhodopsin is formed within 3 ps.²⁴ The fluorescence quantum yield is $\leq 10^{-5}$ and temperature independent between 5 and 40K. This is evidence that the process that competes with fluorescence does not have an activation barrier. When H_2O in the solvent was replaced with D_2O , thereby exchanging the iminium proton for a deuteron, no change in fluorescence quantum yield was observed, so the photoreaction cannot involve bonding changes of the iminium proton.³⁰ This contradicts the conclusions of earlier kinetic absorption studies of the formation of bathorhodopsin at various temperatures between 4K and 30K in which D_2O/H_2O and temperature dependent rates were measured.^{23,31}

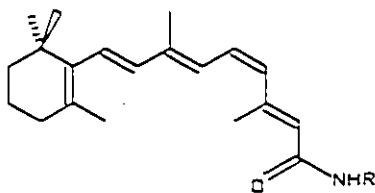
Various theories have been proposed to explain the photoreaction of rhodopsin.² The most commonly accepted is that the excited state decays by isomerizing about the C_{11},C_{12} double bond. This could be accompanied by twisting about an adjacent single bond to accommodate space constraints of the protein.³² The strongest evidence for an isomerization mechanism comes from an experiment using a constrained 11-cis retinal analogue, 3, incorporated into rhodopsin. In this molecule, isomerization cannot occur about the C_{11},C_{12} bond. The rhodopsin analogue containing aldehyde 3 is a non-reactive pigment³³ that fluoresces with a quantum yield of 4×10^{-4} ,

much higher than observed for rhodopsin itself. The process that competes with fluorescence in rhodopsin is not occurring in the analogue, and is thus most likely an isomerization about C₁₁,C₁₂.³⁴



3

The isomerization itself is not enough to cause the protein changes that lead to a nerve impulse. This was shown in a recent study using the rhodopsin analogue 4.



4

R - opsin

In the cellular process derived from the photocycle, an enzyme, GTPase, is activated. In this experiment, GTPase activation was monitored to determine if the rhodopsin analogue could act as a visual transducer. It was found that light absorption by the analogue 4 led to isomerization, but that GTPase was not activated.^{35,36}

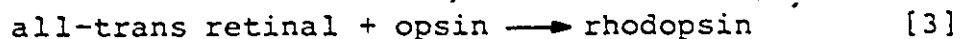
Light absorption by rhodopsin analogue 2 leads to the formation of a meta-rhodopsin I-like intermediate, which slowly hydrolyzes to all-trans retinal and methylated opsin. GTPase

is not activated in the process, suggesting that protonation changes at the nitrogen at the meta-rhodopsin II stage are important in visual transduction.³⁷

Regeneration of Rhodopsin

The second reaction of the cycle of interest in the context of this thesis is the regeneration of rhodopsin.

The equilibrium constant for the reaction shown in Equation 3 is very small. When the bleaching process reaches the all-trans retinal stage, although a small fraction of rhodopsin is regenerated photochemically, the majority is hydrolyzed to all-trans retinal and opsin.^{38,39}



Isomerization of trans retinal to form 11-cis retinal must then occur elsewhere in the membrane or the cell. This could be by a thermal or photochemical pathway. A photochemical process for regenerating rhodopsin has been found in flies and squid. Flies cannot form 11-cis retinal from all-trans retinal in total darkness, but instead require blue light (about 450 nm).⁹ In squid, a retinochrome membrane was found that catalyzes the formation of 11-cis retinal from all-trans retinal, by a photochemical mechanism.⁸ Absorption spectra suggest that retinal is attached to the membrane by an iminium bond. When the membrane containing 90% trans retinal was irradiated for 30 minutes, 70% of the membrane-bound retinal had converted to the 11-cis isomer. Opsin was then incubated

with this irradiated retinochrome membrane in the dark, and rhodopsin was formed.

In frog retinas, thermal isomerization accounts for a small fraction of rhodopsin regeneration.^{40,41}

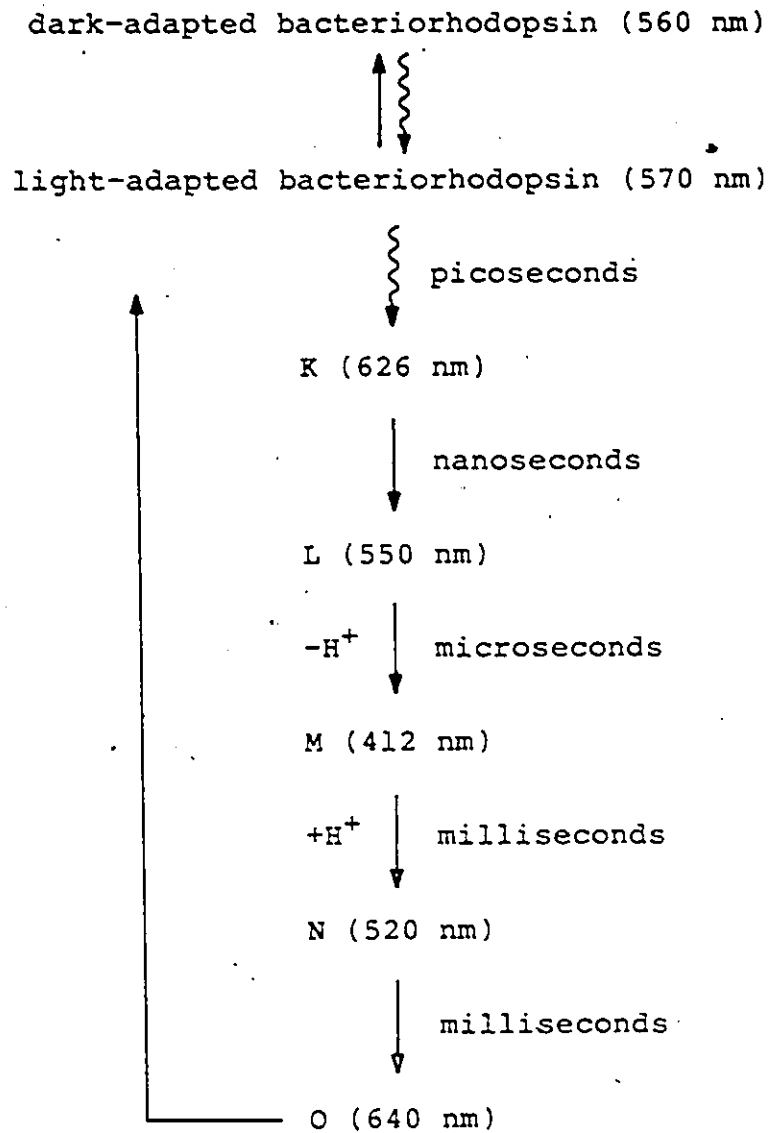
Once trans retinal has isomerized to 11-cis retinal, rhodopsin is regenerated by a condensation reaction of the aldehyde and the amine of the lysine group. This is a pH dependent reaction that is fastest at pH 7. The first step is bimolecular addition, proceeding with a rate constant of $690 \text{ M}^{-1}\text{s}^{-1}$ at pH 7. This is followed by dehydration, $k = 0.055 \text{ s}^{-1}$.⁴²

II. Bacteriorhodopsin

In general, the pigments bacteriorhodopsin and rhodopsin are similar, in that both contain retinal bound to an amino acid of the protein by an iminium bond, and both use light energy to isomerize the chromophore and thus drive cell reactions. The protein backbones are different, however, and some properties of bacteriorhodopsin are not the same as those of rhodopsin. Each protein constrains its chromophore by some interaction. These could be specific ionic interactions, or constraints of the tertiary structures of the proteins and the shape of the pockets in which the chromophores sit.

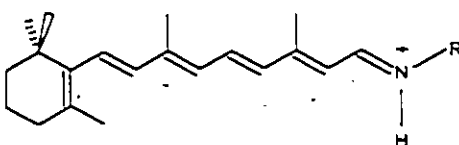
The bacteriorhodopsin photocycle is shown in Scheme 1-2.⁴

In bacteriorhodopsin, retinal is not dissociated from



Scheme 1-2 Bacteriorhodopsin Photocycle

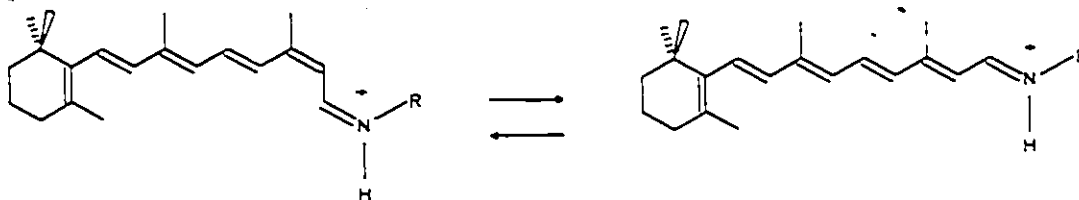
the bacteriorhodopsin during the cycle. In the presence of light, a photoequilibrium is thus maintained, called "light-adapted bacteriorhodopsin". This photostationary state is wavelength dependent.⁴³ When bacteriorhodopsin is irradiated with light >540 nm, the photostationary state is composed of >95% all-trans retinylidene.^{44,45}



R = bacterioopsin

A variety of spectroscopic techniques, including resonance Raman^{18,46}, solution ¹³C NMR^{47,48}, solid state ¹⁵N NMR⁴⁹, solid state ¹³C NMR⁵⁰, and FTIR^{51,52} spectroscopy, indicate that the nitrogen of the C=N bond is protonated in the intact protein. The configuration about the C=N bond is trans.^{50,53}

When the light source is removed, bacteriorhodopsin converts slowly⁵⁴ into what is known as "dark-adapted bacteriorhodopsin", 5. The "dark-adapted" state is a mixture of bacteriorhodopsin containing 60% of the 13,15 dicyc chromophore and 40% all-trans retinylidene.^{45,50,53}



bR₅₄₈

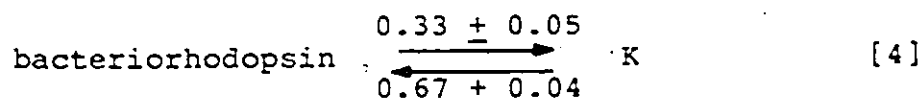
bR₅₆₈

The 13,15-dicis isomer was also characterized by resonance Raman spectroscopy, and found to be protonated.^{18,55} The two isomers are in dynamic equilibrium in the dark-adapted state⁵⁶, and the energy difference between them is small.⁵⁴

Photoisomerization of Bacteriorhodopsin

When dark-adapted bacteriorhodopsin, 5, absorbs light, the 13,15-dicis component converts to the all-trans isomer with no apparent effects on membrane processes.⁵⁴ Light absorption by the all-trans chromophore initiates a photocycle, Scheme 1-2, that results in proton movement through the cell membrane. As in rhodopsin, experimental evidence shows that the photoreaction is an isomerization process, although in bacteriorhodopsin isomerization occurs about the C₁₃,C₁₄ double bond. Retinal analogues that are constrained trans isomers about the C₁₃,C₁₄ double bond form bacteriorhodopsin analogues that do not have photocycles or proton pump activity,⁵⁷⁻⁶⁰ and have prolonged excited state lifetimes relative to the natural pigment.^{61,62}

The photoisomerization is reversible at 77K, and highly efficient, equation 4.^{63,64}



The isomerization reaction accounts for most of the photoprocesses, and at room temperature, bacteriorhodopsin is only weakly fluorescent ($\phi_f = 2.5 \times 10^{-4}$).⁶⁵

The first intermediate formed in the photocycle, K, has a protonated iminium bond at low temperature^{18,52,66-70} and at room temperature⁷¹⁻⁷⁶. Resonance Raman experiments establish that the C=N configuration of K is trans,⁵³ and the spectra have been interpreted to fit a twisted 13-cis structure.⁶⁷ The C=N stretching vibration of K is low, 1609 cm⁻¹. It was calculated that separating the iminium ion from its counterion by 3.4Å accounts for this.⁷⁷ Room temperature and low temperature (77K) spectra of K differ, and in FTIR studies at an intermediate temperature, 135K, two species can be detected.⁷⁸ The identities of these two species are not known.

The decay rate of the excited state of bacteriorhodopsin and the rate of formation of K were measured by femtosecond spectroscopy. The two processes fit a single exponential, with time constants 0.7±0.1 ps in H₂O and 1.0±0.1 ps in D₂O. The reaction was monitored from 570 to 620 nm, and no evidence of other intermediates was found.^{79,80} However, other spectroscopic evidence exists, that J, a precursor to K, is the first ground state product of the photo-reaction.^{61,62,81-84} Part of the difficulty in analysing absorption data is that subtraction techniques must be used, and the errors involved are reflected in the widely varying absorption maxima reported for K. Thus K has been reported to absorb at 610 nm (-196°C)⁸⁵, 631 nm (-25°C)⁸⁶, 590 nm (1°C-50°C)^{85,87}, 610 nm (25°C)⁸¹, 615 nm (25°C)⁷⁹, and

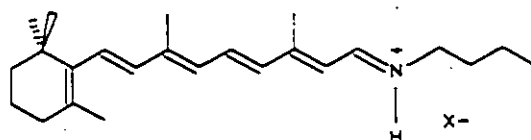
620 nm (37°C)⁸⁰.

Although it is not certain whether an intermediate J precedes K in the photocycle, it is certain that a 13-cis retinylidene chromophore is the product of the photoreaction. Further changes known to occur in the cycle are deprotonation to give M⁴⁶, an imine with a 13-cis C=C bond⁸⁸, and re-protonation and thermal isomerization from a 13-cis to a twisted trans C=C bond isomer, O.⁸⁹ The retinal chromophore remains attached to the protein throughout the cycle.

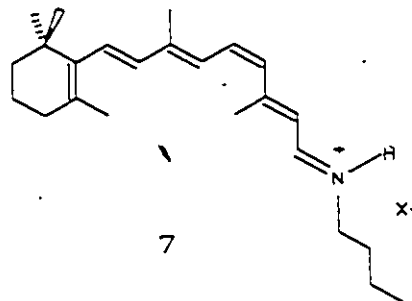
III. Effect of the Protein Environment

The retinylidene chromophore is the common element of the light-absorbing pigments discussed, but the protein component of each pigment is different, and so each type of retinylidene chromophore is in a slightly different environment. Many of the properties of the retinylidene chromophores are species dependent, including the absorption maxima, the quantum yields of the photoreactions, and the thermal equilibria, clearly indicating that the proteins affect the chemical and physical properties of their chromophores. It is possible that there is some specific interaction between each protein and its chromophore, or that the geometry of the chromophore is affected by the shape of the cavity in which it is found. The amino acid sequences of opsin and bacterioopsin have been determined⁹⁰⁻⁹³, however, the three dimensional arrangements of the proteins are not yet known, so interactions between

the amino acids and the retinylidene chromophores can only be speculated on at this point. Some information about the nature of the protein effect comes from comparing the properties of rhodopsin and bacteriorhodopsin to properties of model iminium salts in organic solvents. The chromophore of bacteriorhodopsin can be approximated by the all-trans *N,N*-butylretinylidene iminium salt, 6. Similarly, the 11-cis iminium salt, 7, can represent the chromophore of rhodopsin.



6



7

The ground state structures of rhodopsin, bacteriorhodopsin and their models have been probed by various techniques, including vibrational spectroscopy, and NMR, Table 1-1, and theoretical calculations. The structures, that is the conformations and electron distributions, of the chromophores or the model iminium salts must be elucidated indirectly since structure determinations by X-ray crystallography have not been accomplished yet.

Structure of the Chromophore in Rhodopsin

The π system of the retinylidene chromophore of rhodopsin is thought to be essentially planar. Steric hindrance forces some non-planarity about the C_6, C_7 and the C_{12}, C_{13} single bonds, both of which could be twisted by 30° .

Table 1-1

Some Spectroscopic Data for Rhodopsin, Bacteriorhodopsin and the
All-Trans Retinylidene Iminium Salt

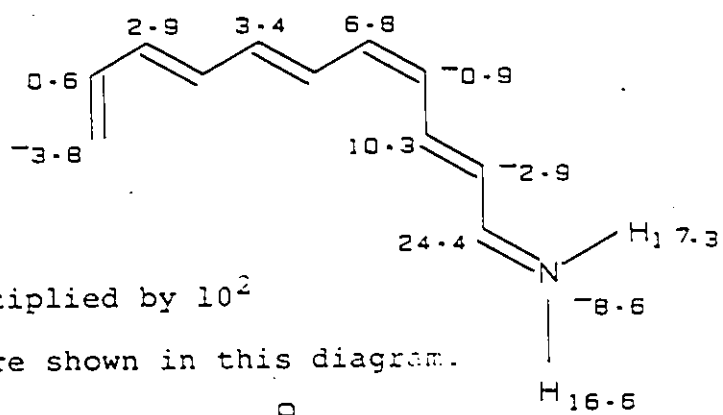
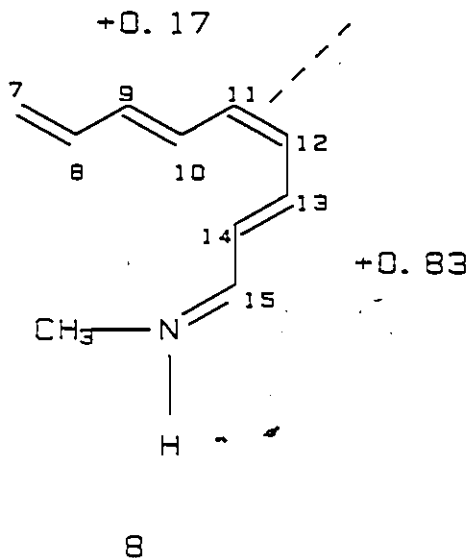
Spectroscopic Technique	Retinylidene Iminium Salt, 6	Rhodopsin	Bacteriorhodopsin bR ₅₆₈	Bacteriorhodopsin bR ₅₄₈
Resonance Raman (cm ⁻¹)				
C=N	1654 ^{100,101}	1655 ¹⁴	1640 ^{67,101}	
C ₁₄ -C ₁₅	1237 ¹⁰¹		1201 ¹⁰¹	
C ₁₀ -C ₁₁	1159 ¹⁰¹		1170 ¹⁰¹	
C ₈ -C ₉	1204 ¹⁰¹		1214 ¹⁰¹	
Solution ¹³ C NMR (ppm)				
C ₁₅	163.7 ¹⁰²⁻¹⁰⁴	165.9 ¹⁰⁵	169 ⁴⁷	166 ¹⁰⁵
C ₁₄	120 ^{50,102-104}	130.8 ^{15,105}	118 ⁴⁷	130 ¹⁰⁵
Solid State ¹³ C NMR (ppm)				
C ₁₅	167 ^{107,106}		163.2 ¹⁰⁶	160.4 ¹⁰⁶ 150 ¹⁰⁵
C ₁₄	122.6 ¹⁰⁷		122.0 ^{50,106}	110.5 ^{50,106}
C ₁₃	161.8 ¹⁰⁷		169.0 ¹⁰⁶	165.3 ¹⁰⁶ 143.7 ¹⁰⁵
Solid State ¹⁵ N NMR (ppm)				
N	X=Cl 172.0 ⁴⁹		151.6 ⁴⁹	144.9 ⁴⁹
	X=Br 166.1 ⁵⁰			

or more. The cyclohexenyl ring is thought to be in an s-cis conformation, and all other single bonds in the linear chain are s-trans.^{94,95}

The electron distributions in the π systems of simplified polyenylidene iminium ions 8 and 9 have been calculated by ab initio and semi-empirical techniques, respectively. The calculations show that the positive charge is distributed mainly within the C₁₂-N part of the molecule, Figure 1-1.^{96,97} These calculations did not optimize geometries, nor did they include a counterion.

The positive charge in rhodopsin is likely more delocalized than it is in the model iminium salt, a conclusion arrived at by comparing resonance Raman spectra of an N-ethanol-retinylidene iminium salt and rhodopsin.⁹⁸

Ground state interactions between the chromophore and the protein could be provided by a general polar environment, or by a point charge in the protein, such as an anionic amino acid side chain, that interacts with the chromophore in a specific location. The first indication of a specific ground state interaction between the chromophore and the protein of rhodopsin came from its solution ¹³C NMR spectrum. The resonance of C₁₄ is 10 ppm downfield from the corresponding peak of the model iminium salt in solution.¹⁵ It was calculated that a negatively charged amino acid near C₁₄ could cause this deshielding.¹⁶ However, systematic examination of the resonance Raman spectra of ¹³C labelled rhodopsins



Charges shown are multiplied by 10^2

Not all the charges are shown in this diagram.

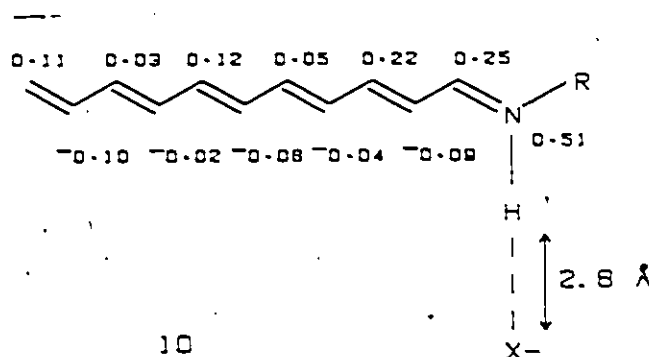
Figure 1-1 Charge Distributions in the Ground States of Model Compounds of Retinylidene Iminium Salts

indicated that the C₈ to C₁₅ region is not perturbed by a point charge interaction.⁹⁹

Structure of the Chromophore in Bacteriorhodopsin

The structure of bacteriorhodopsin has been investigated more thoroughly than that of rhodopsin.

Semi-empirical calculations of a simplified trans polyenylidene iminium salt, 10, predict the positive charge distribution shown.^{103,108}



Analyses of resonance Raman spectra¹⁰¹ indicate that the positive charge of the chromophore of the pigment is more delocalized into the polyene chain than in the model iminium salt in solution, with diminishing effect as the distance from the nitrogen increases. Solid state ¹³C NMR spectra show that the cyclohexenyl ring is in an s-trans configuration relative to the polyene chain of the bacteriorhodopsin molecule.^{106,109} The other single bonds are also s-trans.

It was concluded from ¹⁵N NMR studies of bacteriorhodopsin that the counterion is only weakly interacting with the iminium nitrogen.^{49,106}

NMR spectra suggest that a ground state perturbation such as a negative charge in the protein could contribute to the downfield shift of the resonance of C_5 of the chromophore of bacteriorhodopsin¹⁰⁶, and resonance Raman spectra indicate that no significant perturbations exist from C_8 to C_{15} .¹⁰¹ The structure shown in Figure 1-2 depicts the charge environment predicted from the analysis of the Raman and NMR spectra.¹⁰⁶

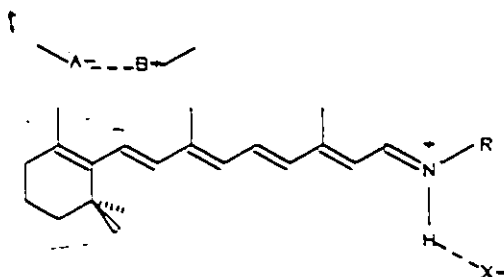
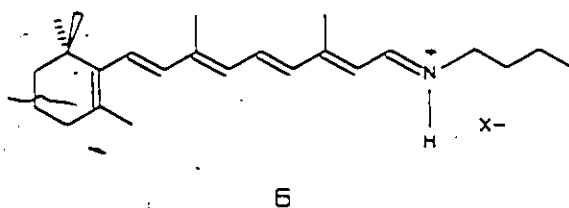


Figure 1-2

The effect that a non-conjugated negative charge would have on the ground state structure has not been determined experimentally, but has been calculated.¹¹⁰ According to the semi-empirical calculations, a retinylidene iminium salt with an additional negative charge near the cyclohexenyl ring has properties similar to the free cation, without a counterion. The molecule has more positive charge delocalized into the polyene chain than found for the iminium salt 10, where a counterion was included in the calculations.

The available structural evidence suggests that the ground state structures of the iminium model compounds are different from the structures of the natural pigments. In addition to the perturbation that might arise from a specific

charge interaction, the chromophores in the pigments might differ from the model iminium salts in the torsional angles of the single bonds of the π system,¹¹¹ or in the distance between the counterion and the iminium ion. Blatz and co-workers proposed that the ground state of the retinylidene iminium ion would be destabilized by moving the counterion away from the iminium nitrogen.¹¹²⁻¹¹⁵ This would lead to increased conjugation within the π system, and a longer wavelength absorption band.^{103,114,107} Three N-n-butyl retinylidene iminium salts, **6**, were synthesized with chloride, bromide and iodide counterions respectively. As the size of the counterion increases from chloride to iodide, and the counterion must move further from the iminium group, the absorption spectrum shifts to longer wavelengths.¹¹²



X	λ_{max} (acetone) ^a
Cl	428 nm
Br	439 nm
I	445 nm

Of the three structural possibilities mentioned above, only the point charge is expected to have an effect on the excited state of the chromophore.

On absorption of light, molecules reach an excited state that differs from the ground state in the distribution of electrons in the π system. In the excited state, the positive charge is calculated to be more delocalized into the

polyene chain of the model retinylidene ions than it is in the ground state.^{96,97,108} This is substantiated by a large increase in the dipole moment of the excited state relative to the ground state of iminium salt 6.^{116,117}

An absorption spectrum measures the energy difference between the ground state and first excited state of a molecule. The absorption maxima of the chromophores in rhodopsin and bacteriorhodopsin are at considerably longer wavelength than those of retinylidene iminium salts in solution, Table 1-2, indicating that the energy gap between ground and excited states is smaller than in the model compounds. The difference in absorption maxima between the chromophore and the model iminium salts is called the "opsin shift". The opsin shift could result from destabilizing the ground state, as proposed by Blatz and co-workers, or stabilizing the excited state.

Although solvent and counterion changes can modify the solution spectra of retinylidene iminium salts, they do not account for the observed absorption maxima of the natural pigments, Table 1-2.

In bacteriorhodopsin, a large fraction of the opsin shift is attributed to the conformation of the cyclohexenyl ring. In solution, the configuration of the cyclohexenyl ring of 6 is s-cis, but in the pigment it is s-trans.^{106,109} The additional double bond in conjugation with the π system should stabilize the excited state.

Specific ionic interactions in the natural pigments

Table 1-2

Absorption Maxima for Rhodopsin, Bacteriorhodopsin and Retinylidene Iminium Salts in Various Solvents

	Solvent	λ_{\max} (nm)	Reference
Bacteriorhodopsin		568	
Rhodopsin		500	
6, X=Cl	acetone	428	114
	benzene	437	112
	acetonitrile	443	114
	dichloromethane	460	114,112
	methanol	440	120
7, X=Cl	3-methylpentane	438	121
	methanol	440	122

are thought to contribute to the opsin shift as well. Kropf and Hubbard originally suggested that, in addition to the counterion of the iminium group, a second negatively charged or polarizable group in the protein backbone interacts with the π system of the chromophore on excitation.³⁹ Various theoretical and experimental approaches have been used to test this, the most elegant by Nakanishi and co-workers^{118,120,121}, and the theory has gained widespread acceptance.

Specific models were proposed based on the experimental results of studies of rhodopsin and bacteriorhodopsin analogues that contain dihydroretinals.^{118,120-122} The dihydro-retinylidene iminium salts and rhodopsin analogues shown in Figure 1-3 were synthesized. The absorption maxima of these pigments differ from the absorption maximum of the natural pigment by amounts that decrease with increasing conjugated chain length. An "opsin shift" was calculated for each of the synthetic rhodopsins.

The largest opsin shift was observed for the C₁₁,C₁₂ dihydroretinal derivative. Combining this result with the calculated effects of negative point charges on the absorption spectra, it was concluded that in rhodopsin an additional negative charge (the dipole of an amino acid, or part of a salt bridge) was held in place about 3 Å from C₁₂ and C₁₄, Figure 1-4.^{16,111} This contradicts ground state structural evidence against interactions in the C₈ to C₁₅ region,

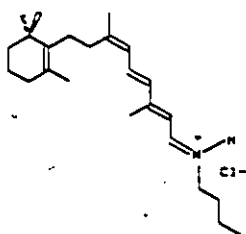
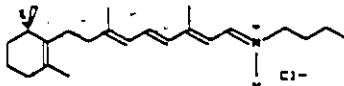
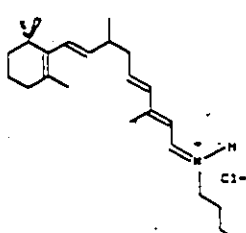
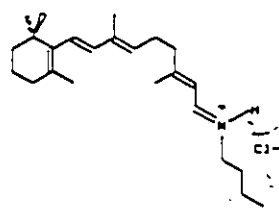
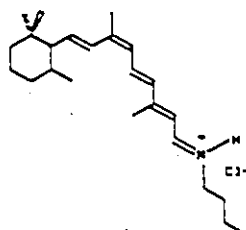
dihydroretinylidene	rhodopsin analogue		bacteriorhodopsin analogue		
	λ_{\max} in MeOH (nm)	λ_{\max} (nm)	opsin shift (cm^{-1})	λ_{\max} (nm)	opsin shift (cm^{-1})
6	440			560	4870
7	440	500	2700		
	392	420	1700		
	392			440	2780
	322	345	2100	325	300
	270	315	5300		
	425	460	1800	476	2500

Figure 1-3 Absorption Maxima of Dihydroretinylidene Iminium Salts

although weak ground state interactions that intensify in the excited state are possible.

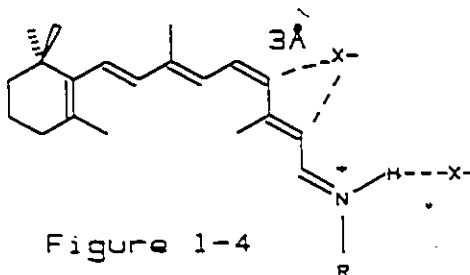


Figure 1-4

The experiments for bacteriorhodopsin, Figure 1-3, were used to predict a charge environment similar to that previously suggested from ground state observations, Figure 1-2.^{118,122}

Various model compounds have been synthesized where a non-conjugated charge is incorporated into the retinylidene iminium ion molecule to attempt to reproduce the spectral shifts observed in the protein environment, Figure 1-5.¹²³⁻¹³⁶ The charged groups can shift the spectra to longer or shorter wavelengths, depending on where they are placed, but the effect is not as large as the opsin shift.

The chromophores in the natural pigments differ from the model retinylidene salts not only in structural and physical properties, but also in the isomerization reactions they undergo.

Effect of the Protein on Thermal Reactions

Retinylidene iminium salts 6 and 7 isomerize by thermal pathways about the C=C and C=N bonds in solution.^{137,138,104} The composition of the thermodynamic equilibrium mixture is

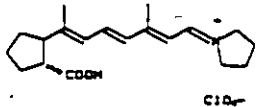
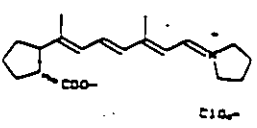
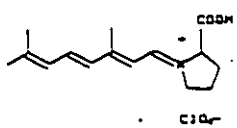
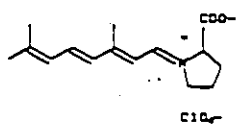
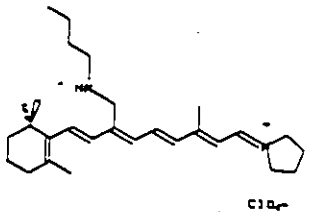
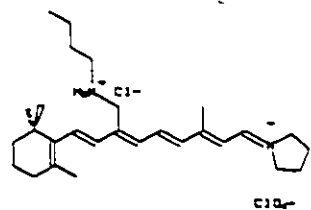
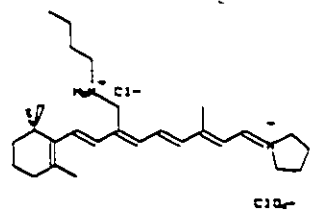
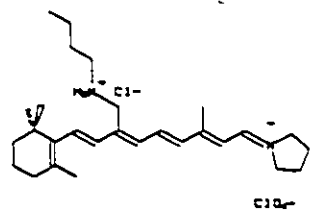
iminium salt	λ_{\max}	solvent	reference
	410	CHCl ₃	125
	420	CHCl ₃ /Et ₃ N	125
	415	CHCl ₃	125
	405	CHCl ₃ /Et ₃ N	125
	450	EtOH	130
	475	CHCl ₃	130
	420	EtOH/Et ₃ N	130
	435	CHCl ₃ /Et ₃ N	130

Figure 1-5 Effect of Non-Conjugated Charged Groups on Absorption Maxima of Rhodopsin and Bacteriorhodopsin Models

not reported in the literature, however it is thought that the ratios of the isomers about the C=C bonds are the same at equilibrium as are the retinal isomers.¹³⁸ It is also known that both cis and trans isomers about the C=N bond are found in solution at equilibrium.^{137,104} Rhodopsin does not reach a thermodynamic equilibrium at room temperature, since only the 11-cis isomer of the chromophore remains attached to the protein. In bacteriorhodopsin, the equilibrium contains only two species, the 13,15-dicis isomer, and the all-trans isomer in a 60:40 ratio, 5.

The rates of isomerization of the iminium salts have been measured by two groups,^{137,138} with conflicting mechanistic conclusions. In one report, the authors suggest that isomerization barriers are determined by the extent of double bond alternation within the conjugated chain.¹³⁷ 13-cis N,n-butylretinylidene iminium chloride in CDCl₃ isomerized to the all-trans isomer with a rate constant of $3 \times 10^{-5} \text{ s}^{-1}$. A larger, less nucleophilic counterion such as perchlorate induced a faster isomerization rate than did halide counterions. It was concluded that as the counterion moves closer to the iminium nitrogen, the positive charge becomes localized at the nitrogen. This increases double bond alternation in the rest of the polyene chain, and increases the activation barrier to isomerization. In another report, C=C bond isomerization in retinylidene salts was found to be nucleophile catalyzed.¹³⁸ The chloride salt of the 13-cis retinylidene

isomer disappeared with a rate constant of $3 \times 10^{-2} \text{ s}^{-1}$ in heptane, and the 11-cis isomer isomerized to the all-trans isomer with a rate constant of $2 \times 10^{-2} \text{ s}^{-1}$. When the counterion was a less nucleophilic one, trifluoroacetate, a slower rate of isomerization of the 11-cis isomer was measured, $k = 2.6 \times 10^{-6} \text{ s}^{-1}$.

The isomerization of all-trans retinylidene to the 13,15-dicis isomer in bacteriorhodopsin proceeds with a rate constant of $2 \times 10^{-4} \text{ s}^{-1}$.⁵⁴ Although it seems that the rate of thermal isomerization of the chromophore in bacteriorhodopsin is within the range of the rate constants reported for thermal isomerization of the retinylidene salts in solution, it has been calculated that the negative point charge near the ring has the added effect of reducing the isomerization barrier of bacteriorhodopsin.¹¹⁰

Effect of the Protein on Photochemical Isomerization

Rhodopsin photoisomerizes exclusively about the 11-cis C=C bond, as does the model iminium ion, 7, in solution.^{139,140} The quantum yields are not the same, however. Rhodopsin isomerizes with a quantum yield of 0.67, whereas the 11-cis N,n-butylretinylidene iminium trichloroacetate isomerizes less efficiently, with a quantum yield of 0.23.^{139,140,57} This photoisomerization is both solvent and wavelength independent. C=N isomerization could not be observed in these model studies as identification of the products required hydrolysis of the iminium bond.

The photoisomerization of bacteriorhodopsin is also regiospecific, the C₁₃,C₁₄ bond isomerizing in the reaction with a quantum yield of 0.33. The all-trans iminium salt, 6, isomerizes about several bonds in solution, with a quantum yield of 0.14 and relatively low regioselectivity.^{140,141,57} The major product is the 11-cis isomer (70% in hexane). The 13-cis isomer (19%), the 9-cis isomer (11%) and a trace amount of the 7-cis isomer are also formed. In these model studies the iminium salts were also hydrolyzed before analysis, and isomerization about the C=N bond could not be detected.

Photoisomerization is thought to originate in the singlet state in the model chromophores, as intersystem crossing yields are less than 0.001.¹⁴² Isomerization in the triplet state was thought to have been observed using anthracene or phenanthrene as sensitizers^{142,143}, however the possibility of electron transfer in the excited state was overlooked. At room temperature, retinylidene iminium salts do not fluoresce, but weak fluorescence has been observed at 77K in 3-methylpentane glasses, $\phi_f=0.098$.¹⁴⁴

The rates of photoisomerization of the iminium salts in solution and in the pigments are similar. The lifetime of the 11-cis retinylidene salt, 7, was found to be less than 8 ps in methanol at room temperature.^{145,146} The rhodopsin photoreaction occurs within 3 ps²⁴, and the bacteriorhodopsin isomerization takes place in about 1 ps.⁸⁴ As in the thermal isomerizations, the proteins seem to influence the regio-

selectivity of the isomerizations more than the rate of the reaction.

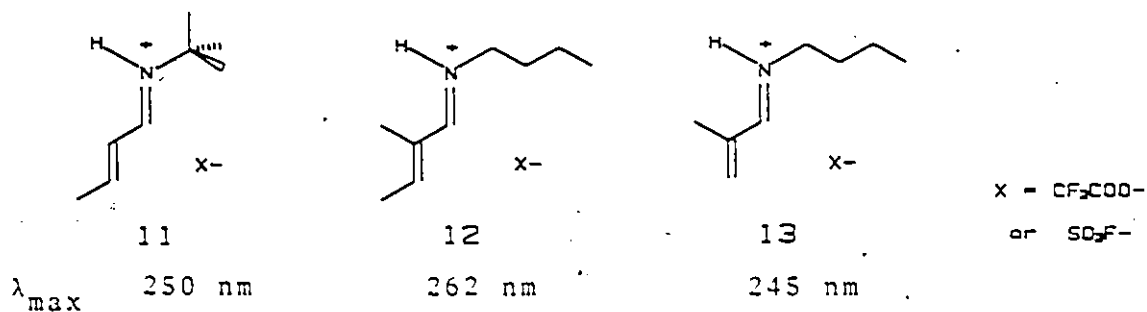
Although our knowledge of the visual system, and related light-absorbing pigments such as bacteriorhodopsin, is extensive and growing daily, there is still a great deal to be learned about the interactions between the proteins and the chromophores. Before these can be understood, the properties of the model iminium salts themselves, and other simple conjugated iminium salts, need to be better characterized. A recent review summarizes the photochemistry of iminium ions.¹⁴⁷

One approach to an understanding of the reactions of retinylidene iminium ions has been to study simple molecules such as α, β unsaturated iminium salts where only two bonds can isomerize, the C=C bond and the C=N bond.

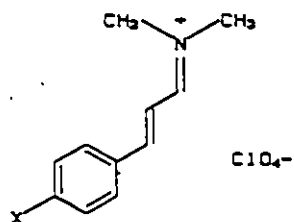
IV. α, β Unsaturated Iminium Ions

Absorption Studies

Alkyl iminium ions 11, 12 and 13 absorb light in the ultraviolet region.^{148,149}



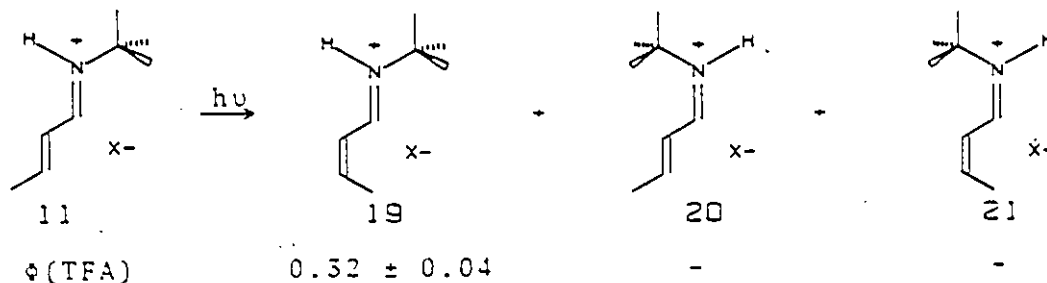
An aryl group on C₃ greatly reduces the excitation energy. The iminium salts 14 to 18 absorb in the visible region, and appear yellow. Changing the substituent on the phenyl ring from nitro to methoxy shifts the absorption maximum to longer wavelengths by 61 nm.¹⁵⁰



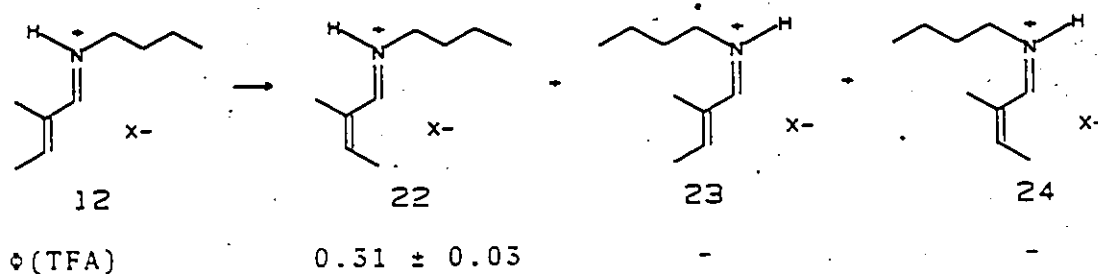
	X	λ_{\max} (nm)
14	NO ₂	323
15	Cl	350
16	H	341
17	CH ₃	359
18	OCH ₃	384

Photochemical Isomerization

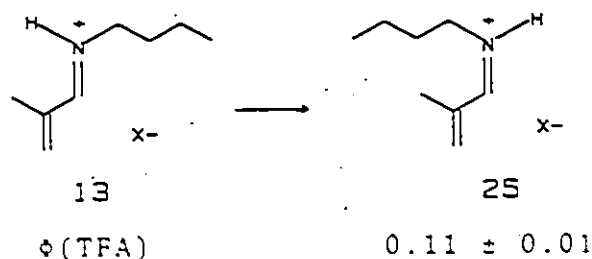
Simple alkyl substituted iminium ions photoisomerize about both the C=C and the C=N bonds in solution.^{148,149} For example, 11 isomerizes to give 19, 20, and 21. The only initial product is the Z C=C bond isomer, 19 ($\phi=0.32$ in trifluoroacetic acid, TFA). This means that C=N isomerization to form 20 has a quantum yield less than 0.10, and the Z,Z isomer, 21, is presumed to be a secondary product.



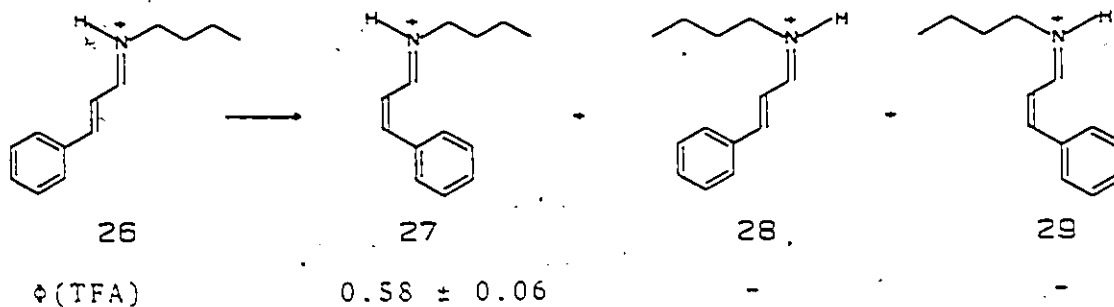
Methyl substitution at C₂ and a less bulky substituent at nitrogen have no effect on the quantum yields.



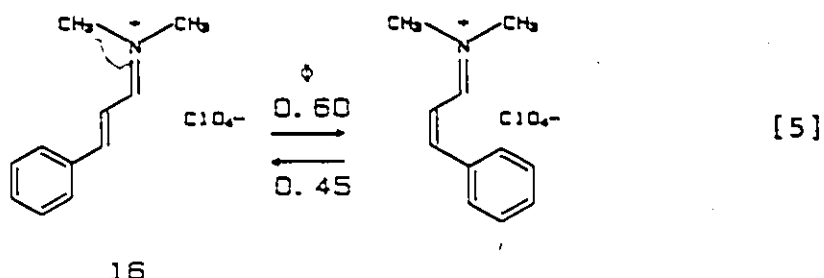
Only C=N isomerization is detected in the absence of the methyl substituent at C_3 . Iminium ion 25 is produced with a quantum yield of 0.11, close to the upper limit determined for C=N isomerization of 11 and 12 to form isomers 20 and 23, respectively.



An aryl substituent at C_3 increases the efficiency of isomerization about the C=C bond at the expense of C=N bond isomerization.¹⁵⁰ Efficient isomerization could be detected about the C=C bond of the E,E isomer, 26 ($\phi=0.58$), but C=N isomerization occurred only very inefficiently. After irradiation for one week, small amounts of the Z C=N isomers, 28 and 29, could be detected.

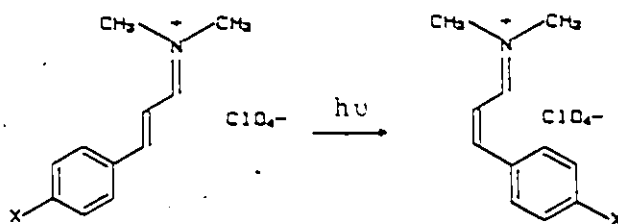


Isomerization about the C=C bond in salt 16 is thought to account for most of its excited state processes since the molecules do not fluoresce, and the quantum yields for the forward and reverse isomerizations add up to one, Equation 5.



Isomerization about the C=N bond could not be detected, but is thought to be inefficient by analogy to the photoisomerization of iminium salt 26.

When the electronic nature of the aryl substituent was changed from chloro to methoxy, no effect on the quantum yield of C=C bond isomerization was observed.¹⁵⁰ However, the salt with a para nitro substituent, 14, isomerizes with a significantly lower quantum yield.



X			ϕ
NO ₂	14	30	0.27 ± 0.02
Cl	15	31	0.58 ± 0.09
H	16	32	0.60 ± 0.06
CH ₃	17	33	0.52 ± 0.05
OCH ₃	18	34	0.59 ± 0.04

Charge Delocalization in α, β Unsaturated Iminium Salts

Several different methods of calculating charge densities and electron distributions have been used for the eneiminium ion 35.^{149,151,152} The calculations optimize the geometry of the molecule, but do not include a counterion. A semi-empirical calculation, using MINDO/3, predicts that the positive charge of the molecule is partially delocalized to C₃.¹⁴⁹ The charge densities and electron distributions calculated by ab initio techniques show no positive charge at C₃.^{151,152}

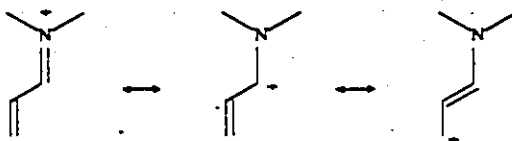
Net Charges (ab initio)	electron densities (MINDO/3)							
	N	(π)	C ₁	(π)	C ₂	(π)	C ₃	(π)
<p>35</p>	6.91	1.46	5.68	0.66	6.12	1.14	5.81	0.74

Experimental techniques that have been used to determine charge distributions in conjugated systems are ¹³C NMR spectroscopy and X-ray crystallography. Since the chemical shifts of carbon nuclei vary with the extent of shielding or deshielding of the nuclei by the electrons surrounding them, the ¹³C NMR technique has been used to predict the charge distributions at carbon atoms in ionic molecules. The extent of charge delocalization has been determined for a number of cyclic, conjugated polyenes.¹⁵³ Comparisons of chemical shifts of the carbon atoms of related neutral and ionic molecules and the differences in π electron densities at each

carbon from theoretical calculations, led to the prediction that the resonance of a carbon atom would move downfield by 160 ppm for each net positive charge unit on the carbon atom. Using this value, the extent of charge delocalization in a conjugated system could be estimated. This technique was extended to linear conjugated molecules, and used to probe the retinylidene iminium salt structure.¹⁰³ It was found that a linear relationship existed between the chemical shift differences of the imine and the iminium ion of retinal, and the differences in π electron density calculated for each carbon of these two molecules, but the downfield shift was about 100 ppm per charge unit. The analysis suggested that positive charge was delocalized at least as far as C₇. A similar relationship was found for the eneiminium ion, 35.¹⁴⁹ Calculated π electron density differences between the eneiminium ion and related imine correlate with ¹³C NMR chemical shift differences, and indicate that the positive charge is partially delocalized to C₃.

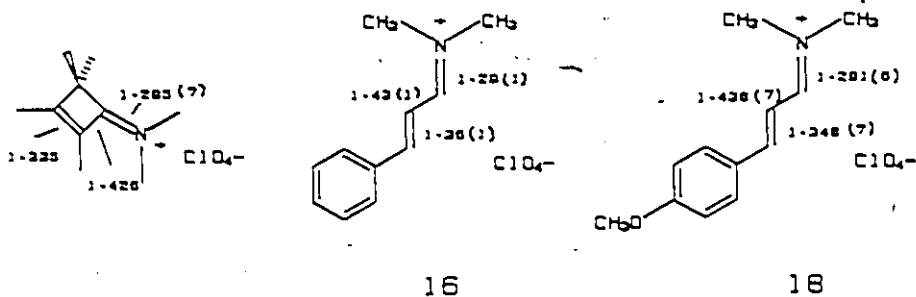
The retinylidene iminium salt structure has not been corroborated by other experimental techniques, but in the case of the eneiminium salt it was concluded, on the basis of crystallography data, that the combined approach of using ¹³C NMR chemical shift data and π electron density calculations did not correctly predict charge distributions in the eneiminium salts.¹⁴⁹ The use of X-ray crystallography data is another approach to studying charge delocalization. Charge

delocalization must be accompanied by changes in bond lengths, to reflect the increased importance of the resonance forms shown.



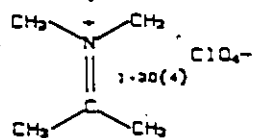
Single bonds between the double bonds of a π system should shorten if conjugation is increased, and double bonds should lengthen, to approach a fully conjugated system where the bond lengths are the same. One structure of a simple iminium salt has been solved, and numerous examples of structures with considerable delocalization of positive charge are known, Figure 1-6.¹⁵⁶⁻¹⁶¹

The structures of three α, β -unsaturated iminium salts have been solved.^{149,155} The bond lengths suggest that the positive charge of the molecule is not delocalized, as bond alternation is large, and C=C and C-C bonds are not lengthened or shortened, respectively, relative to non-conjugated molecules.

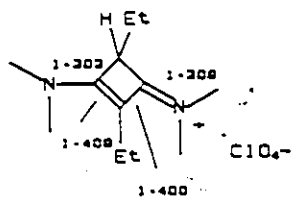


Iminium Salt

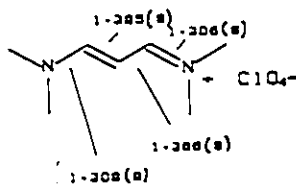
reference



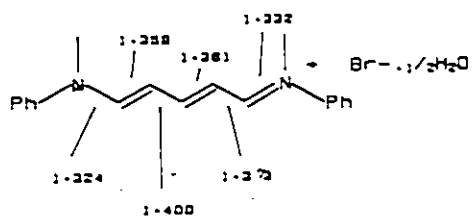
156



157



158



161

Figure 1-6 Bond Lengths of Some Iminium Salts

The bond lengths of salts 16 and 18 are the same within error limits, even with the possibility of a charge-stabilizing interaction between the positive charge and the methoxy substituent in 18.

V. Longer Chain Iminium Ions

Absorption Studies

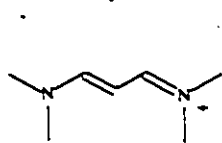
Absorption spectra of a series of retinal iminium ion homologues show that a relationship exists between absorption maxima and the length of a conjugated chain. Each additional double bond increases the absorption maximum by 30-50 nm.^{144,108} E isomers absorb at slightly higher wavelength and with higher extinction coefficients than Z isomers.

Photoisomerization

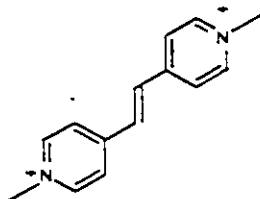
Photoisomerizations of longer chain iminium salts other than the retinylidene salts already mentioned have not been studied.

VI. Photoisomerizations in Related Systems

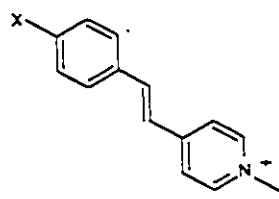
C=C isomerization in conjugated iminium ions has been observed in cyanine dyes, 36¹⁶¹⁻¹⁶⁴, the 4,4'-bipyridyl-ethylene dication, 37¹⁶⁵, and in 1-alkyl-4-styrylpyridinium salts, 38-43.¹⁶⁶⁻¹⁷⁰



36

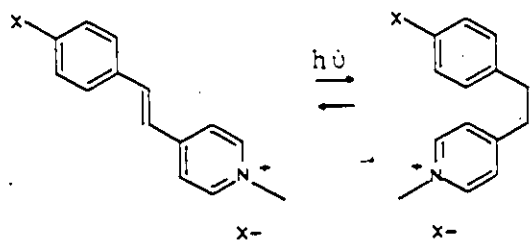


37



	X
38	H
39	CN
40	CH ₃
41	OCH ₃
42	NO ₂
43	N(CH ₃) ₂

The dication 37 isomerizes with a high quantum efficiency in the singlet state, $\phi_{E \rightarrow Z} = 0.5 \pm 0.1$. For salt 38, the effect of aryl substituents on the photoisomerization was explored, and several mechanisms of photoisomerization were elucidated. Quantum yields of E to Z isomerization about the C=C bond were measured for the salts with various para substituents, 38-43, Equation 6. Pyridinium salts 38-42 isomerize with essentially the same quantum yields, and have similar photostationary states. In spite of this, two mechanisms are operative. Salts 38-41 isomerize in the singlet excited state, and the nitro substituted salt, 42, in the triplet.^{166,169} When a dialkyl amino substituent is present, 43, isomerization is inefficient, with an activation barrier of 24 kcal mol⁻¹,¹⁶⁷ considerably higher than the 2-4 kcal mol⁻¹ barrier to isomerization in the unsubstituted salt, 38. This led to the conclusion that for 43, deactivation was occurring by internal conversion from the planar excited state. A fourth isomerization pathway was shown to be electron transfer initiated, and will be discussed below.¹⁷⁰

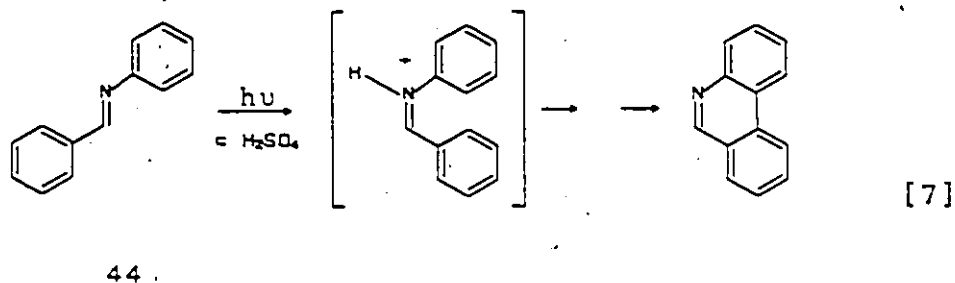


[6]

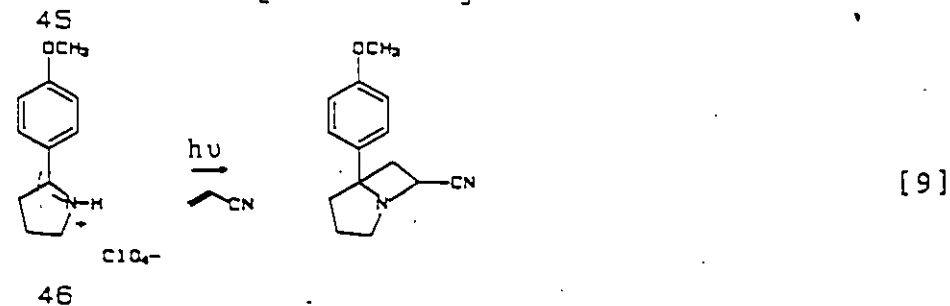
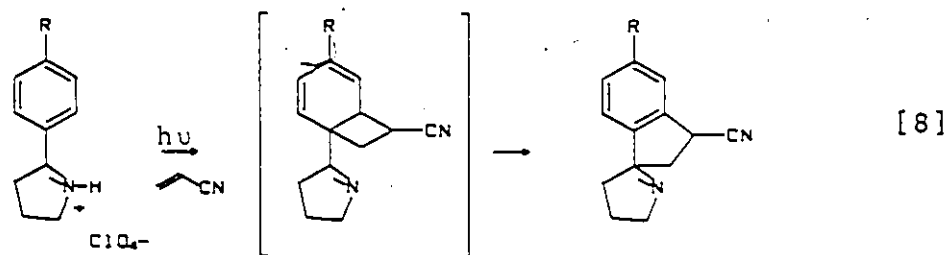
VII. Other Photoreactions

An example of a cyclization reaction involving a

conjugated iminium ion is shown in Equation 7. The photo-reaction of **44** requires an initial photoisomerization about the C=N bond.^{171,172}



The addition of electron-poor olefins to aryl iminium ions has been observed.^{173,174} These reactions were found to be substituent dependent. The iminium salts **45**, with fluoride, chloride, bromide and methyl substituents appear to add olefins at the conjugated aryl ring, equation 8. An electron-donating group, methoxy, induces addition to the C=N group of **46**, equation 9.



Other cyclization and cycloaddition reactions have been reported.^{175-179,147}

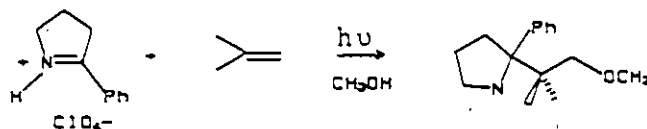
VIII. Photoinduced Electron Transfer

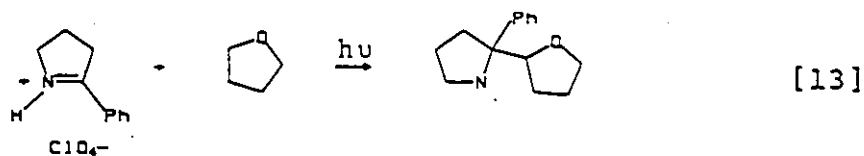
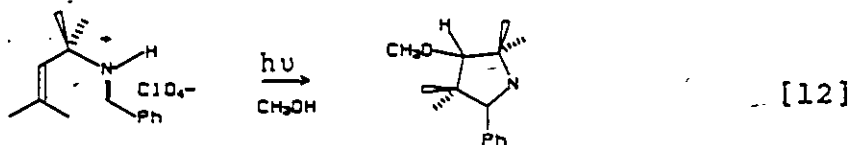
The energy gained on absorption of a photon can be used, not only for isomerization, but also for donating or accepting an electron in the excited state. The empirically derived relationship, equation 10, proposed by Weller, relates the energy of the absorbed photon ($\Delta E_{0,0}$), the energies of oxidation of the donor ($E_{1/2}(+)$) and reduction of the acceptor ($E_{1/2}(-)$) in the system to the probability of electron transfer. C is a constant that is solvent dependent.¹⁸⁰

$$\Delta G = E_{1/2}(+) - E_{1/2}(-) - \Delta E_{0,0} - C \quad [10]$$

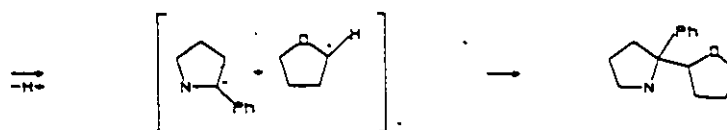
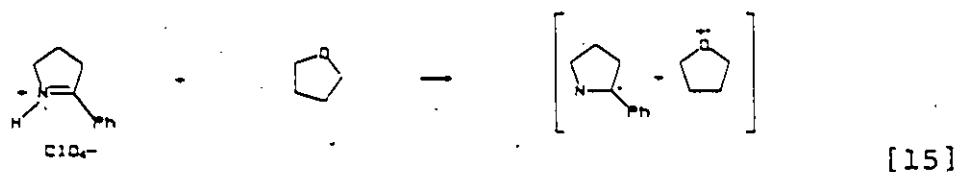
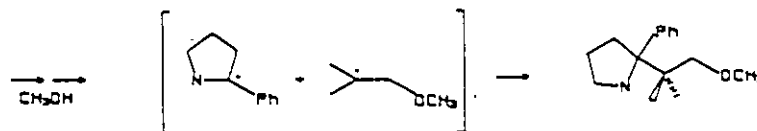
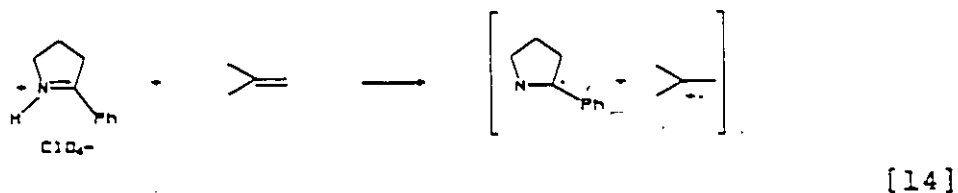
When ΔG is less than zero, electron transfer should occur, at rates approaching the diffusion controlled limit.¹⁴⁷ In general, iminium ions readily accept electrons in the excited state or from excited donors.

Photoinitiated electron transfer reactions have been used to add a variety of electron donors to iminium ions. Donors fall into two classes: π -type donors (arenes and electron-rich olefins) and n-type donors (alcohols and ethers). Some examples are given in equations 11-13.



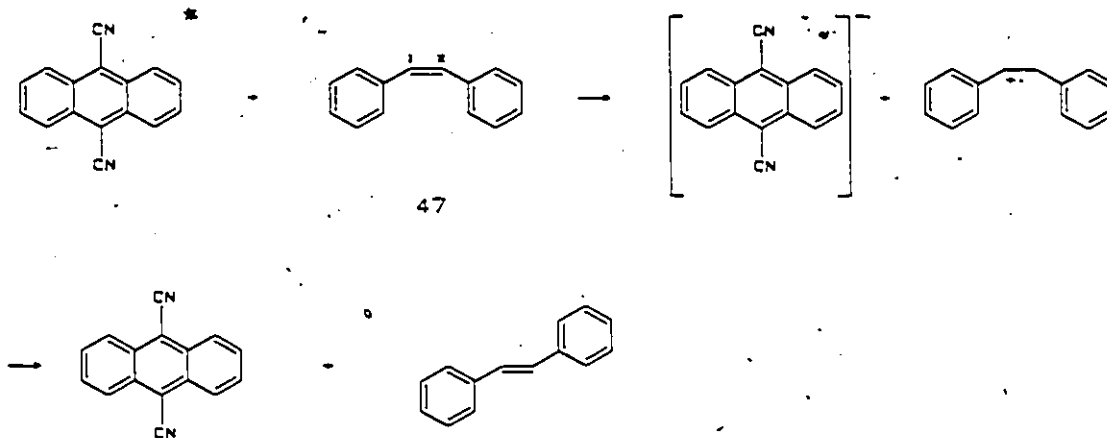


The initially produced radical cation can react with a nucleophile in two ways, either by addition, Equation 14, or by loss of a proton, Equation 15. The products of the reactions are then formed by radical coupling.¹⁴⁷



A photoinitiated electron transfer mechanism for C=C bond isomerization has been observed for stilbenes¹⁸¹, as well as for molecules where the C=C bond is conjugated to iminium groups, as in 37¹⁶⁵ and 42¹⁷⁰.

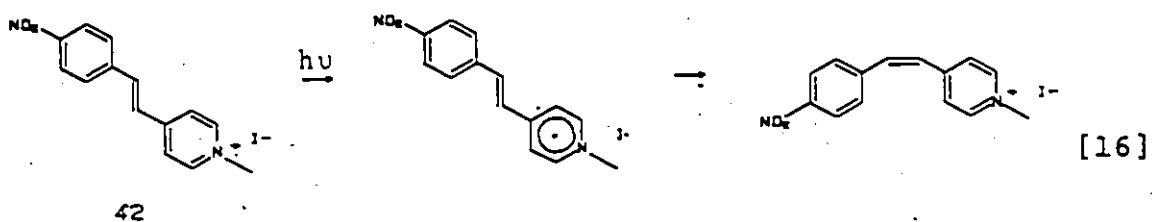
The photoinitiated electron transfer mechanism for isomerization of Z-stilbene, 47, is shown here.



In this example, the excited dicyanoanthracene molecule accepts an electron from 47. The stilbene radical cation produced can rotate easily about the C_1, C_2 bond, and can then react further, or can accept an electron to return to stilbene. About 98% of the stilbene molecules isomerize to E-stilbene, the remainder revert to Z-stilbene.

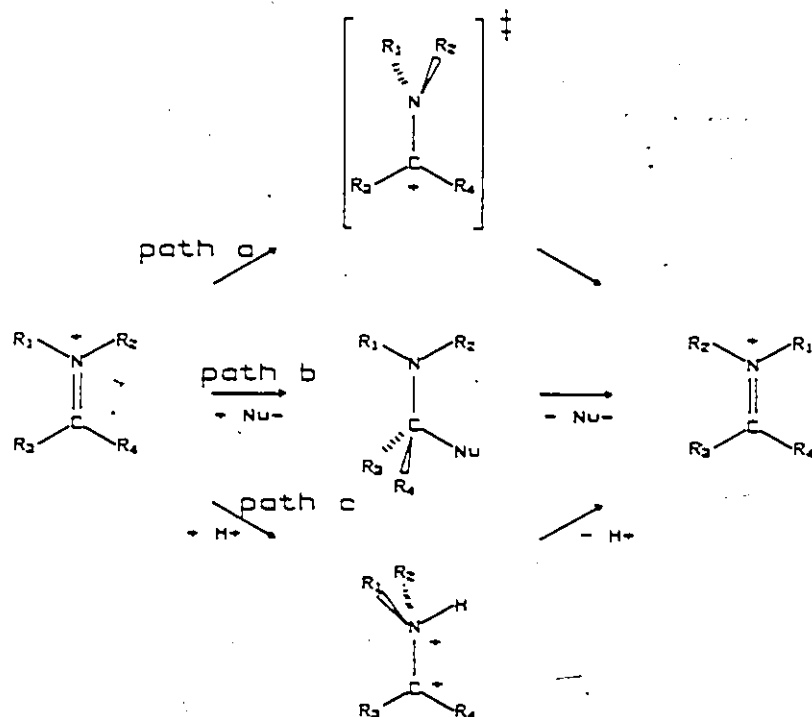
Electron transfer from haloaromatic molecules to the excited singlet state of 37 is thought to lead to intersystem crossing to the triplet state, from which isomerization occurs.

Electron transfer from the counterion, I^- , to the excited styrylpyridinium ion, 42, is observed in non-polar solvents, Equation 16. The main product of the reaction is the starting isomer, 42, with some Z C=C isomer also formed.



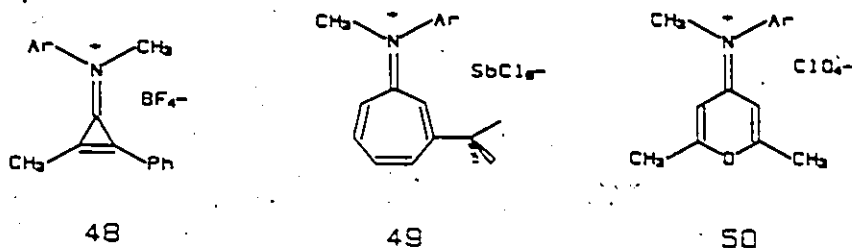
IX. Thermal Isomerization

Thermal E-Z isomerizations of iminium C=N bonds and C=C bonds conjugated to iminium groups have been observed in numerous cases.^{150,182-188} Experimental evidence has been found for three isomerization mechanisms, shown in Scheme 1-3.

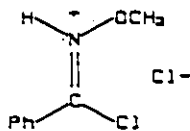


The iminium ions 48-50 are thought to isomerize by a rotation mechanism.^{183,184} The transition state in each case

is highly stabilized since it has aromatic character.

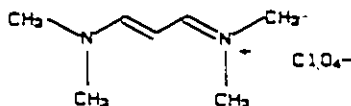


In several molecules where the rotational transition state is not stabilized significantly, catalyzed isomerization mechanisms have been observed. These are shown as paths b and c in Scheme 1-3. The iminium chloride, 51, isomerizes by the nucleophile catalysed path, b.¹⁸⁵ Radioactive chloride counterion exchanged with the chlorine in the molecule at a rate equal to one-half the rate of isomerization.



51

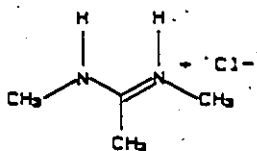
An acid catalysed isomerization path, c, has been observed in a cyanine salt, 52.¹⁸⁶ The site of protonation was not established, although exchange of the C₂ proton for deuterium was observed when deuterated acid solvent was used.



52

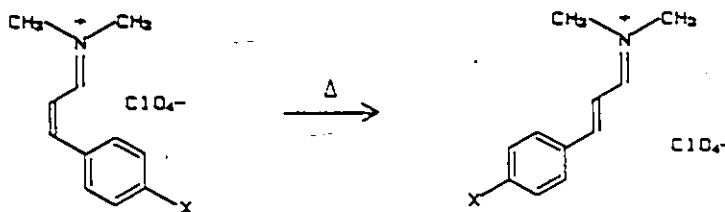
An amidinium salt, 53, also isomerizes in an acid

catalysed reaction. Protonation on the nitrogen was thought to be the most likely mechanism.¹⁸⁷



53

Iminium salts 30-34 contain Z C=C bonds conjugated to iminium groups, and isomerize about the C=C bonds by one of two mechanisms.¹⁵⁰ Electron-withdrawing substituents on the phenyl ring promote a nucleophile catalysed isomerization mechanism, and electron-donating groups induce an acid catalysed mechanism when the reaction takes place in a strong acid such as trifluoroacetic acid.

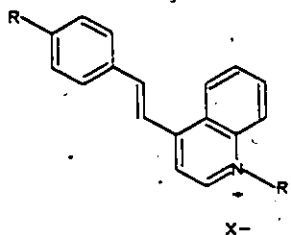


30 - 34

14 - 18

A mechanistic study of thermal C=C isomerization of the styrylquinolinium salt, 54, revealed that the isomerization rate did not depend on the nature of the counterion, but decreased with increasing solvent polarity.¹⁸⁸ Electron-withdrawing substituents on the phenyl ring increase the rate of isomerization, however replacing the counterion with a more nucleophilic one leaves the reaction rate virtually unchanged. The authors conclude that isomerization proceeds

by a rotation mechanism, but this is difficult to reconcile with the observed substituent effect.



54

In recent years, great progress has been made towards an understanding of the properties of the retinylidene-containing pigments, rhodopsin and bacteriorhodopsin, but questions about their chemistry still need to be answered. Although it has been established that the photocycles of these chromophores begin with a fast isomerization about a specific C=C double bond, it is not clear whether the protein surrounding the chromophore determines the reaction rate, or whether iminium salts in solution behave similarly. The proteins certainly influence the regioselectivity of the reaction, but this could be caused by an electronic interaction with a charged species in the protein, or a constraining influence on the geometry of the retinylidene chromophore determined by the three-dimensional structure of the protein. In addition, the mechanisms of thermal isomerization are not agreed upon, and are important in the chemistry of bacteriorhodopsin.

The photochemical isomerizations of simple iminium salts where more than one bond can isomerize have not been

examined in detail before. There are many properties of a molecule that can conceivably determine regioselectivity in a photoreaction, such as electronic or steric factors. In this thesis, the electronic properties of an α,β -unsaturated iminium salt were varied by changing the substituents on phenyl rings at either end of the molecule. The ground and excited state properties of these iminium salts are discussed in terms of the substituents, and the photoisomerization quantum yields of C=C and C=N isomerization were measured as a function of these substituents.

Two other reactions of these iminium salts were investigated: a photo-initiated electron transfer pathway for C=N isomerization, not previously observed in an iminium salt, and thermal isomerization.

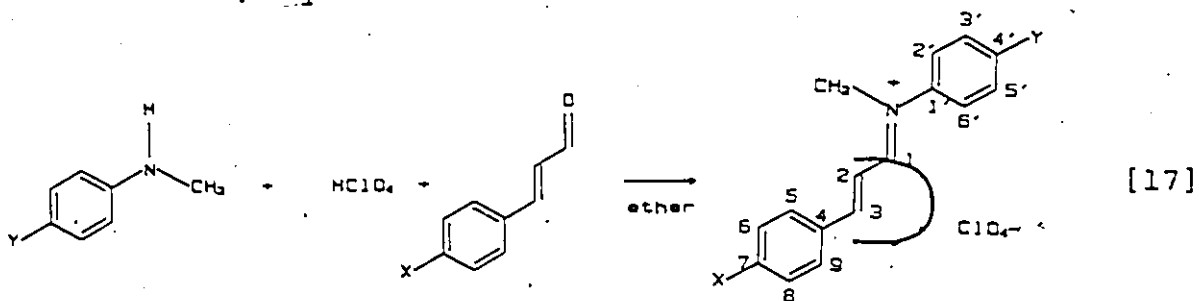
The mechanisms of thermal C=C isomerization in conjugated iminium salts had been studied previously. The thermal isomerization mechanisms about the C=N bond in α,β -unsaturated iminium salts are reported in this thesis.

RESULTS AND DISCUSSION

CHAPTER 2
SYNTHESIS AND STRUCTURE

I. Synthesis

The N-aryl, N-methyl 3-arylpropenylidene iminium perchlorate salts 55-63 were synthesized by combining N-methylaniline or para-substituted N-methylaniline, an equimolar amount of 70% perchloric acid and cinnamaldehyde, or its appropriate derivative, in ether. The product precipitated from solution, Equation 17.



	X	Y
55	NO ₂	H
56	Cl	H
57	H	H
58	CH ₃	H
59	OCH ₃	H
60	H	NO ₂
61	H	Cl
62	H	CH ₃
63	H	OCH ₃

A single product (>98% by ^1H NMR) was isolated as a coloured solid in each reaction. The salts 55-63 were characterized by their melting points, elemental analyses and infrared spectra, Table 2-1. Solutions of the salts in trifluoroacetic acid were analyzed by absorption spectroscopy, Table 2-2, ^1H NMR, Table 2-3, and ^{13}C NMR, Table 2-4.

The signals of the ^1H NMR spectra were assigned by comparison with spectra of 14-18^{149,150}, and by selective decoupling experiments. ^{13}C NMR signals were assigned by comparison to the spectra of 14-18, and by using calculated substituent parameters for the resonances of the aryl ring carbons.¹⁸⁹

The solids are unreactive to air or moisture in the air, insoluble in non-polar solvents and ethers, dichloromethane, and water. They dissolve readily in methanol, acetonitrile, nitromethane, sulfur dioxide, and strong acids such as trifluoroacetic acid. Traces of water in the aprotic solvents cause hydrolysis of the iminium salts.

II. Geometric Isomerization

In solution, a thermal reaction takes place to produce a mixture consisting of approximately equal amounts of the starting material and a product that was identified as a geometric isomer. This reaction is fast at room temperature in acetonitrile and nitromethane, but slow in trifluoroacetic acid. A solution left standing for several days at room

Table 2-1
Physical Data for Iminium Salts 55-63

Iminium Salt	M.W.	C=N stretch ^a (cm ⁻¹)	melting range (°C)	elemental analyses					
				found		calculated			
				%C	%H	%N	%C	%H	%N
55	366.76	1618	186-187	52.20	4.14		52.40	4.12	
56	356.21	1620	151-152	53.96	4.15	3.96	53.95	4.24	3.93
57	321.76	1628	185-185.5	59.82	5.01	4.17	59.73	5.01	4.35
58	335.79	1620	142.5-144	60.49	5.42		60.81	5.40	
59	351.79	1620	165-166	58.01	5.14		58.04	5.16	
60	366.76	1620	219-220	52.29	4.12		52.40	4.12	
61	356.21	1614	193-194.5	53.72	4.22		53.95	4.24	
62	335.79	1618	168-169.5	60.49	5.36		60.81	5.40	
63	351.79	1624	173.5-174.5	58.18	5.19	3.92	58.04	5.16	3.98

^aby FTIR, in KBr discs

Table 2-2
Absorption Data for Iminium Salts 55-63^a

Iminium Salt	λ_{\max} (nm)	log ϵ	$\Delta\nu_{1/2}$ (10^{-5}cm^{-1})
55	348	4.51	1.4
56	368	4.60	1.6
57	361	4.60	1.6
58	378	4.58	1.7
59	408	4.63	1.4
60	370	4.56	1.6
61	361	4.53	1.6
62	360	4.49	1.5
63	372	4.46	1.1

^ain trifluoroacetic acid

Table 2-3

 ^1H NMR Chemical Shift Data for Iminium Salts 55-63^{a,b}

Iminium Salt	H ₁	H ₂	H ₃	Aryl H	CH ₃	Other	J _{1,2} (Hz)	J _{2,3} (Hz)
55	8.59d	7.55dd	8.08d	8.17d, 7.89d, 7.4m	4.05s		10	15
56	8.42d	7.31dd	7.95d	7.62d, 7.47-7.33m	3.94s		11	15
57	8.42d	7.4 ^c	8.01d	7.70d, 7.45-7.30m	3.94s		11	15
58	8.35d	7.3 ^c	7.95d	7.58d, 7.46-7.31m, 7.22d	3.90s	2.29s	11	15
59	8.30d	7.16dd	7.92d	7.71d, 7.44-7.30m, 6.96d	3.87s	3.83s	11	15
60	8.60d	c	8.17d	8.30d, 7.74-7.36m	3.99s		11	15
61	8.42d	7.33dd	8.03d	7.69d, 7.53-7.28m	3.92s		11	15
62	8.39d	7.4 ^c	7.98d	7.68d, 7.50-7.26m	3.92s	2.29s	11	15
63	8.38d	7.31dd	7.98d	7.68d, 7.50-7.33m, 7.03d	3.92s	3.83s	11	15

^aIn ppm, referenced to N(CH₃)₄⁺BF₄⁻ at 3.10 ppm, in trifluoroacetic acid

^bs = singlet, d = doublet, dd = doublet of doublets, m = multiplet(s)

^cpeaks hidden

Table 2-4

 ^{13}C NMR Chemical Shift Data^a

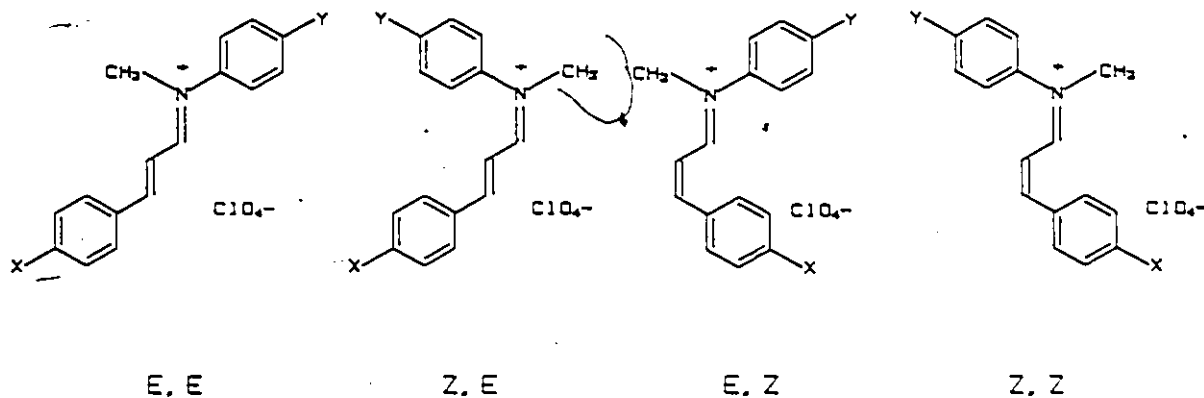
Iminium Salt	C ₁	C ₂	C ₃	C ₄	C _{5,9}	C _{6,8}	C ₇	C _{1'}	C _{2',6'}	C _{3',5'}	C _{4'}	$\overline{\text{CH}}_3$	Other
55	169.9	120.0	161.4	139.3	131.3	124.5	150.4	144.3	122.0	130.6	132.0	42.4	
56	169.6	116.4	164.8	131.9	132.0	130.1	142.6	144.5	122.1	130.6	131.5	41.8	
57	169.8	115.9	167.1	133.4	131.1	129.8	135.6	144.6	122.2	130.7	131.5	41.6	
58	169.3	114.7	167.2	131	131.4	130.6	148.9	144.6	122.1	130.6	131.3	41.4	20.6
59	168.6	113.4	166.3	127.3	134.2	115.7	166.1	144.7	122.1	130.6	131.1	41.1	55.4
60	171.4	115.9	170.3	133.5	131.8	129.9	136.6	148.8	124.3	126.2	149.3	41.6	
61	169.9	115.8	167.8	133.4	131.2	129.8	135.9	142.8	123.6	130.9	138.4	41.7	
62	168.9	115.7	166.2	133.2	130.9	129.5	135.3	143.0	121.5	130.7	142.0	41.3	19.3
63	168.0	115.9	166.3	133.5	130.9	129.7	135.4	138.3	123.9	116.1	161.3	41.7	55.6
56 ^b	171	119	163	131	131	131	139	144	124	131	131	41	

^ain ppm, referenced to $\overline{\text{CF}}_3\text{CO}_2\text{H}$ at 114.7 ppm, in trifluoroacetic acid or deuterated trifluoroacetic acid

^bsolid state CP/MAS ^{13}C NMR

temperature in trifluoroacetic acid contains only small amounts of the thermally produced isomer. Solutions of the iminium salts absorb light of 366 nm and react to produce mixtures of four compounds, one is the starting material, the others were shown to be geometric isomers by ^1H NMR. The thermally produced isomer was among these photoproducts.

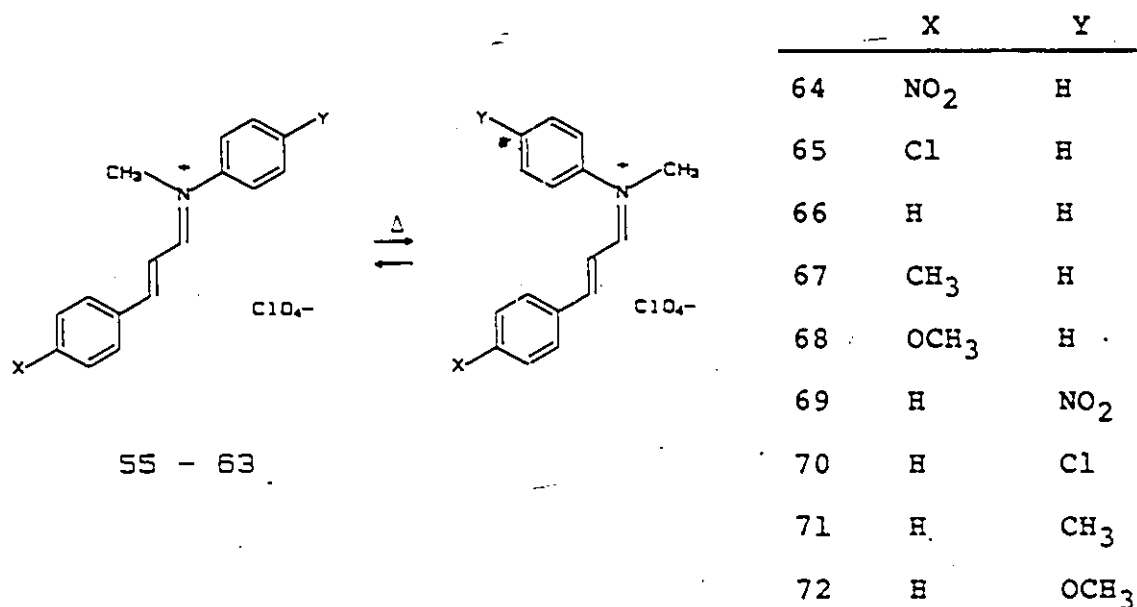
Four stereoisomers are possible in these iminium salts, produced by E-Z isomerization about the two double bonds.



^1H NMR spectra show that in each case only one ($>98\%$) of the isomers is formed by the synthesis described above, with $\leq 2\%$ of another isomer present in some cases. The major isomer was shown to be the E,E isomer by ^1H NMR spectroscopy and X-ray crystallography. The size of the coupling constant across the C=C bond, $J_{2,3}$, 15 Hz, fits an E double bond, as these are generally in the range 11-18 Hz, and Z isomers have coupling constants that are smaller.¹⁹⁰ The configuration about the C=N bond could not be determined in this way, so an X-ray crystallographic structure determination was used. It

was found that the C=N bond of 56 has an E configuration.¹⁹¹ It is assumed that the other salts are also E C=N isomers.

The ¹H NMR spectra of the thermally produced compounds are similar to those of the starting materials, Figure 2-1, Table 2-5. On the basis of the coupling constants $J_{2,3}$, the C=C bond is E as in the starting isomers, so the configuration of the C=N bond must be Z, 64-72.



The remaining stereoisomers could be generated photochemically, along with 64-72, from 55-63 respectively, and were characterized by their ¹H NMR spectra only, Figure 2-1. These two isomers have Z C=C bonds, $J_{2,3} = 11$ Hz, Table 2-6. It was assumed that only one of the two double bonds isomerizes on absorption of a photon,¹⁹² so the compounds that appear first in an irradiation of the E,E isomers 55-63 are the Z C=N, E C=C isomers, 64-72, and the E C=N, Z C=C isomers, 73-81. The remaining isomers, 82-90, are not present

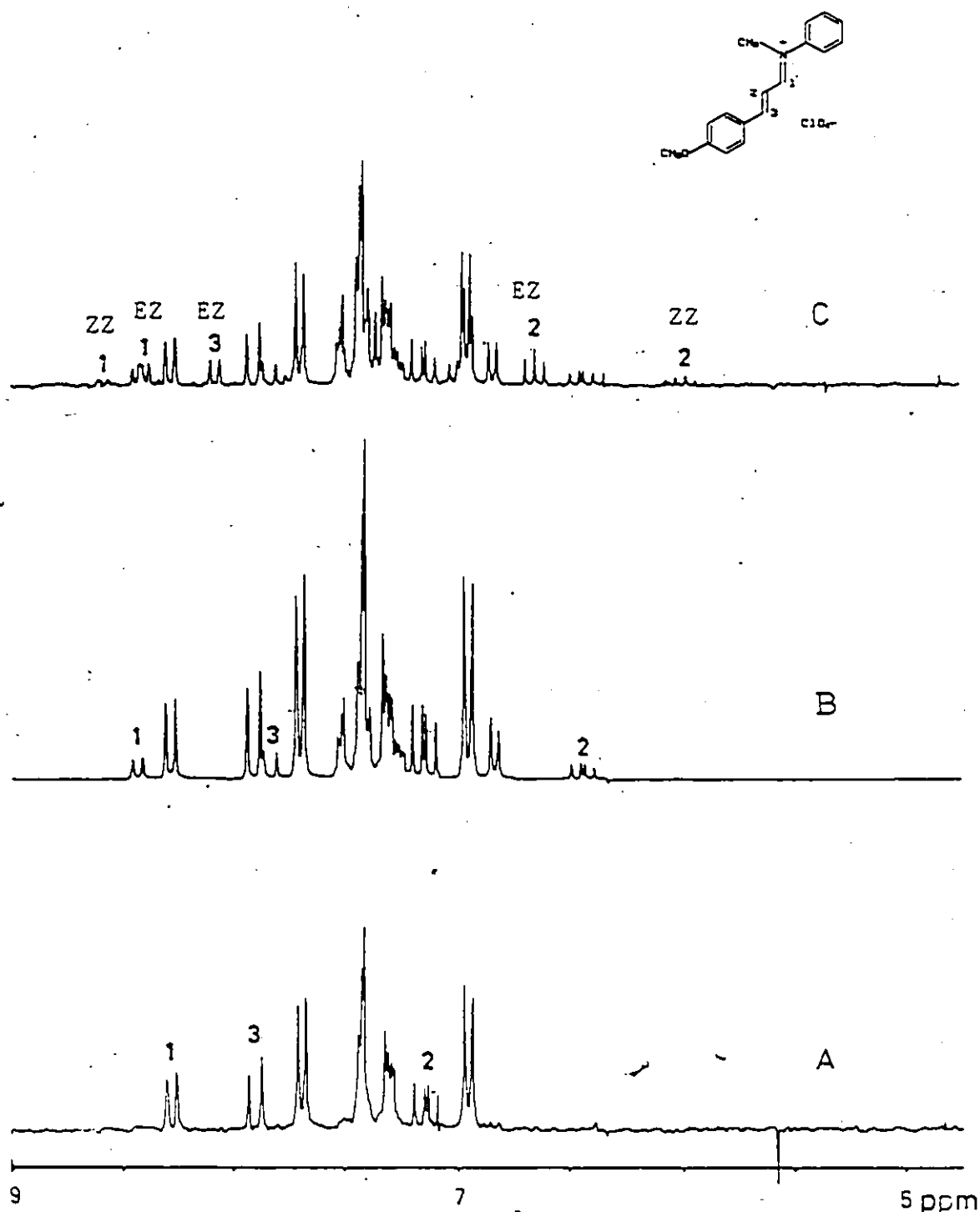


Figure 2-1 Vinyl Region of the ^1H NMR spectra of N-methyl, N-phenyl-3-(p-methoxyphenyl)-2-propenyldene iminium perchlorate, 59, in TFA (A) E,E isomer, (B) Z,E isomer in a thermally produced mixture, and (C) E,Z and Z,Z isomers in an irradiated mixture.

Table 2-5

¹H NMR Data for Iminium Salts 64-72^{a,b}

Iminium Salt	H ₁	H ₂	H ₃	Aryl H	CH ₃	Other	J _{1,2} (Hz)	J _{2,3} (Hz)
64	8.75d	6.74dd	8.01d	8.11d, 7.62-7.31m	3.98s		10	16
65	8.59d	6.55dd	7.88d	7.53m, 7.37-7.21m	3.90s		10	15
66	8.58d	6.60dd	7.92d	7.53m, 7.47-7.22m	3.90s		10	15
67	8.50d	6.53dd	7.87d	7.52m, 7.35-7.27m, 7.09d	3.86s	2.26s	11	15
68	8.45d	6.45dd	7.84d	7.53-7.24m, 6.84d	3.83 ^c	3.77s	11	15
69	8.69d	6.57dd	8.05d	8.43d, 7.64d, 7.45-7.25m	3.94s		11	16
70	8.59d	6.59dd	7.95d	7.53-7.23m	3.88s		11	15
71	8.54d	6.64dd	7.90d	7.50-7.15m	3.87s	2.33s	11	15
72	8.54d	6.65dd	7.91d	7.47-7.23m, 7.10d	3.87s	3.85s	10	16

^a in ppm, referenced to N(CH₃)₄⁺BF₄⁻ at 3.10 ppm, in trifluoroacetic acid

^b s = singlet, d = doublet, dd = doublet of doublets, m = multiplet(s)

^c peaks hidden

Table 2-6
¹H NMR Data for Iminium Salts 73-90^{a, b}

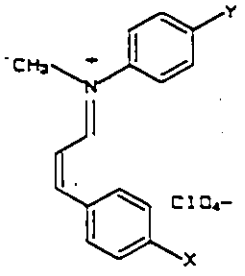
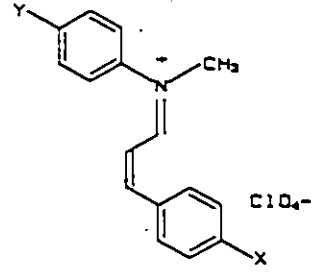
Iminium Salt	H ₁	H ₂	H ₃	CH ₃	Other	J _{1,2} (Hz)	J _{2,3} (Hz)
73	8.45d	7.08dd	<u>c</u>	4.05 ^c		11	11
82	8.52d	6.30dd	<u>c</u>	3.98 ^c		11	11
74	8.42 ^c	6.83dd	8.11d	3.97s		11	11
83	8.61d	6.11dd	7.77d	3.93s		11	11
75	8.45d	6.82dd	8.21d	3.97s		11	11
84	8.61d	6.12dd	7.87d	3.92s		11	11
76	8.44d	6.73dd	8.15d	3.93s	2.22s	11	11
85	8.61d	6.03dd	7.80d	3.90 ^c	2.29 ^c	11	11
77	8.40d	6.67dd	8.08d	3.91s	3.79s	11	11
86	8.59d	5.98dd	7.8 ^c	<u>c</u>	<u>c</u>	10	10
78	8.52d	6.90dd	<u>c</u>	4.02s		11	11
87	8.73d	6.10dd	7.98d	3.98s		11	11
79	8.43d	6.82dd	8.22d	3.95s		11	11
88	8.62d	6.11dd	7.89d	3.92s		11	11
80	8.43d	6.80dd	8.17d	3.95s	2.27s	11	11
89	8.58d	6.15dd	7.84d	3.90s	2.32s	11	11
81	8.39d	6.80dd	8.14d	3.95s	3.79s	11	11
90	8.57d	6.17dd	7.85d	3.89s	3.84s	11	11

^ain ppm, referenced to N(CH₃)₄⁺BF₄⁻ at 3.10 ppm, in trifluoroacetic acid

^bs = singlet, d = doublet, dd = doublet of doublets, m = multiplet(s)

^cpeaks hidden

in the irradiated mixture until more than ten percent of the starting isomer has reacted (with one exception, 60). These are secondary photoproducts and must have the Z,Z configuration. The distinguishable resonances of the ^1H NMR spectra of the isomers 64-90 are given in Tables 2-5 and 2-6.

	X	Y
		
73 - 81		
		
82 - 90		
	73, 82	NO ₂ H
	74, 83	Cl H
	75, 84	H H
	76, 85	CH ₃ H
	77, 86	OCH ₃ H
	78, 87	H NO ₂
	79, 88	H Cl
	80, 89	H CH ₃
	81, 90	H OCH₃

If any of these iminium salts is allowed to crystallize from a solution containing the E,E and Z,E isomers, the crystals isolated are only E,E, and the solution does not contain increased concentrations of the Z,E isomer. This phenomenon has been observed previously,¹⁹³ and was called "diastereomeric transformation".

Separation of C=N Isomers

Several attempts were made to separate the isomers by column or thin-layer chromatography. When the packing materials (alumina or silica) and eluting solvents were carefully dried, hydrolysis could be minimized, but no degree of

separation of the isomers was ever achieved. This is attributed to fast isomerization about the C=N bond in either the eluting solvents or on the solid supports used. Selective crystallization as a separation technique was also unsuccessful because of the isomerization that occurs on crystallization.

III. Structures of the E,E Iminium Salts

The X-ray crystal structure of 56 shows that the molecule adopts an s-trans configuration about the C₁, C₂ single bond in the solid state. The relative energies of the s-cis and s-trans conformers are thought to be similar,^{149,151} so it is possible that in solution an equilibrium exists between the conformers. If so, the conformers must be rapidly interconverting at room temperature, as no evidence for two species was observed by NMR spectroscopy. A solid state CP/MAS ¹³C NMR spectrum of the salt 56 can be compared to the solution ¹³C NMR spectrum, Figure 2-2, Table 2-4. The two spectra are remarkably similar, suggesting that the conformation and structure of the molecule in solution is the same as observed in the solid state.

Charge Distribution

In order to understand the reactions of these iminium salts, some knowledge of their ground state structures is necessary. The structure determination of salt 56 by X-ray crystallography (solved by G.S. Shaw, McMaster University)

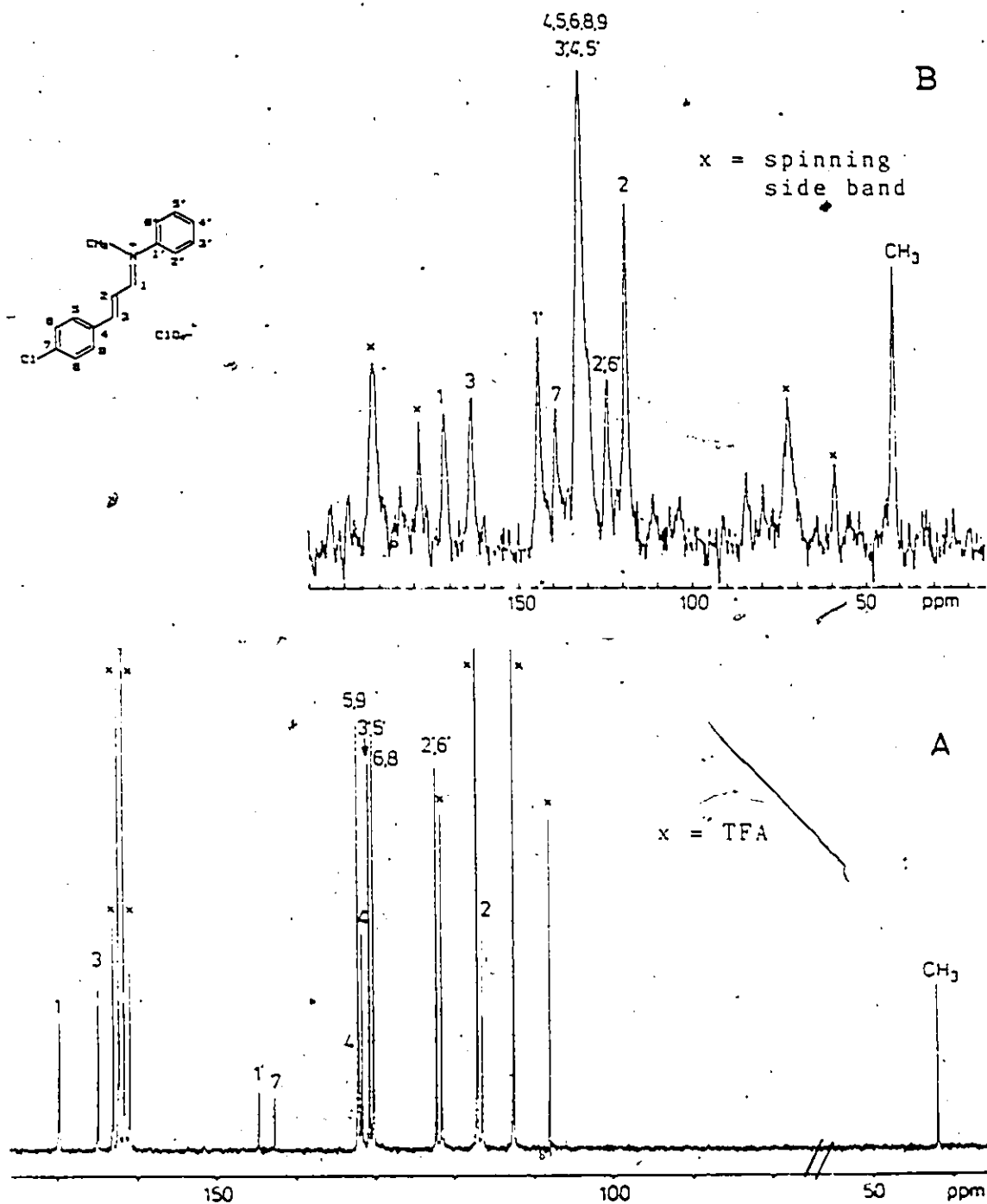
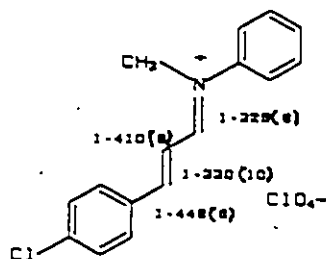


Figure 2-2 ^{13}C NMR spectra of N-methyl, N-phenyl-3-(p-chlorophenyl)-2-propenylidene iminium perchlorate, 56 (A) TFA solution, and (B) solid state

can be used to determine the extent of charge delocalization in the molecule. Analysis of the bond lengths found in the crystal structure indicate that the positive charge of the molecule is not delocalized farther than C_1 .¹⁹¹



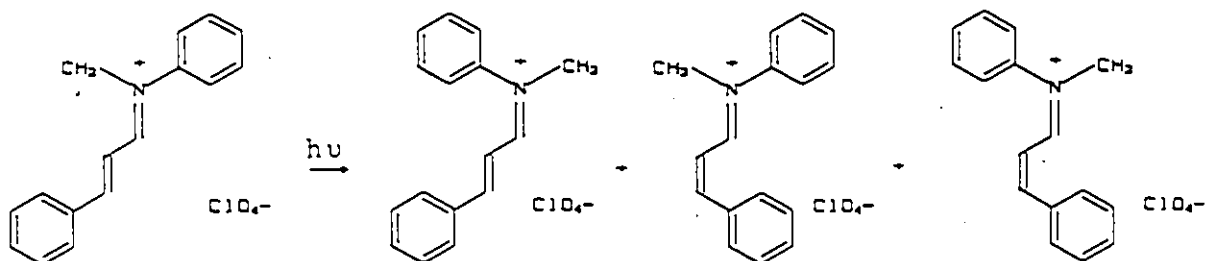
55

Solvent Effects

It is difficult to predict the effect that solvents will have on the ground state structures. The similarity of the solid state and trifluoroacetic acid solution ¹³C NMR spectra suggest that there are no major solvent effects on the ground state. The effect of solvation of the counterion on the spectrum is not known, however.

CHAPTER 3
PHOTOCHEMISTRY

The iminium salts 55-63 isomerize about the C=C and C=N bonds on absorption of light. Various excited state processes of these molecules were examined--the absorption and emission of light, photoisomerization, and intersystem crossing from the excited singlet to a triplet state. The results, together with experimental and theoretical information in the literature, are used to attempt to describe the nature of the excited state that leads to isomerization in the conjugated iminium salts.



I. Absorption and Emission Studies

The absorption spectra of the iminium salts 55-63 were obtained in trifluoroacetic acid. Each of the iminium salts 55-63 has an intense long wavelength $\pi \rightarrow \pi^*$ absorption band extending into the visible region, Table 2-2. The extinction coefficients of the absorption bands are large,

$\geq 10^4$, the bands are broad and have no vibrational structure, as is shown for salt 57 in Figure 3-1.

After recording spectra of the E,E isomers, 55-63, the solutions were irradiated to produce mixtures of isomers. In all cases, the absorption decreased in intensity, indicating that the Z isomers, E,Z, Z,E, or Z,Z, absorb with smaller extinction coefficients than the E,E isomers. This has also been observed with other iminium ions.¹⁴⁴ The isomers could not be separated, so individual absorption spectra could not be measured.

Fluorescence was not observed in acetonitrile solutions of iminium salts 55-63 at room temperature. The quantum yield of fluorescence for these salts can be estimated as $<10^{-4}$. Salt 57 was dissolved in a mixture of sulfuric acid, trifluoroacetic acid and acetic acid (2:2:1), which forms a glass at 77K. Luminescence was not observed under these conditions, possibly because of experimental difficulties. Some closely related iminium salts have been reported to luminesce in powder form.¹⁹⁴

The absorption of light by a molecule leads to the creation of an excited singlet state, S_1 . In the ground state, a molecule in solution is normally in its lowest vibrational level, but on excitation, one of many vibrational levels of S_1 can be reached. For a non-rigid molecule in solution, these vibrational levels are often close together, so that the many transitions observed appear as a continuum,

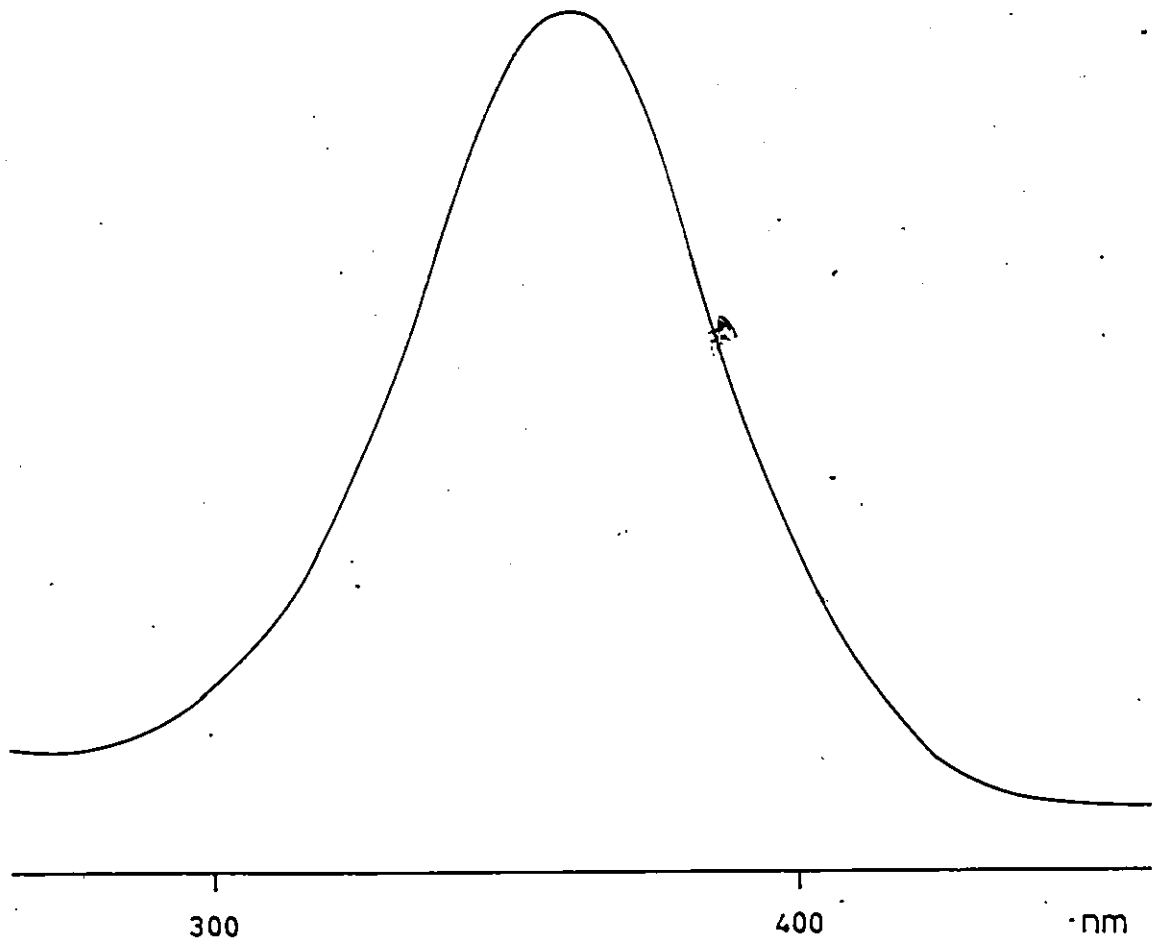
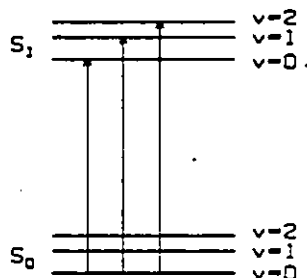


Figure 3-1 Absorption Spectrum of N-methyl, N-phenyl-3-phenyl-2-propenylidene iminium perchlorate, 57, in TFA.

and the spectra are broad and featureless as observed for the iminium ions 55-63.



The λ_{\max} of the absorption band corresponds to the most probable transition, often to a vibrationally excited level of S_1 . The size of the extinction coefficient at the maximum (ϵ_{\max}) is a measure of the strength or probability of this transition. The large extinction coefficients of the absorption spectra of salts 55-63 indicate that the transition from ground to excited state is a formally spin-allowed and electronically-allowed process.¹⁹⁵

The vibrationally excited molecules are thought to decay to the lowest vibrational level of S_1 before further excited state processes take place, so it is desirable to know the energy of this level. The energy difference between the lowest vibrational level of the ground state and the lowest vibrational level of the excited state is $E_{0,0}$. This corresponds to the energy at the origin, the highest energy vibrational band, of the fluorescence spectrum. The origin can also be approximated by the onset of fluorescence in a broad spectrum, or by the lowest energy absorption band in a

structured absorption spectrum.¹⁹⁶ Since fluorescence was not observed for the iminium salts 55-63 and the absorption spectrum is unstructured, assignment of the 0,0 band is not possible. Rather than using $E_{0,0}$ to determine the excited-state energy levels, the trends observed in the absorption maxima of these compounds will be assumed to reflect changes in the energy level of S_1 .

Structure of the Excited State

The ground state structures of the iminium salts 55-63 have been discussed in Chapter 2. The positive charge of the ion is mostly localized at the iminium group. The structure of the related iminium salt 16 is not affected by an electron-donating substituent on the C_3 phenyl ring (see Chapter 1). This is assumed to hold true for the salts 55-63 as well. However, the absorption maxima depend strongly on substituent. Salt 59, with a positive charge stabilizing methoxy group on the C_3 phenyl ring, is a red solid and forms a red solution in trifluoroacetic acid. Its absorption maximum is 408 nm, the lowest energy transition of the series. Salt 55 has an electron withdrawing substituent on the C_3 phenyl ring which would destabilize a positive charge. This iminium salt is yellow, and its absorption maximum is at higher energy, 348 nm. Since the ground state structures, and presumably also the ground state energy levels, are unaffected by substituents, the observations are consistent with a shift of the positive charge toward the C_3 aryl ring

in the Franck-Condon state. This positive charge is stabilized by the electron-donating methoxy group and destabilized by the nitro substituent. The initially-formed excited state can be represented as a combination of resonance forms with varying degrees of positive charge migration towards the C₃ phenyl ring. The extent of charge delocalization is not known, and might vary with substituent.

Substituents on the nitrogen aryl ring have little effect on the absorption maxima. The N-phenyl ring may be twisted out of the plane of the π system, and so conjugative effects are not observed.

Similar correlations between absorption maxima and substituent can be made for the iminium salts, 14-18,¹⁵⁰ the styrylpyridinium salts, 38-43,¹⁶⁸ and the tetraphenylethylenes, 91-94,¹⁹⁷ Table 3-1.

The Franck-Condon principle states that the geometry of the excited state reached on absorption of a photon is the same as the ground state geometry of the molecule. Absorption of a photon takes place in about one femtosecond (10^{-15} s). Vibrations of organic molecules take a relatively long time on this scale (10^{-13} s for a C-H stretch and 10^{-12} s for a C-C bend), so the molecule has no time for vibrational relaxation within the absorption process. Electron movement is much faster than nuclear motion (10^{-15} s), therefore changes in the molecule must correspond to changes in electron configuration. The absorption spectrum then reflects differences

Table 3-1

Absorption Maxima as a Function of Substituent

Compound	Substituent X	λ_{\max} (nm)	Reference
55 ^a	NO ₂	348	this work
57 ^a	H	361	" "
59 ^a	OCH ₃	408	" "
14 ^a	NO ₂	323	150
16 ^a	H	341	"
18 ^a	OCH ₃	384	"
42 ^b	NO ₂	345	168
38 ^b	H	358	"
41 ^b	OCH ₃	404	"
43 ^b	N(CH ₃) ₂	512	"
91 ^c	H	306	197
92 ^c	OCH ₃	318	"
93 ^c	CN	326	"
94 ^c	X=OCH ₃ , Y=CN	353	"

^ain trifluoroacetic acid

^bin dichloromethane

^cin 95% ethanol

in electron distribution between the ground and excited states.

The substituent effects observed on the absorption maxima of the iminium salts 55-63 indicate that the structures of the initially formed excited states, identical in geometry to those of the ground states by the Franck-Condon principle, have decreased electron density in the C₃-phenyl to C₁ regions of the molecules.

Absorption of light by the retinylidene-iminium salts results in a similar charge migration. This was predicted from theoretical calculations,^{96,97} and has been experimentally verified by measuring the change in dipole moment of the molecule on excitation.^{116,117} The dipole moment of the excited state is much larger than that of the ground state, indicating that charge separation has occurred. In the ground state the positive charge is close to a negative counterion. On excitation, the dipole moment increases when the positive charge moves away from the counterion, into the polyene chain.

Lifetime of the Excited State

The lifetime of an excited state can be measured in several ways. A direct measurement of the fluorescence decay gives the most accurate excited state lifetime. When this information is not available, a decay rate can be calculated from the fluorescence and absorption spectra.¹⁹⁸ In addition, the absorption spectrum can give an estimate of the

fluorescence decay rate, assuming it is the only pathway for excited state deactivation, using the relationship in Equation 18.¹⁹⁹

$$k_e = 3 \times 10^{-9} \nu_0^2 \epsilon_{\max} \Delta\nu_{1/2} \quad [18]$$

k_e = rate constant for emission (s^{-1})

ν_0 = absorbance maximum (cm^{-1})

ϵ_{\max} = extinction coefficient at the absorbance maximum

$\Delta\nu_{1/2}$ = width of absorbance band at half height (cm^{-1})

The lifetime of the excited state is the inverse of the rate constant for emission, k_e^{-1} .

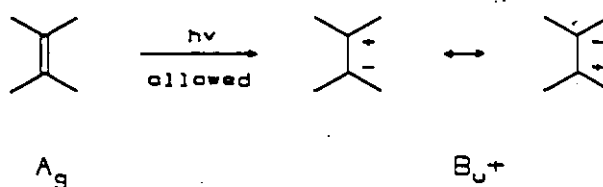
The lifetimes of the excited states of the iminium salts 55-63 calculated using Equation 18 are about 10^{-11} s. Since fluorescence is not observed in these iminium salts, a non-radiative competing process must occur in less than 10^{-11} s.

Excited state lifetimes of other iminium salts have been reported in the nanosecond range at 77K¹⁴⁴, and a more recent report found that the retinylidene iminium salt has an excited state lifetime of $<10^{-11}$ s at room temperature.¹⁴⁶

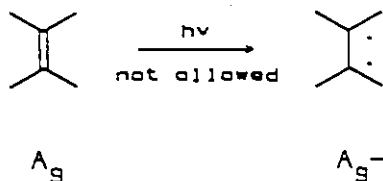
Planar Excited States of Alkenes, Polyenes and Iminium Ions

The excited states of conjugated iminium ions have been described in the literature in terms of valence bond theory derived for the isoelectronic linear polyenes. The symmetry properties of the polyenes are used to generate descriptions of the ground and excited states.²⁰⁰ The lowest

energy ground state of a linear polyene of C_{2h} symmetry is a singlet state, 1A_g . The two singlet excited states, which differ from the ground state only in electron distribution, are described as ${}^1B_u^+$ and ${}^1A_g^-$. The ${}^1B_u^+$ state is of ionic character, although the state has a permanent dipole only if some dissymmetry exists in the molecule.



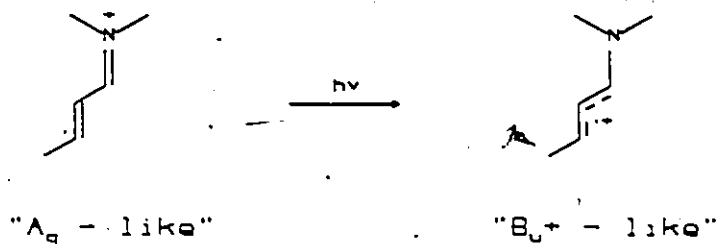
The transition from the 1A_g ground state to the ${}^1B_u^+$ excited state is allowed. This is seen experimentally as an absorption band with large extinction coefficient at the maximum. The ${}^1A_g^-$ state is neutral in character, and the transition to it is not formally allowed.



Absorption in linear polyenes is normally strong, indicating that an allowed 1A_g to ${}^1B_u^+$ transition is observed. This does not necessarily mean that the ${}^1B_u^+$ state is of lower energy than the ${}^1A_g^-$ state. In fact, longer chain polyenes such as diphenylhexatrienes are thought to have lower energy ${}^1A_g^-$ states, while in molecules such as stilbene and diphenylbutadiene the ordering of excited

states is reversed.

Replacing a carbon of a polyene with a nitrogen to form an iminium ion reduces the symmetry of the system. This in turn changes the properties of the excited states. Nevertheless, analyses in the literature have based their arguments on the linear polyenes, assigning " A_g^- -like" and " B_u^+ -like" states.²⁰⁰ The allowed transition, the one causing strong absorption, is to the ionic ${}^1B_u^+$ -like state. Because of the greater electronegativity of the iminium nitrogen versus carbon, this is a state with a permanent dipole.



The strong absorption bands of iminium salts 55-63 are in agreement with an allowed ${}^1A_g^-$ to ${}^1B_u^+$ -like transition. The substituent effects on the absorption spectrum also support the assignment of an ionic excited state. However, it is important to remember that the reduced symmetry in the molecules is expected to result in increased mixing between the A_g^- and B_u^+ states, so that the properties of each are not purely "ionic" or "covalent".

The state reached on absorption is not necessarily the state from which fluorescence or other photoprocesses take place.. If the ${}^1A_g^-$ state lies below the ${}^1B_u^+$ excited

state, the former state can be reached before further reactions occur. The state where fluorescence initiates can be observed experimentally in several ways. If the excited molecule internally converts to a lower energy excited state, and fluoresces from the latter state, then the 0,0 band of the fluorescence spectrum will be separated from the 0,0 band of the absorption spectrum by an energy difference equal to the energy difference between the initially formed excited state and the fluorescing state. If the fluorescing state is $^1A_g^-$, then the transition to the ground state is not a formally allowed process. The lifetime of fluorescence is then longer than that calculated from the absorption and fluorescence spectra.^{198,201} Two-photon spectroscopy can be used to detect directly the $^1A_g^-$ state. In this technique, absorption between 1A_g states is allowed.²⁰⁰

Stilbene and diphenylbutadiene show behaviour attributed to absorption and fluorescence from the same state, the $^1B_u^+$ state. Longer polyenes, such as diphenylhexatriene fluoresce from the $^1A_g^-$ state.

Little information exists about the fluorescing state of iminium ions. One difficulty is their broad absorption and emission spectra which makes assignment of the 0,0 band difficult. An exception is the iminium ion of decapental, for which structured emission can be observed at 77K. The fluorescence spectrum is separated from the absorption spectrum, and the measured fluorescence lifetime is longer than

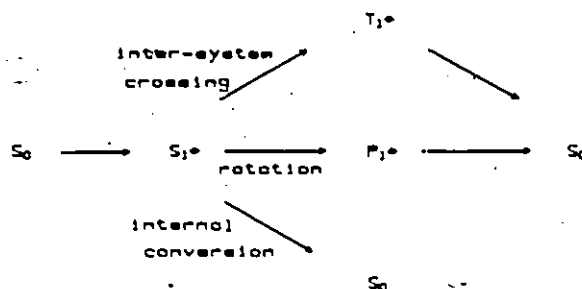
that calculated from the absorbance and emission spectra, indicating that emission originates from the ${}^1A_g^-$ state.²⁰¹

Retinylidene iminium ions have broad fluorescence spectra even at low temperature, so a similar analysis is not possible. However, the ${}^1A_g^-$ state was found by two-photon spectroscopy, and lies above the ${}^1B_u^+$ state, although the separation is small.²⁰² Similar results were obtained for a rhodopsin analogue containing an 11-cis constrained retinal chromophore.²⁰³

The studies of these conjugated iminium salts agree that the ${}^1A_g^+$ and ${}^1B_u^-$ states are close together, although the ordering is reversed for the decapentenylidene iminium ion, suggesting that in iminium salts, significant mixing between the states influences the character of the excited state. It is important to bear in mind that, although the absorption spectra indicate an ionic excited state for the iminium salts 55-63, the fluorescence studies of other molecules indicate that a covalent state may be reached before further photoprocesses take place. The states discussed so far are thought to be planar, although some geometric relaxation will have taken place after the Franck-Condon state was reached.

In the conjugated iminium salts studied to date, a rapid radiationless process deactivates the planar excited state at room temperature. Processes that might compete with fluorescence in these molecules are twisting about a double

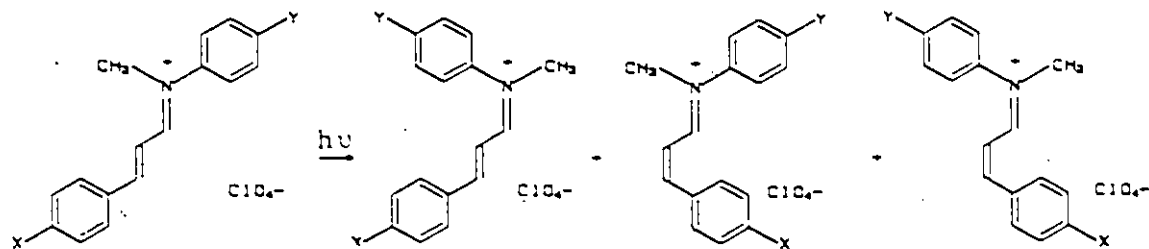
bond, intersystem crossing, or internal conversion.



S = singlet
T = triplet
P = perpendicular

II. Photochemical E-Z Isomerization

Iminium salts 55-63 in solution isomerize on irradiation about both the C=C and C=N bonds. On prolonged irradiation of the E,E isomer of each salt, mixtures containing the four possible stereoisomers are obtained.



55 - 63

64 - 72

73 - 81

82 - 90

Compound

X

Y

55, 64, 73, 82	NO ₂	H
56, 65, 74, 83	Cl	H
57, 66, 75, 84	H	H
58, 67, 76, 85	CH ₃	H
59, 68, 77, 86	OCH ₃	H
60, 69, 78, 87	H	NO ₂
61, 70, 79, 88	H	Cl
62, 71, 80, 89	H	CH ₃
63, 72, 81, 90	H	OCH ₃

The products were identified by ^1H NMR, Chapter 2. Chemical shifts are given in Tables 2-3, 2-5 and 2-6. No products other than the geometric isomers were formed in the irradiation in amounts detectable by NMR. The solvent used in these experiments is trifluoroacetic acid, chosen because thermal isomerizations are slow in this medium.

Quantum Yields

At low conversions, <10%, it was observed that the E,E isomers convert only to the E,Z and Z,E isomers, with the exception of salt 60. In this case, the Z,Z isomer is formed earlier in the irradiation. This isomer could still be a secondary product, however frequent stirring during the irradiation to ensure that local concentrations of E,Z or Z,E isomers were low did not affect the formation of the Z,Z isomer.

Quantum yields of the photoisomerizations of iminium salts 55-63 were measured using an optical bench, and are given in Table 3-2. A silicon photodetector with digital output was calibrated by ferrioxalate actinometry and used to quantitate the light absorbed by the solution. Relative isomer concentrations were determined by 250 MHz ^1H NMR analysis.

Thermal controls showed that small amounts of isomers 64-72 were present before irradiation, and, with the exception of 68, these did not increase under the conditions of the experiment and analyses. The quantum yields given are

Table 3-2
Quantum Yields of Photoisomerization^{a,b,c}

Iminium Salt	ϕ_{CN}	ϕ_{CC}	$\phi_{\text{CC+CN}}$	$\phi_{\text{CN}}/\phi_{\text{CC}}$	$\phi_{\text{CN}} + \phi_{\text{CC}}$
55	0.31 ± 0.04	< 0.05			0.31 ± 0.04
56	0.19 ± 0.02	0.18 ± 0.01		1.1	0.37 ± 0.03
57	0.20 ± 0.01	0.26 ± 0.03		0.8	0.46 ± 0.04
58	0.14 ± 0.02	0.17 ± 0.01		0.8	0.31 ± 0.05
59	$0.25 \pm 0.03^{\text{d}}$	0.11 ± 0.01		2.3^{d}	
60	0.19 ± 0.01	0.22 ± 0.03	0.13 ± 0.05		
61	0.15 ± 0.02	0.16 ± 0.02		0.9	0.31 ± 0.04
62	0.23 ± 0.05	0.18 ± 0.03		1.3	0.41 ± 0.08
63	0.17 ± 0.01	0.12 ± 0.02		1.5	0.29 ± 0.03

^a0.04M - 0.08M iminium salt in trifluoroacetic acid

^bmeasured relative to the photodecomposition of potassium ferrioxalate at 366 nm

^cerrors are standard deviations of at least 3 runs

^dincludes some thermal isomerization

corrected for these isomers, to the detection limit of about 0.5%.

In the case of salt 59, some thermal isomerization during the experiment accounts for the high quantum yield of C=N isomerization. This can be seen by comparison to a measurement in the weaker acid medium, 0.01 M sodium trifluoroacetate in trifluoroacetic acid, in which thermal isomerization is expected to be slower (see Chapter 5), Table 3-3.

Concentration Effects

The quantum yields were measured over a small concentration range. The lowest concentration, about 0.04 M, was the practical limit for the analysis method used. The quantum yields were not affected by doubling the concentration of the samples, indicating that bimolecular effects are not important in the photoreaction.

Effect of Dissolved Oxygen

Preliminary experiments showed that the quantum yields were not affected by degassing the samples before irradiation. Triplet states formed in a photoreaction can be quenched by dissolved oxygen. This is often used to determine the multiplicity of an excited state reaction, since quenching of a reaction should change the quantum yields measured. In these experiments the result is ambiguous because the concentration of dissolved oxygen in trifluoroacetic acid (about 2×10^{-3} M) is small relative to

Table 3-3

Medium Effects on Photoisomerization Quantum Yields^{a,b}

Iminium Salt	Solvent	ϕ_{CN}	ϕ_{CC}
55	0.01M sodium trifluoroacetate in TFA	0.30 \pm 0.05	-
55	0.1M sodium trifluoroacetate in TFA	0.34	-
55	0.1M (CH ₃) ₄ NCl in TFA	0.28	-
59	0.01M sodium trifluoroacetate in TFA	0.13	0.13
59	0.03M H ₂ SO ₄ in TFA	0.15	0.12

^arelative to the photodecomposition of potassium ferrioxalate, measured at 366 nm

^bestimated error \pm 10%

the concentration of reactant and therefore quenching, if occurring, would be insignificant.

Medium Effects on Photochemistry

It is important for the interpretation of the results of these experiments to know that only simple E-Z isomerization reactions were observed, and that constituents of the medium do not play a role in determining product ratios. In the ground state, slow isomerization by nucleophile addition or protonation can be observed (Chapter 5). The electronic changes in the excited state could increase the rate of one or both of these reactions. For salt 55, the effect of increased concentrations of nucleophiles on the quantum yield was measured. Solutions that were 0.1 M in sodium trifluoroacetate or tetramethyl ammonium chloride had no significant effect on the quantum yields of isomerization outside experimental error, Table 3-3. Likewise, increased or decreased acidity of the medium had no effect on the quantum yields of isomerization of iminium salt 59. It was thus established that the photoisomerization is a unimolecular excited state process.

Photostationary States

Solutions of the salts 55-63 were irradiated in a Rayonet photoreactor with 350 nm lamps for periods of time greater than 36 hours. The mixtures were analyzed by ^1H NMR, and their compositions are given in Table 3-4.

Table 3-4
Photostationary State Compositions^{a,b,c}

Iminium Salt	%E,E	%Z,E	%E,Z	%Z,Z
55	25	56	9	10
56	40	25	23	12
57	37	26	24	13
58	42	20	27	11
59	54	16	22	8
60	37	24	27	12
61	38	26	24	12
62	43	26	21	12
63	48	25	19	8

^adetermined by ¹H NMR

^bsolutions in TFA, irradiated at 350 nm for 36 hours

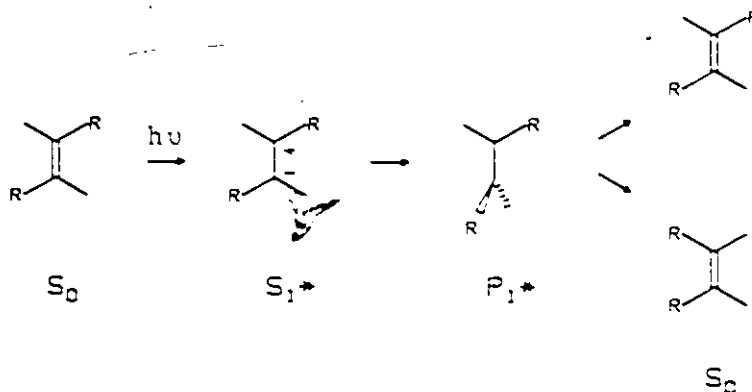
^cestimated errors ±10%

Photoisomerization Energy Surface

The photoisomerizations of iminium salts 55-63 were examined in an attempt to understand the factors that can affect the regioselectivity of photoisomerization of iminium ions.

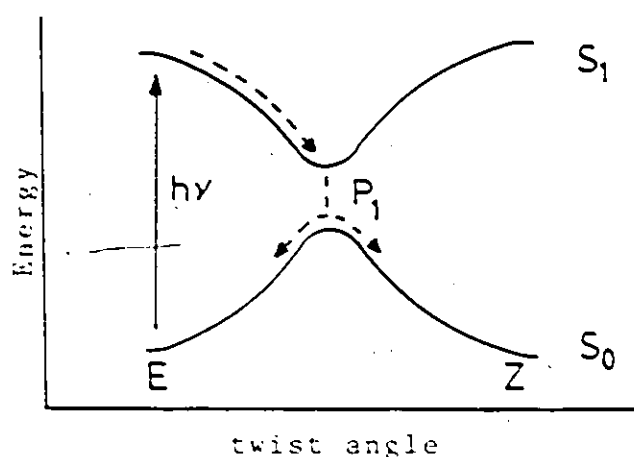
The iminium salts 55-63 isomerize from the E,E configuration with total quantum yields of 0.3 to 0.5, as given in Table 3-2. The quantum yields for the reverse processes, E,Z to E,E or Z,E to E,E, could not be measured because the E,Z and Z,E isomers could not be obtained in pure form.

The planar excited states of chromophores containing a double bond, either C=C or C=N, can relax by twisting about the double bond, a process facilitated by the electron rearrangement that occurs on light absorption.



Calculations have shown that the 90° twisted

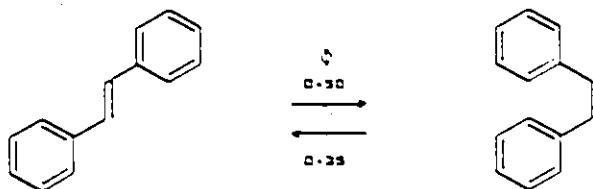
structure, P_1^* , is the lowest energy excited state configuration of polyenes¹⁵² and of molecules containing double bonds conjugated to iminium functional groups.^{96,97,204,205} The energy minimum in S_1 coincides with an energy maximum in the ground state, and as a result the S_1 and S_0 energy surfaces are close together at the perpendicular state. This creates a funnel for excited state processes, in which radiationless crossing to the ground state is faster than escape from the energy minimum.²⁰⁶



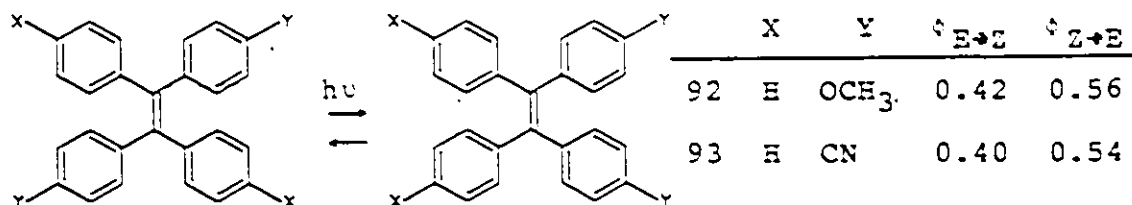
According to the model, the product ratio is determined on the ground state energy surface. For most molecules the distribution is expected to be statistical. 50% of the excited molecules decay to the starting isomer, and 50% form the opposite isomer. Since the formation of starting material cannot be detected, the quantum yield of isomerization, in the absence of other excited state processes, should be

0.5.²⁰⁷ Likewise, the quantum yield for the back reaction should also be 0.5. Only a few examples have appeared in the literature where isomerization quantum yields for both the forward and back reactions have been measured in molecules with only one isomerizable double bond. In the examples described below, the quantum yields for the forward and reverse isomerizations deviate somewhat from the expected values of 0.50.

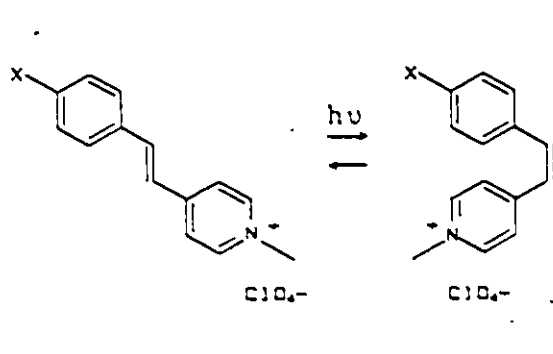
E-stilbene isomerizes to Z-stilbene with a quantum yield of 0.50. The reverse isomerization yield is 0.35.²⁰⁸



The tetraphenylethylenes, 92 and 93, isomerize about the C=C bond with approximately equal probability from either the Z or E isomers.¹⁹⁷



Similar results were found for the styrylpyridinium salts, 38-41.¹⁶⁸



	X	$\phi_{E \rightarrow Z}$	$\phi_{Z \rightarrow E}$	solvent
39	CN	0.5		CH ₂ Cl ₂
38	H	0.5		CH ₂ Cl ₂
38	H	0.5	0.4	CH ₃ CN
40	CH ₃	0.4		CH ₂ Cl ₂
41	OCH ₃	0.5		CH ₂ Cl ₂

In these examples, fluorescence is inefficient, $\phi_f \leq 0.05$.

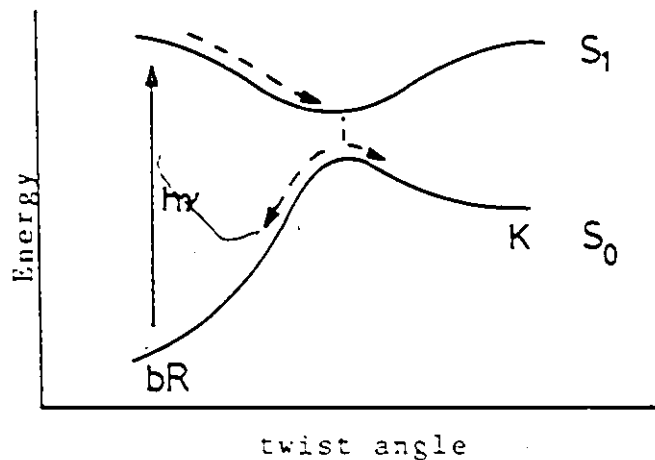
The equal distribution of isomers at the perpendicular state might be perturbed in highly unsymmetrical molecules, or in cases where the excited state decays before thermal equilibration.^{207,97,209} It is also possible that energy barriers on the ground state surface influence the product formation.

Systems where two or more bonds can isomerize have not been thoroughly examined. The assumption has been made in analyzing the results in this thesis, that the excited state decays with equal probability to starting isomer or to product isomer. Since two products are possible, the sum of the quantum yields, $\phi_{CX} + \phi_{CC}$, should equal 0.5. In some cases, the total quantum yield for disappearance of the E,E isomer is considerably less than 0.5, as in salts 55, 59, and 63. It is not certain whether this indicates that the above assumption is not correct, or whether some undetectable process is deactivating the excited state. The latter

possibility is discussed below.

Rhodopsin and bacteriorhodopsin, although multi-double bonded molecules, isomerize about only one C=C bond. Rhodopsin isomerizes about the C₁₁,C₁₂ bond with a quantum yield of 0.67, higher than the expected yield of 0.5.²⁸

Bacteriorhodopsin isomerizes about the C₁₃,C₁₄ double bond to form the intermediate K with a lower quantum yield, 0.33, but the reverse reaction is considerably more efficient, $\phi=0.67$.^{63,64} This does not agree with the prediction that forward and backward isomerization quantum yields should be the same. One major difference between these isomerizations and those of polyenes in solution is that the products, bathorhodopsin and K, are considerably higher in energy than the starting isomers. The product ratios may be disturbed if the steepness of the descent on the ground state surface plays a role in determining product formation.²⁰⁶



The bacteriorhodopsin quantum yields can be explained

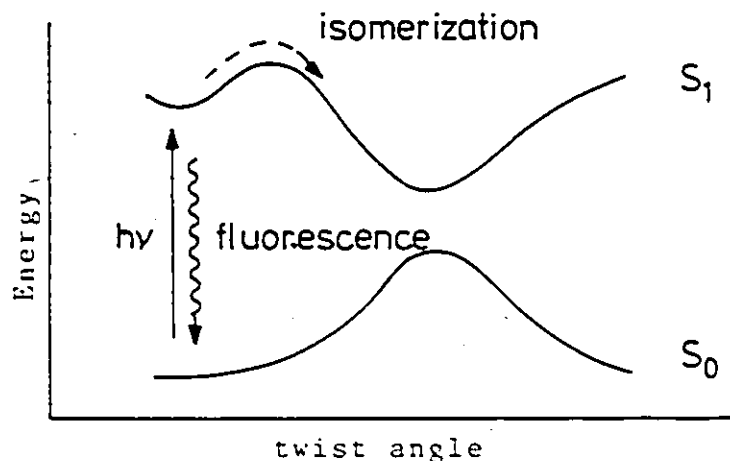
in this way, but not the rhodopsin photoisomerization. Theoretical calculations of the trajectory a molecule such as rhodopsin would follow in the excited state have suggested that the high quantum yield can be explained by assuming that the molecule does not equilibrate in the twisted excited state, but crosses to the ground state at a geometry that favours product formation, rather than return to its initial geometry.^{97,209} Another possibility is that the energy surface is perturbed by the protein environment. Since little is known about the energy surface in the vicinity of the 90° twisted state in either the ground or excited states, conclusions cannot be reached at this time.

Energy Barriers on Excited State Surfaces

The presence of energy barriers on excited state energy surfaces would cause competition to take place between various processes, such as competition between a photophysical process, e.g. fluorescence, and isomerization reactions. The data presented on the iminium salts 55-63 indicate that isomerization competes successfully with fluorescence. The sums of the quantum yields, $\phi_{CN} + \phi_{CC}$, approach the expected limit of 0.5 in most cases, and the fluorescence quantum yields were estimated to be less than 10^{-4} for all the salts.

An upper limit to an isomerization energy barrier for these iminium salts can be derived from fluorescence studies of stilbene and diphenylbutadiene. It has been shown experimentally that in stilbene and diphenylbutadiene, an energy

barrier separates the fluorescing state from the perpendicular state.



When the activation barrier is increased, the quantum yield of fluorescence increases, as does the fluorescence lifetime, and the quantum yield of isomerization decreases. Viscosity and solvent polarity affect the height of the barrier in the photoisomerizations of stilbene and diphenylbutadiene. The energy barrier to isomerization of stilbene is low, so fluorescence is inefficient, with a quantum yield of 0.05 in methylcyclohexane/isopentane.²⁰⁸ More viscous solvents increase the isomerization barrier, thereby decreasing the isomerization quantum yield, and increasing the quantum yield of fluorescence. By measuring the activation energy at constant viscosity at various temperatures, an intrinsic energy barrier, E_0 , was calculated. In hydrocarbon solvents, this barrier is 2.4 kcal/mol.²¹⁰ In alcohol solvents, E_0 is <1 kcal/mol.²¹¹ The more polarizable alcohol solvents stabilize the transition state, indicating that it

has ionic character. The barriers to isomerization of diphenylbutadiene are higher; E_0 is 4.7 kcal/mol in hydrocarbon solvents and 0.7 kcal/mol in alcohol solvents. In pentane, the quantum yield of fluorescence is 0.35 ($\eta=0.24$ cP). In the more viscous decane, $\eta=0.92$ cP, the fluorescence quantum yield is 0.51.²¹²

By comparison, the energy barrier to isomerization in the iminium salts 55-63 must be much less than 1 kcal/mole or non-existent.

Other iminium ions also do not fluoresce at room temperature. However, in a rigid matrix such as an organic glass at 77K, fluorescence is observed.¹⁴⁴ Under these conditions, a significant viscosity induced barrier to isomerization exists. Temperature dependent fluorescence is observed for retinyl iminium ions,¹⁴⁴ as well as styrylpyridinium salts.¹⁶⁸ As the temperature is decreased, and the solvent becomes viscous or solid, the quantum yield of fluorescence increases. Rhodopsin fluorescence is not affected by decreasing the temperature. At room temperature the quantum yield of fluorescence is $1.2(+0.5) \times 10^{-5}$ and at 5K the quantum yield is the same within experimental error, $6.5(+1.5) \times 10^{-6}$,^{29,30} indicating that isomerization, the excited state process that competes with fluorescence, does not have an energy barrier. This result is expected at room temperature, by analogy to the iminium ions studied in solution. The protein must have properties of a nonviscous,

and possibly polarizable solvent in the vicinity of the isomerizing bond. It is interesting that this apparently does not change even at low temperatures.

The presence of viscosity induced barriers, provided by the protein to isomerization about bonds other than C_{11}, C_{12} , is an attractive explanation for the regiospecificity of isomerization of the visual pigments.

Electron Distribution of the Twisted State

It was concluded above that iminium ions 55-63 have planar excited states of ionic character. The photoisomerization process could be influenced by the planar states or the transition state for isomerization, although the latter is probably not important in the isomerizations of iminium ions at room temperature. It is also possible that the character of the energy surface as the molecule twists about the double bond plays a role in the photoisomerization process.

Some theoretical calculations predict that the lowest energy perpendicular state of polyenes is of neutral, biradical character,²¹³ others predict that for polyenes²⁰⁴ and conjugated iminium ions,^{96,97,152,214} the lowest energy perpendicular state is ionic in character. The twisted states of symmetrical polyenes should be non-polar whether ionic or biradical, but unsymmetrical molecules such as iminium ions would have permanent dipoles in an ionic twisted state. The calculations do not agree on the direction of this dipole.

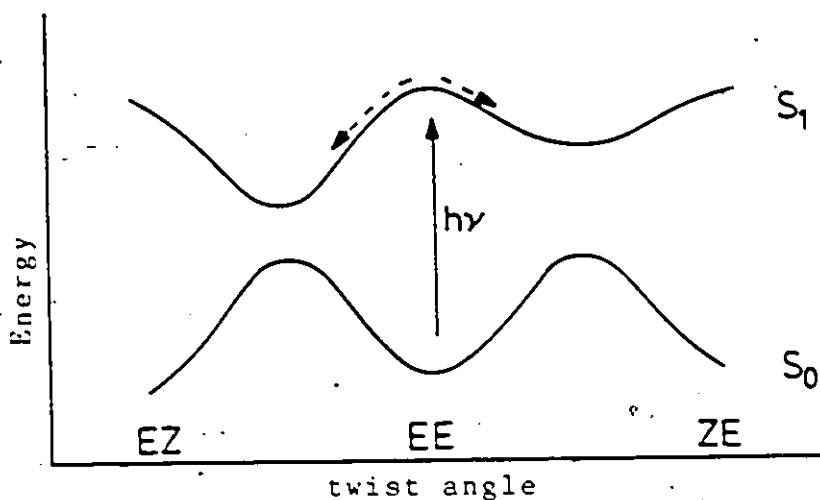
The term "sudden polarization" describes the charge migration that accompanies a twisting double bond of a conjugated iminium ion, as calculated by Salem and co-workers using ab initio methods.^{96,204} The positive charge of the molecule shifts away from the nitrogen only when the molecule is within 5° of the perpendicular conformation.

These calculations do not bring us any closer to an understanding of the nature of the excited state energy surface for an isomerization process because of the discrepancies in their conclusions. An experimental approach that might provide an insight into the photoisomerization process is to examine the effects that substituents have on the regioselectivity of isomerization in molecules where more than one conjugated double bond can isomerize.

Regioselectivity in Photoisomerization

In a molecule where more than one double bond can isomerize, the isomerization efficiency about each bond is not necessarily the same. In a flexible molecule such as a polyene in solution, energy absorbed is distributed throughout the conjugated chain before reactions take place. However, in the excited singlet state, only one bond of a multiply double bonded molecule will isomerize at a time.¹⁹² Regioselectivity might be observed when the various isomerizations have different activation barriers. Theoreticians have predicted that, even in the absence of barriers, selectivity could still be attained if the energy wells of the

various perpendicular states were of different depths.^{206,215}



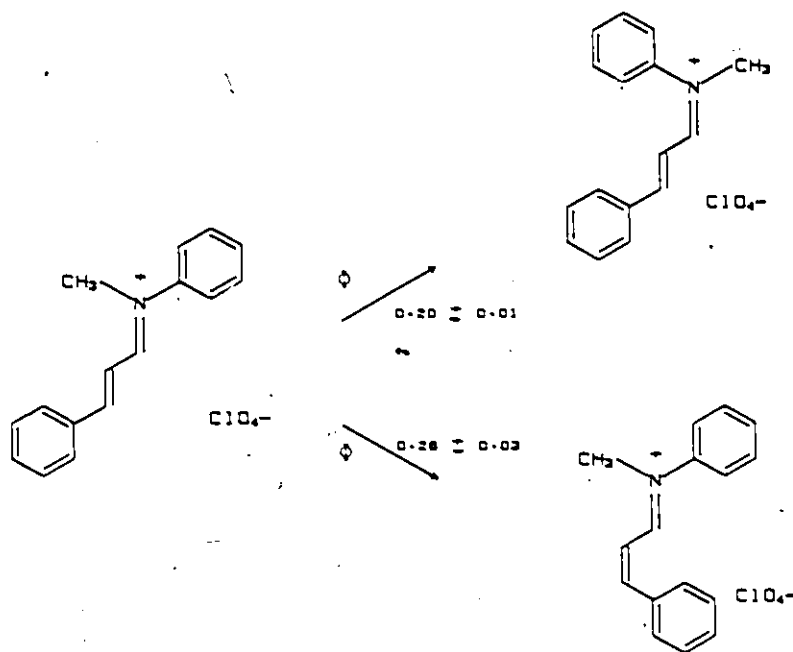
If one energy well is deeper, that is, one perpendicular state is stabilized relative to the other, the approach to the lowest energy conformation is steeper, therefore a molecule may be more likely to follow this path. The factors which determine barrier heights or well depths are not understood at this point. The excited state surface should respond to substituent and environmental effects in much the same way as does the ground state. The time spent in the excited state is so short, however, that effects analogous to thermal effects may not be important.

A systematic study of the effects that substituents in a molecule can have on the regioselectivity of photoisomerizations had not been undertaken previously. The photoisomerizations of iminium salts 55-63 would reveal whether electronic effects could play a role in determining isomerization efficiencies.

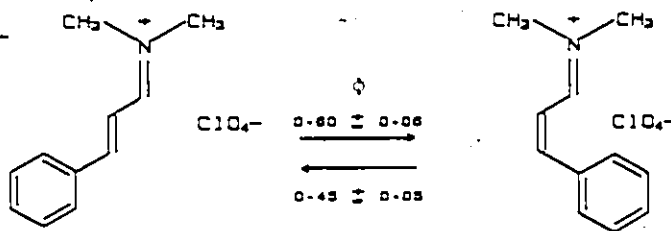
The unsubstituted salt, 57, isomerizes about both the

C=C and the C=N bonds with approximately equal efficiency.

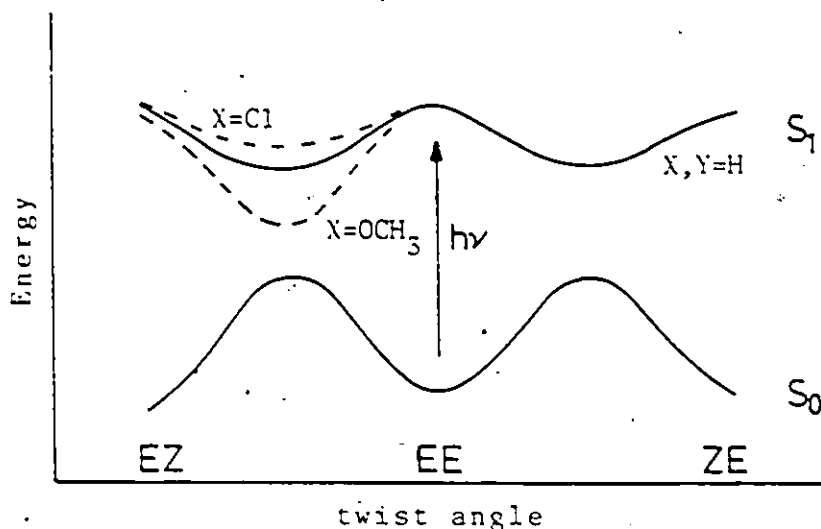
It was concluded above that barriers to isomerization were very small or non-existent at room temperature, and it seems, from the isomerization efficiencies, that the C=C and C=N bonds are affected equally.



Comparison of these results with the quantum yields of isomerization of 16 indicates that the N-phenyl ring plays an important role in encouraging isomerization about the C=N bond.¹⁵⁰



If this is an electronic effect, then changing the electronic nature of either phenyl ring by adding electron-withdrawing or -donating substituents might also alter the relative ratios of isomerization of the two isomerizing bonds. On the basis of Salem's model, a positive charge stabilizing substituent on the C₃ phenyl ring should increase the stability of the structure that is twisted about the C=C bond, and enhance isomerization about the C=C bond at the expense of the C=N bond isomerization. Likewise, an electron-withdrawing substituent such as chlorine should destabilize the perpendicular state for C=C isomerization.



The results of the experiments did not concur with these predictions. When the substituents were varied from chloro to methoxy on either phenyl ring, no change was observed in relative quantum efficiencies of isomerization outside experimental error, Table 3-2. The nitro substituted salts 55 and 60 behaved anomalously, and their isomerization

will be discussed below. It is possible that, in the absence of energy barriers, changing the depths of the wells of the twisted intermediates does not affect regioselectivity. It is also possible that the twisted intermediates do not have significant polar character, so their stabilities are not greatly affected by positive charge stabilizing or destabilizing substituents. The effect of the N-phenyl ring is substantial however, and needs to be examined. The data suggest that, assuming the energy levels of the perpendicular states determine regioselectivity, the perpendicular states of conjugated iminium ions have biradical rather than ionic character, and therefore can be greatly stabilized by adjacent phenyl rings, but are not significantly affected by charge-stabilizing substituents on those rings.



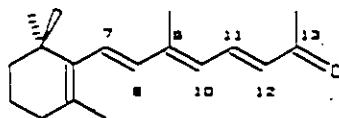
Regioselectivity in Polyenes and Related Neutral Molecules

In polyenes, a trend has been observed in regioselectivity in that molecules isomerize preferentially about the more highly substituted double bond, suggesting that stabilization of an ionic transition state or twisted state

by substituents may be important.²¹⁶⁻²²⁰ This generalization often fails in cases where isomerization about a Z disubstituted C=C bond competes with isomerization about a tri-substituted double bond, the former being preferred. In stilbene, Z-E isomerization is barrierless, while E-Z isomerization has a small activation barrier.²²¹ The same effect might operate in the polyenes.

Electronic effects also seem to play a role in determining regioselectivity. Some examples are shown in Figure 3-2.

Polyenals behave in a similar manner to the polyenes, Figure 3-3. Retinal isomerizes about the tri-substituted 9,10 and 13,14 double bonds only, in non-polar solvents, with a preference for the bond closer to the aldehyde.²²³ This preference is not changed by increasing the length of the conjugated chain. In the retinal homologue shown below, the 11,12 double bond, although only disubstituted, becomes the favoured isomerizing bond, possibly because of the charge-stabilizing carbonyl group now adjacent.



In polar solvents, the regioselectivity of retinal photoisomerization changes somewhat, with the C₁₁, C₁₂ double bond isomerizing more efficiently.

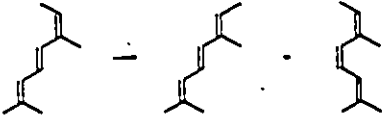
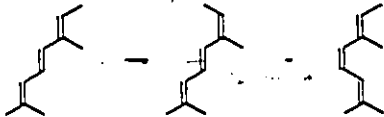
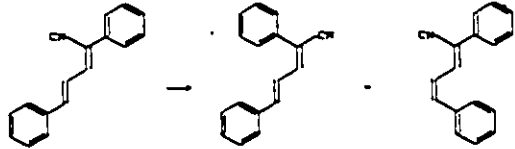
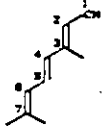

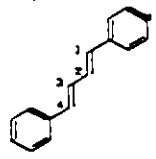
	initial product ratios		Reference
	0.5	0.6	216
initial product ratios			
	1.4	0.1	216
initial product ratios			
	0.08	0.003	218
ϕ (benzene)			
ϕ (acetonitrile)	0.09	0.013	
	initial product ratios		219
	4-cis/2-cis	6-cis/2-cis	
cyclohexane	0.07	-	
acetonitrile	0.14	-	
	=		220
\downarrow		\downarrow	
Z,E isomer		E,Z isomer	
$\phi = 0.026$		$\phi = 0.34$	
	$\phi_{EE \rightarrow ZE}$ 0.30	$\phi_{EE \rightarrow EE}$ 0.07	
	$\phi_{ZE \rightarrow EE}$ 0.24	$\phi_{ZE \rightarrow ZE}$ 0	222
	$\phi_{EE \rightarrow EE}$ 0	$\phi_{EE \rightarrow ZE}$ 0	

Figure 3-2 Photoisomerization Regioselectivity in Some Polyenes

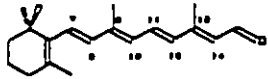
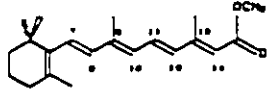
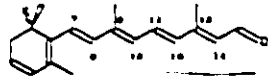
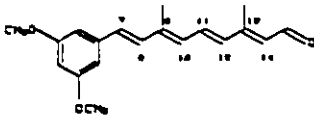
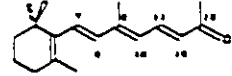
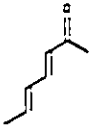
	initial product ratios			Reference
	13-cis	11-cis	9-cis	
	4	-	1	225
	13	-	1	
	3.4	-	1	
	3.6	-	1	
		1.5	1	
	ϕ EE-EC	0.16		224
	ϕ EE-JE	0.35		

Figure 3-3 Photoisomerization Regioselectivity in Some Polyenals

An additional factor that must be considered is that different double bonds in the molecule require different volumes in which to rotate. This could lead to steric inhibition of rotation of some double bonds, a factor that could be governed by the solvent cage.²²³

In the above examples, the position of the double bond within the conjugated chain is not a factor in determining regioselectivity. This strongly suggests that regioselectivity is determined at a stage such as an early transition state where the twist angle about the isomerizing double bond is not large enough to break conjugation within the chain. At a perpendicular state, the two ends of the molecule are no longer conjugated, and the stabilization received by having the length of the conjugated chain as long as possible on each end of the isomerizing bond is expected to be of great importance.

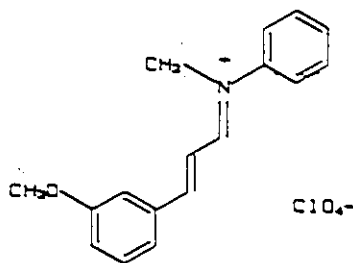
Regioselectivity in Charged Molecules

The introduction of a charge into a polyenal seems to affect the regioselectivity of photoisomerization from the few examples studied. In isooctane solution, complexation of trans retinal with $\text{Eu}(\text{fod})_3$ (tris(6,6,7,7,8,8,8,heptafluoro-2,2-dimethyl-3,5-octanedionato)-europium(III)) causes more of the 11-cis isomer to be formed on photolysis, compared to retinal isomerization in a non-polar solvent.²²⁵ Coordination of retinal to silica gel has a similar effect on the photoisomerization,²²⁶ as does formation of the iminium

salt.¹⁴⁰ This seems to agree with the proposal given above, that stabilization of a perpendicular state, with the maximum number of conjugated double bonds at either end of the isomerizing bond, is determining regioselectivity. Thus it is not surprising that the regioselectivities observed in these salts differ from those of the polyenes and polyenals, where factors that are important in stabilizing an ionic transition state apparently control regioselectivity.

Effect of a Meta Substituent

An iminium salt with a meta methoxy substituent on the C₃ aryl ring, 95, was synthesized. Its absorption maximum and relative quantum yields of photoisomerization are given in Table 3-5, and compared with data for the para methoxy salt, 59.



95

Zimmerman and co-workers²²⁷ have suggested that the $\pi\pi^*$ excited states of substituted benzene derivatives have electron distributions where a substituent, either electron-withdrawing or electron-donating, exerts an influence on the ortho and meta positions, and not on the ortho and para

Table 3-5

Absorption Maxima and Relative Quantum Yields of
Photoisomerization of the Para and Meta Methoxy Iminium Salts
59 and 95

Iminium Salt	λ_{max} (nm)	$\phi_{\text{CN}}/\phi_{\text{CC}}^{\text{a}}$
59	408	1.1
95	346	1.7

^aestimated error \pm 20%

positions as in the ground state. Photosolvolysis studies of 3- and 4-methoxybenzyl acetates support this prediction. The meta methoxy group stabilizes the alpha carbonium center of the solvolysis intermediate, and the para substituent does not. Similarly meta methoxy, fluoro, and methyl benzyl alcohols form benzyl cations in the excited state. The products of the reaction of the para substituted alcohols are generally derived from radical intermediates, since the para substituent cannot stabilize the alpha carbonium ion.^{228,229}

Iminium salt 95 has a higher energy absorption band than the para substituted salt, 59, indicating that the planar excited state reached on absorption into the long wavelength absorption band is best described by resonance forms as they are drawn for the ground state, with positive charge at the para position of the phenyl ring. In addition, C=C bond isomerization was not enhanced relative to C=N bond isomerization, Table 3-5. The patterns of positive charge delocalization observed in the benzyl cations are not important in the isomerizations of the iminium salts.

III. Intersystem Crossing

Direct experimental information about the multiplicity of the excited states of iminium salts 55-63 was not obtained.

Although a singlet state is normally reached on light absorption, mechanisms often exist that allow the multiplici-

ty of the excited state to change to triplet before the molecule returns to the ground state. Information about whether a molecule reaches a triplet state can be obtained in several ways experimentally. Sometimes the phosphorescence spectrum can be observed, indicating that intersystem crossing is occurring. This is not proof that excited state reactions are also occurring in the triplet state, however, if quenching the triplet emission also quenches the reaction, the triplet state must be involved. Another experimental method is to generate a triplet state directly by sensitization. A molecule (donor) that is known to cross efficiently to the triplet excited state is irradiated in the presence of the molecule of interest (acceptor). If the triplet energy levels are compatible, exchange can occur with the acceptor in its ground state leaving it in an excited triplet state. The triplet sensitizer is then in the ground state.



If reaction products differ from those obtained in the direct irradiation, then the triplet state is likely not involved in the photoreaction.

Triplet energy levels are determined experimentally from phosphorescence spectra, by quenching phosphorescence, quenching triplet reactions, or by sensitizing the triplet state with sensitizers of known triplet energy.

There are severe experimental limitations involved in studying the multiplicity of the photoisomerization reaction

of salts 55-63. If product studies are required, then the reaction must be run in a strong acid such as trifluoroacetic acid to limit unwanted thermal isomerizations. Few triplet sensitizers or quenchers are soluble or unreactive in this solvent. The product analysis must be by NMR, therefore high concentrations of material are required. In addition, the reactants remain in solution, and cannot be separated from added sensitizers and quenchers before analysis. These additives often interfere with the analysis. Another major constraint is that iminium salts are easily reduced in the excited state or by excited state donors, and therefore sensitizers and quenchers must be chosen that cannot participate in this unwanted side reaction.

It was found that triplet quenching or sensitization experiments, followed by product analysis, were not practical because of these limitations.

One alternative approach is to sensitize a known phosphorescing compound by irradiating the iminium salt. If the triplet state of the iminium salt is reached by direct irradiation, it might act as a donor. The acceptor would in turn phosphoresce. Because this is a spectroscopic experiment, some of the experimental difficulties discussed earlier, such as solvent and concentration, are avoided. An attempt was made to sensitize the triplet state of benzil (E_T 53 kcal/mole) with salt 60. When a solution of benzil in acetonitrile was irradiated at 310 nm, emission was observed

with a maximum at 500 nm. The iminium ion was added to this solution in excess, so that it would absorb all the light. On irradiation at 370 nm, no emission was detected. It is difficult to base conclusions on one experiment, however it appears that if the triplet state of salt 60 is reached by direct irradiation, its energy is not being transferred to benzil. This could mean that the triplet energy of 60 is below that of benzil ($E_T=53$ kcal/mol), or that the lifetime of the triplet state is too short to allow energy transfer. Based on the position of the absorption spectrum, it would not be unreasonable to expect a lower energy triplet state. Unfortunately, available lower energy phosphorescing compounds are also good electron donors.

Information about the multiplicity of the photoisomerizations of iminium salts 55-63 will have to be obtained indirectly.

Experimental information that suggests that the nitro substituent is causing intersystem crossing in the iminium salts 55 and 60 comes from the anomalous quantum yields measured for the isomerization reaction, Table 3-2. These are not attributable to electronic effects since the other substituents do not affect the quantum yields. Salt 55 isomerizes much more efficiently about the C=N bond than the C=C bond, and in the case of 60, it appears that the Z,Z isomer is formed directly from the E,E isomer.

In the styrylpyridinium salts, 38-41, isomerization

occurs in the singlet state, however when the molecule has a nitro substituent, 42, intersystem crossing to the triplet state is observed. Isomerization then proceeds from the triplet state.^{166,169}

The only other iminium salts studied, the retinylidene iminium salts, do not deactivate via the triplet state. The quantum yield for intersystem crossing is less than 0.001.¹⁴²

The tentative conclusion from this indirect information is that the iminium salts 56-59 and 61-63 isomerize in the singlet state, and salts 55 and 60 isomerize in the triplet state.

IV. Internal Conversion

Iminium salt 59 isomerizes with lower quantum yields than observed for the other iminium salts, Table 3-2. It is also the salt with the lowest excitation energy, $E_{0,0} \leq 60$ kcal/mol.

When the excited and ground states are closer together than about 50-60 kcal/mol, an additional mechanism for returning to the ground state becomes probable, namely internal conversion.²³⁰ In this process, energy is dissipated through vibrational modes, and isomerization does not necessarily occur. The low isomerization quantum yields observed for salt 59 could mean that internal conversion is occurring at the planar configuration or the partly twisted configura-

tion, and that a fraction of the excited molecules cross to the ground state before reaching the 90° twisted intermediate.

The amino styrylpyridinium salt, 43,¹⁶⁷ and dimethoxy dicyanotetraphenylethylene, 94,¹⁹⁷ are two molecules for which internal conversion was proposed. Both have low absorption energies and low isomerization quantum yields. Rhodopsin and bacteriorhodopsin also have low energy absorption bands, however internal conversion is not indicated from the high quantum yields observed. One effect that the protein has on the chromophores seems to be to channel excited molecules efficiently into the excited state energy minimum.

V. Summary

The absorption spectra of iminium salts 55-63 indicate that electronic effects play a role in determining the energy levels of the planar excited state. The evidence suggests that the positive charge of the molecule is delocalized towards the C₃ phenyl ring in the excited state. These iminium salts photoisomerize about both the C=C and C=N bonds in a barrierless process with no evidence that electronic effects determine regioselectivity. The N-phenyl ring does affect regioselectivity, leading to the suggestion that the excited state that determines regioselectivity has biradical character. A nitro substituent on either phenyl ring likely causes inter-system crossing to the triplet state, a longer-

lived state with different electronic properties than the singlet state. As a result, the relative quantum yields of the salts 55 and 60 differ from those of the other molecules.

Steric effects on photoisomerization, especially related to the solvent cage around the molecule, require further study. The regioselectivity of rhodopsin and bacteriorhodopsin isomerization is likely based on viscosity induced barriers provided by the protein to isomerization about all double bonds except the C₁₁,C₁₂ and C₁₃,C₁₄ isomerizations respectively. Although we have shown that conjugated charge-stabilizing groups do not influence the regioselectivity of photoisomerization, the effect of non-conjugated charged groups such as might be found in the protein needs to be explored.

CHAPTER 4

E/Z ISOMERIZATION BY PHOTOINITIATED ELECTRON TRANSFER

Iminium salts are electrophilic and so are easily reduced in the ground state. This can be accomplished by hydride reducing agents, such as sodium borohydride, to form amines²³¹, or by one-electron donors to form reactive radicals. The addition of electron donors to iminium salts via electron transfer has been extensively studied by Mariano and co-workers, and recently reviewed.¹⁴⁷

I. Cyclic Voltammetry

The energy required to add an electron to an iminium salt can be measured by quantitative electrolysis techniques such as cyclic voltammetry or polarography. The reductions of iminium salts 55-63 were observed by cyclic voltammetry. A constant current flows through the cell until a sufficiently negative voltage is reached to allow reduction of the molecule, and the current increases rapidly. The reduction products accumulate on the working electrode, and since diffusion away from the electrode is normally slow, further reaction is hindered by the layer of reduction product on the electrode surface, and the current decreases. The pattern observed is a reduction wave, shown in Figure 4-1. When the voltage reaches a pre-set switching potential, it reverses to become less negative. If the reduced product remains on the

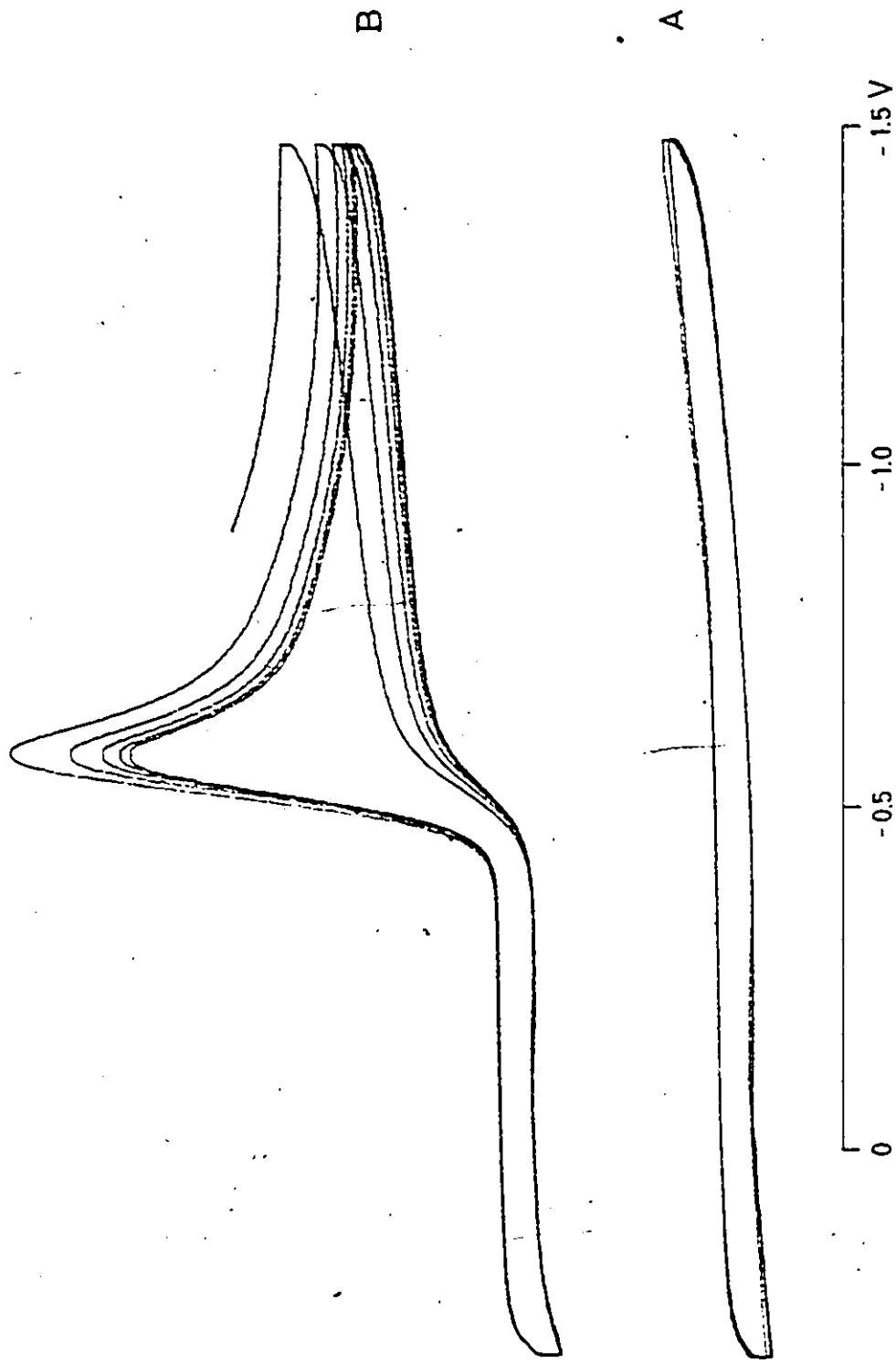


Figure 4-1 Cyclic Voltammogram of N-methyl, N⁺-phenyl-3-(p-chlorophenyl)-2-propenylidene iminium perchlorate, 56 (A) background (B) iminium salt

electrode surface, the current will decrease as this reduction product reoxidizes, producing an inverted wave. The reduction potential, $E_{1/2}$, is halfway between the reduction and re-oxidation peaks, which, in a reversible one-electron reaction, are separated by 57 mV.²³² In some instances, the reduced species will have reacted further with itself or with solvent before the re-oxidation voltage is reached. The reaction is then said to be irreversible, and no inverse wave will be observed, as in Figure 4-1.

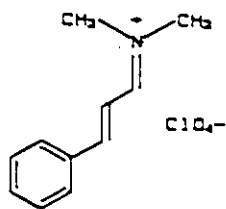
The electrolytic cell contains a working electrode, a platinum wire auxiliary electrode, and a saturated calomel electrode that is separated from the bulk solution by a glass frit. The solution must be dry to avoid hydrolysis of the iminium salts, and the glass frit serves to keep the aqueous calomel solution separate from the bulk solution.

A background scan of a degassed solution of 0.1 M electrolyte, tetrabutylammonium perchlorate, in acetonitrile gave the flat baseline voltammogram shown in Figure 4-1. Oxygen has a reduction potential of about -1.2 V, and so interferes with the measurement when present. In the presence of iminium salt (3×10^{-3} M solution), a reduction wave is observed in the cyclic voltammogram. The sample scan, for iminium salt 56, shown in Figure 4-1 was obtained at a scanning rate of 0.5 V/s, with output directly to an X-Y recorder.

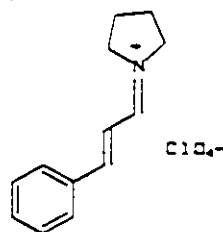
Cyclic voltammograms were recorded for each of the

iminium salts 55-63. E_p values for the reduction waves are given in Table 4-1. The iminium salts exhibit substituent dependent reduction waves ranging from -0.38 V to -0.68 V. The nitro aryl salts, 55 and 60, have additional, partially reversible reduction waves at E_p -1.30 V and -1.39V respectively, Figure 4-2. These are attributed to reduction of the nitro groups. The E_p values given are measured at the top of the reduction peak, since the reaction is irreversible at the scan rate of 0.5 V/s. E_p is an estimate of $E_{1/2}$, not an accurate measurement, and is dependent on the scan rate. As the rate is increased, E_p moves to more negative voltages, as shown for iminium salt 57 in Table 4-2. If the equipment had allowed measurements at much faster scan rates, a scan rate that is greater than the rate of reaction of the reduced product could presumably be reached, and a reversible wave would be observed.

The accuracy of the measurements can be deduced by comparing the E_p value measured for iminium salt 16, -0.84 V, with the reduction potential; $E_{1/2}$, of salt 96, -0.97 V, measured by polarography.²³³



16



96

Table 4-1
Reduction Potentials^{a,b}

Iminium Salt	E _p (V)
55	-0.380
56	-0.585
57	-0.610
58	-0.650
59	-0.735
60	-0.425
61	-0.575
62	-0.640
63	-0.680
16	-0.84
6, X=ClO ₄	-0.73

^ameasured by cyclic voltammetry, at 0.5 V/s, vs. SCE

^b0.003M iminium salt in 0.1M tetrabutylammonium perchlorate
in acetonitrile

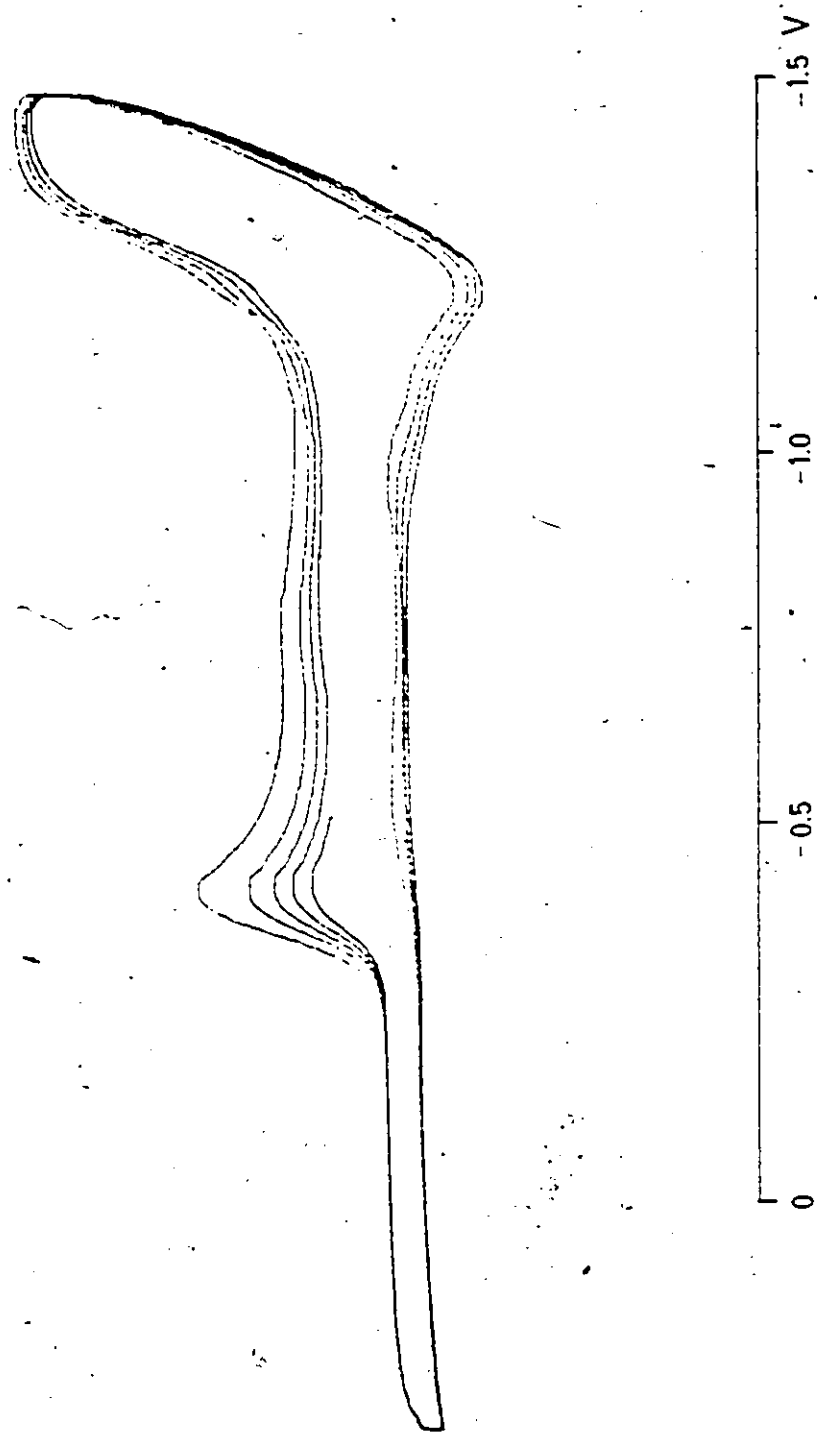


Figure 4-2 Cyclic Voltammogram of N-methyl, N-(p-nitrophenyl)-3-phenyl-2-propenylidene iminium perchlorate, 60

Table 4-2
Variation of E_p with Scan Rate for Iminium Salt 57^{a,b}

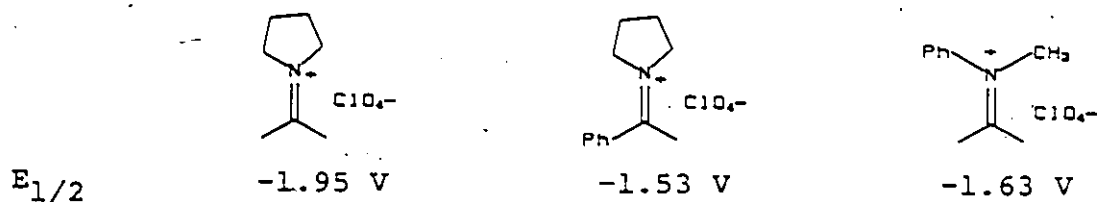
Scan Rate (V/s)	E_p (V)
0.1	-0.585
0.3	-0.605
0.5	-0.610
0.7	-0.620
1.0	-0.625
2.0	-0.67

^ameasured by cyclic voltammetry, vs. SCE

^b0.003M iminium salt in 0.1M tetrabutylammonium perchlorate
in acetonitrile

An E_p value for the *N,N* dimethylretinylidene perchlorate salt was also measured, Table 4-1.

Phenyl rings on the carbon or nitrogen of an iminium C=N bond make the molecule easier to reduce. The trend is clearly shown in the half-wave reduction potentials reported for the iminium salts shown below,²³³ and by comparing E_p for salt 16 (-0.84 V) to that of salt 57 (-0.61 V).

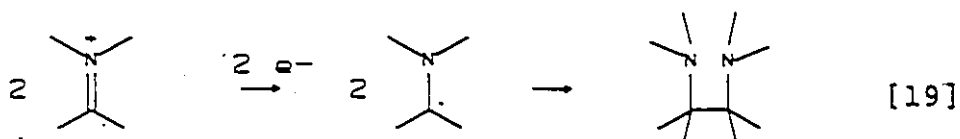


A similar effect can be achieved by increasing the number of double bonds conjugated to the iminium group, as in the retinylidene iminium salt, E_p -0.73 V.

Electron-donating substituents on either aryl ring of the iminium salts 55-63 increase E_p , and electron-withdrawing substituents decrease E_p , making the iminium salt easier to reduce. The methoxy-substituted salts 59 and 63 have E_p values of -0.735 and -0.680 V respectively, while the nitro-substituted salts 55 and 60 have much lower E_p values, -0.380 and -0.425 respectively.

The reduction values measured for these iminium salts indicate that they are easily reduced compared to other stable organic molecules. For example, the $E_{1/2}$ of stilbene is -2.07 V vs. SCE, that of anthracene, -1.41 V, and anthraquinone, -0.94 V.²³⁴

Iminium salts reduced by electrolysis have been shown to react by coupling of two radical fragments to produce dimers, Equation 19. The dimerization reaction is fast in most iminium salts studied, and so the reduction is irreversible.²³³



II. Electron Transfer in the Excited State

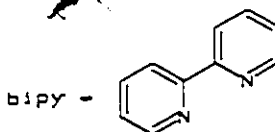
The low reduction potentials measured for the iminium salts 55-63 suggest that electron transfer between molecules in solution might be achieved if a suitable donor is present. Electron transfer requires energy, which can be provided by heat or light energy. As mentioned in the Introduction, the feasibility of photo-initiated electron transfer can be derived from Equation 10.¹⁸⁰ The energy required for the reaction comes from exciting either the electron donor or the acceptor.

Isomerization Initiated by Electron Transfer

On an electrode surface, the radicals generated by reduction of the iminium salts couple because of the high concentrations of radicals present. Radicals generated at low concentrations in solution should undergo other reactions,

and possibly re-oxidize to iminium salts. By analogy to the reactions of stilbenes, 47, and styrylpyridinium salts, 42, it was thought that isomerizations about the C=C or C=N bonds might be observed in iminium salts 55-63.

An electron donor, tris(2,2'-bipyridine)ruthenium(II) dichloride, 97, was synthesized. This compound is ideal for the reaction because it absorbs light of lower energy than the iminium salts, λ_{max} 448 nm, so that energy transfer in the excited state becomes unlikely, it is soluble and thermally stable in trifluoroacetic acid, and its oxidation potential is suitable for the electron transfer reaction (1.3 V). The complex has previously been shown to donate electrons to organic dications.²³⁵ The luminescence lifetime of 97 is about 600 ns, and it emits light with a maximum at 600 nm.²³⁴



97

Qualitative quenching experiments were performed to determine if iminium salts 55-60 could quench the luminescence of 97. It was found that iminium salts 55, 56, 57, 58 and 60 did quench the luminescence of solutions of 97, but iminium salt 59 did not. Conditions of the experiments,

and results are given in Table 4-3. In each case, the solutions were irradiated at a wavelength that allowed absorption by 92, but minimized absorption by the iminium salt.

A change of solvent to trifluoroacetic acid did not affect the result, as shown by the luminescence quenching of 97 by salt 60.

The experiment is based on the premise that electron transfer rather than energy transfer from the triplet excited state of the ruthenium complex is causing the quenching. The triplet energy of 97 is 49 kcal/mol. There are two experimental observations that suggest that electron transfer is the predominant process. The first excited states of the iminium salts studied decrease in energy in the order 55 to 59, and the triplet state energies should follow this trend. If so, it is unlikely that triplet energy transfer would be seen for salts 55-58, but not for salt 59, the molecule with the lowest energy triplet state. However, the reduction values, E_p , of these salts increase in the order 55 to 59, and as expected, the iminium salt that is the most difficult to reduce does not quench the luminescence of 97. The second experimental observation is from product analyses and will be discussed below.

The photolyses were repeated at higher concentrations in trifluoroacetic acid for iminium salts 57 and 60, to allow product analysis by ^1H NMR. A solution of iminium salt 60 ($4.5 \times 10^{-2}\text{M}$) and 97 ($2.6 \times 10^{-2}\text{M}$) in trifluoroacetic acid

Table 4-3

Quenching of Tris (2,2'-bipyridine) ruthenium (II) dichloride
(97) Luminescence by Iminium Salts 55-60 in Acetonitrile

Iminium Salt	Approx. Conc. (M)		λ_{ex} (nm)	abs. increase ^a	lum. decrease
	Iminium Salt	97			
55	1×10^{-4}	2×10^{-6}	460	-	53% ^b
56	1×10^{-3}	1×10^{-6}	520	.006 (24%)	85% ^c
57	1×10^{-3}	1×10^{-5}	520	.004 (11%)	80% ^c
58	2×10^{-3}	1×10^{-5}	540	.005 (20%)	75% ^c
59	1×10^{-2}	1×10^{-5}	550	.57 (3000%)	41% ^c
60	1×10^{-3}	1×10^{-5}	480	.02 (20%)	65% ^b
			460	.20 (120%)	77% ^b

^aincrease in absorption peak height (percentage increase) at the exciting wavelength, λ_{ex}

^bpercentage decrease in peak area of luminescence peak

^cpercentage decrease in peak height of the luminescence peak, at the maximum (about 600 nm)

was irradiated with light of wavelength >425 nm, to maximize absorption by 97. The reaction was stopped at regular intervals, and monitored by ^1H NMR. At 30 minutes irradiation, the percentage of E,E isomer, 60, had decreased to 73% from $>95\%$. The only product observed was the Z C=N isomer, 69. The ratios approach a steady state resembling the thermodynamic ratio within about three hours, Table 4-4. 250 MHz ^1H NMR analysis confirms that the Z C=C isomers, 78 and 87, are not formed in the reaction.

The isomerization to form a mixture of the E and Z C=N isomers of salt 57 was accomplished starting from the E,E isomer 57, or from a photomixture containing the four isomers, 57, 66, 75, and 84. In the first experiment, a mixture of 35% E,E isomer, 57, and 65% Z,E isomer, 66, was obtained within three hours. In the second experiment, a photoequilibrium was generated by irradiating a trifluoroacetic acid solution of the E,E isomer. Compound 97 was added to this solution, and irradiation was continued at a higher irradiating wavelength, >425 nm. After 30 minutes irradiation, the Z C=C isomers, 75 and 84, had disappeared.

It is unlikely that a triplet excited state isomerization would lead to a thermodynamic ratio of isomers, so the reaction is most likely an electron transfer process. This is the first reported example of E-Z isomerization of an iminium salt by electron transfer. The proposed mechanism is similar to that outlined for stilbene isomerization.¹⁸¹

Table 4-4

Isomerization of Iminium Salt 60 on Irradiation of
Tris (2,2'-bipyridine) ruthenium (II) dichloride, 97^{a,b}

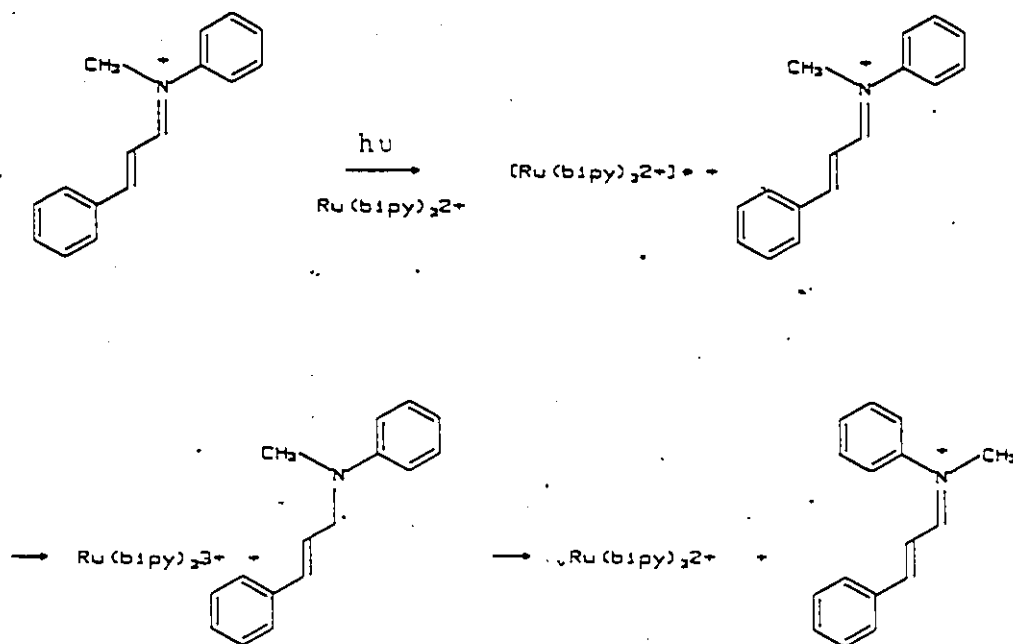
time (min)	% E, E ^c	% Z, E ^c
0	>95	<5
30	73	27
60	63	37
83	62	38
120	60	40
150	58	42
24 hr	54	46

^a concentrations: 60, $5 \times 10^{-2} \text{M}$; 97, $2.5 \times 10^{-2} \text{M}$
in trifluoroacetic acid

^b $\lambda_{\text{ex}} > 425 \text{ nm}$

^c measured by ^1H NMR, the peak height of the NCH_3 signal,
relative to the sum of the heights of the two CH_3 peaks

The intermediate radical could be long-lived enough to allow free rotation about both the C=C and C=N bonds, and thermal equilibration. The initial electron transfer process could be to either the C=C bond or the C=N bond, or delocalized throughout the π system.



The ground state radical produced by electron transfer returns to an iminium ion by donating the excess electron. No other products were observed in the reaction. The electron acceptor can be the oxidized donor, tris(2,2'-bipyridine)-ruthenium(III), or another ground state iminium ion. If electron donation to the latter species becomes predominant, a catalytic reaction ensues.²³⁴ This can be detected by measuring quantum yields of reaction as a function of concen-

tration of reactant. In the photoisomerization studies discussed in Chapter 3, a possible reaction mechanism that was considered was electron transfer from a donor in solution to the excited iminium salt. This was ruled out by two observations. First, increased concentrations of the iminium salt had no effect on the quantum yields of either C=C or C=N isomerization. Second, increased concentrations of the only reasonable donor in the system, the trifluoroacetate anion, also had no effect on the quantum yields of isomerization of salts 59 and 60.

The ^1H NMR spectrum of 97 consists of four aromatic signals, at the start of the reaction. By four hours irradiation only a broad singlet remains, and by 24 hours, the aromatic peak has completely disappeared, and a peak at about 2 ppm is found. These changes take place in the presence and in the absence of iminium salt. A disproportionation reaction has been observed under other reaction conditions and might be responsible for this observation, Equation 20.²³⁶ In solution the back reaction is normally fast, so the products are not observed, but in the strong acid used in these experiments, protonation of the reduced bipyridine ligand could take place. If the process continues, the bipyridine groups might eventually be completely reduced. This would explain the disappearance of the aromatic peaks, and the emergence of an aliphatic proton signal in the NMR spectrum.

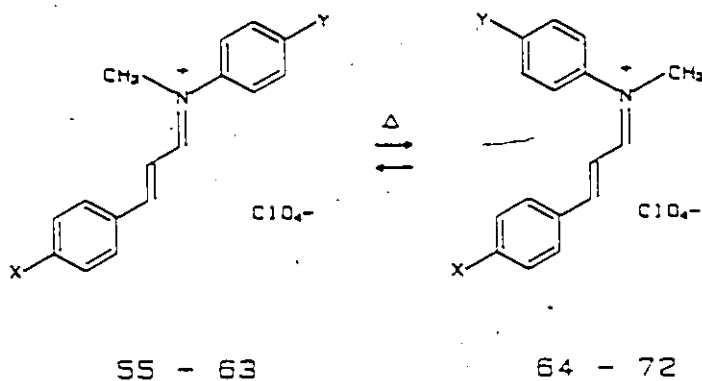
The line broadening of the spectra might also be

and acceptor are fixed in positions suitable for electron transfer to occur.

CHAPTER 5

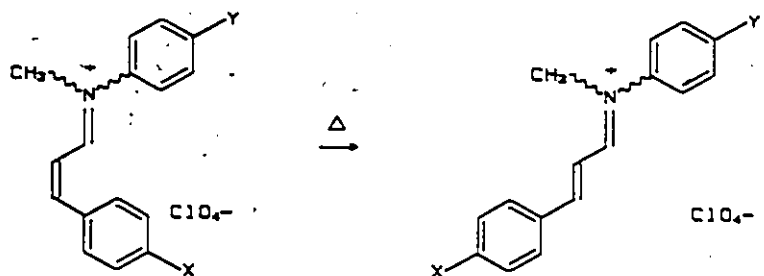
THERMAL E/Z ISOMERIZATION

The iminium salts 55-63 isomerize in solution about the C=N bond, in a thermally initiated process. At equilibrium, a mixture of the E,E isomer and the Z,E isomer exists, with the latter generally favoured. The equilibrium constants, K , measured at 100°C are given in Table 5-1. The equilibrium constants do not vary with substituent, within the error limits of the determination.



	X	Y
55, 64	NO ₂	H
56, 65	Cl	H
57, 66	H	H
58, 67	CH ₃	H
59, 68	OCH ₃	H
60, 69	H	NO ₂
61, 70	H	Cl
62, 71	H	CH ₃
63, 72	H	OCH ₃

Thermal isomerization about the C=C bond cannot be observed in salts 55-63, but does occur from the E,Z and Z,Z isomers. At equilibrium, only the E,E and Z,E isomers remain.



On prolonged heating, an additional product (or products) forms in solution that is not a geometric isomer, and is apparently not in equilibrium with the isomers. This product was not characterized.

The isomerization mechanisms were elucidated from a study of the reaction.²³⁷ The approach used was to measure electronic substituent effects on the reaction rates to learn about the nature of intermediates or transition states in the reaction, and to examine the effect of the medium to determine if the reaction is unimolecular or bimolecular.

I. Kinetic Measurements

The rates of the isomerization reaction about the C=N bonds of iminium salts 55-63 were measured at 100°C. Solutions of iminium salt in trifluoroacetic acid (about 0.2 M), with an internal standard, tetramethylammonium tetrafluoroborate, were sealed in NMR tubes, and heated until equilibrium was reached. The samples were analysed at regular intervals by ¹H NMR to determine the concentration of starting isomer, or product isomer. The analysis permitted the determination of the rate constants for the forward and

reverse isomerizations. These are given in Table 5-1. The isomerization reactions followed pseudo first-order kinetics with one exception, 63. In this case, the rate constants were estimated from the half reaction time.

Substituent Effect

The rate constants of the isomerization reactions vary over a large range, from $7 \times 10^{-7} \text{ s}^{-1}$ for salt 62 to $3 \times 10^{-4} \text{ s}^{-1}$ for salt 59. Electron-withdrawing or electron-donating substituents on either phenyl ring substantially enhance the rate of the reaction relative to that of the unsubstituted iminium salt, 57.

Solvent Effect

The solvent used in the reaction, trifluoroacetic acid, is a strong acid, with an H_0 of -4.3, measured by the Hammett indicator method. This falls within the range previously measured, -4.4 to -2.77²³⁸. An impurity in the acid, HCl, is thought to contribute to the acidity. Other components of the solution are traces of the counterion, trifluoroacetate, the iminium salt and its counterion, perchlorate, and the internal standard, tetramethylammonium ion, and its counterion, tetrafluoroborate. The anions listed are weak nucleophiles, and trifluoroacetate is present in low concentrations, about $2 \times 10^{-7} \text{ M}$.²³⁸

To study medium effects, the acidity of the solvent was increased by the addition of a small amount of 100% sulfuric acid. This decreased H_0 to -5.4, and presumably

Table 5-1

Isomerization Rate Constants at $100 \pm 1^\circ\text{C}$ in TFA and 0.01M
 $\text{H}_2\text{SO}_4/\text{TFA}^{\text{a,b}}$

Reaction	TFA		$\text{H}_2\text{SO}_4/\text{TFA}$		K^{c}
	$10^7 k_{\text{f}},$ s^{-1}	$10^7 k_{\text{r}},$ s^{-1}	$10^7 k_{\text{f}},$ s^{-1}	$10^7 k_{\text{r}},$ s^{-1}	
55 → 64	110	79	22	16	1.4
56 → 65	12	9.6			1.3
57 → 66	8.9	7.1	3.2	2.5	1.3
58 → 67	12	11			1.1
59 → 68	3400	2850	13000	11000	1.2
60 → 69	370	430	170	190	0.86
61 → 70	22	20	4.6	4.2	1.1
62 → 71	7.3	6.1	6.4	5.4	1.2
63 → 72	140 ^d	110 ^d	350	290	1.2

^aError $\pm 10\%$

^b $k_{\text{f}}, k_{\text{r}}$ = rate constants for the forward and reverse reactions, respectively; average of two runs

^c K = equilibrium constant $[\text{Z,E}]/[\text{E,E}]$ at 100°C .

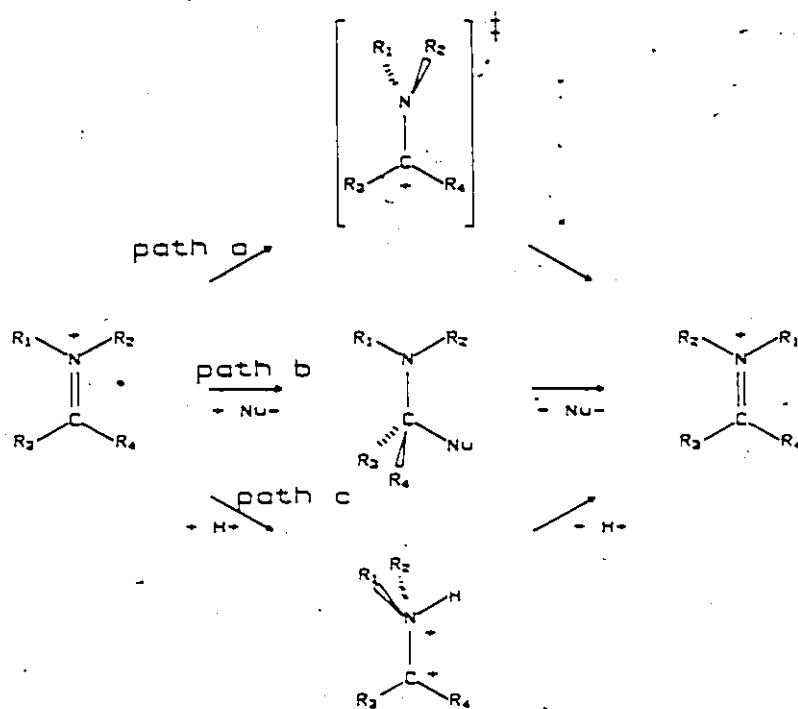
^destimated from the half reaction time

also decreased the nucleophilicity of the solution.

The rate constants of isomerization of all the iminium salts, 55-63, were affected by the solvent change, Table 5-1, indicating that the isomerization reaction is not unimolecular, but catalysed by the solvent or a constituent of the solution.

II. Mechanisms of Isomerization

Isomerization mechanisms that have been observed or postulated previously are shown in Scheme 1-3.



Path a, a rotation mechanism, can be eliminated as the isomerization mechanism of the iminium salts 55-63 on the basis of the observed medium effect. The intermediates formed in paths b and c, the nucleophile and proton catalyzed

paths respectively, are of considerably different characters. The former intermediate has less positive charge than the iminium salt, and the latter has increased positive charge.

No direct evidence for the formation of either of these intermediates was found by ^1H NMR, indicating that, if present, they are of considerably higher energy than either the E,E or Z,E isomers of the iminium salts. The rate-determining step of the reaction must then be the initial interaction of catalyst and iminium salt.

To better understand the intermediates involved in the isomerization reaction, the rate constants were correlated with Hammett substituent constants. The results are shown in Figures 5-1 and 5-2. In the postulated mechanisms shown above, isomerization is via an initial transition state where the carbon of the iminium system carries some positive charge. Therefore, correlations of the rate constants of isomerization of the salts 55-59, with different substituents on the C_3 phenyl ring that can interact by resonance with C_1 , are made with σ^+ , Figure 5-1.

Electron density at the nitrogen of the iminium system is affected by either mechanism. Substituents on the N-phenyl ring should influence the nitrogen, and therefore correlations of the rate constants of isomerization of iminium salts 60-63 were made with σ^- , Figure 5-2.

In both cases, two lines of opposite slope fit the data, indicating that at least two mechanisms of

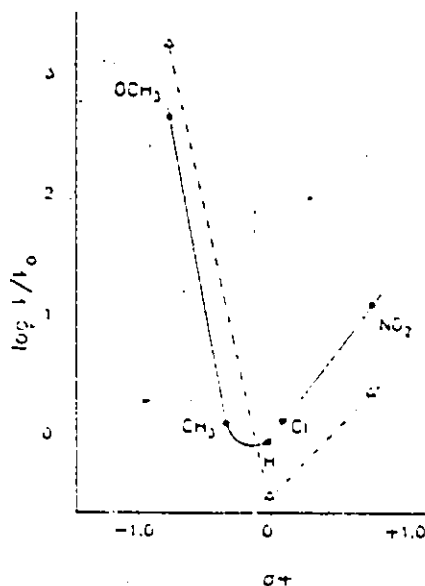


Figure 5-1 Hammett correlations for the rate constants for isomerization of iminium salts with substituents on the C₃ aryl ring, 55-59, in TFA (—) and 55, 57, 59 in H₂SO₄/TFA (---). The latter values are plotted using $\log k(H)$ in TFA as the reference point.

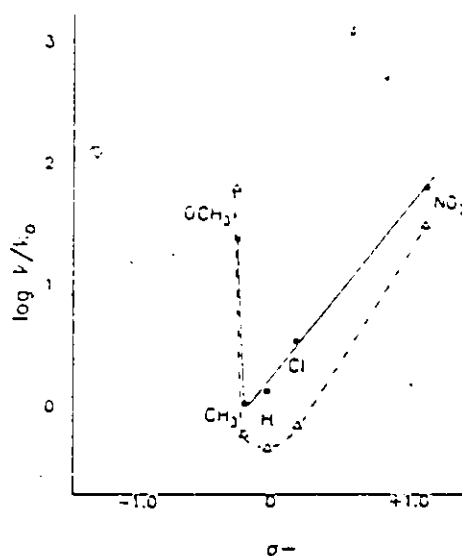
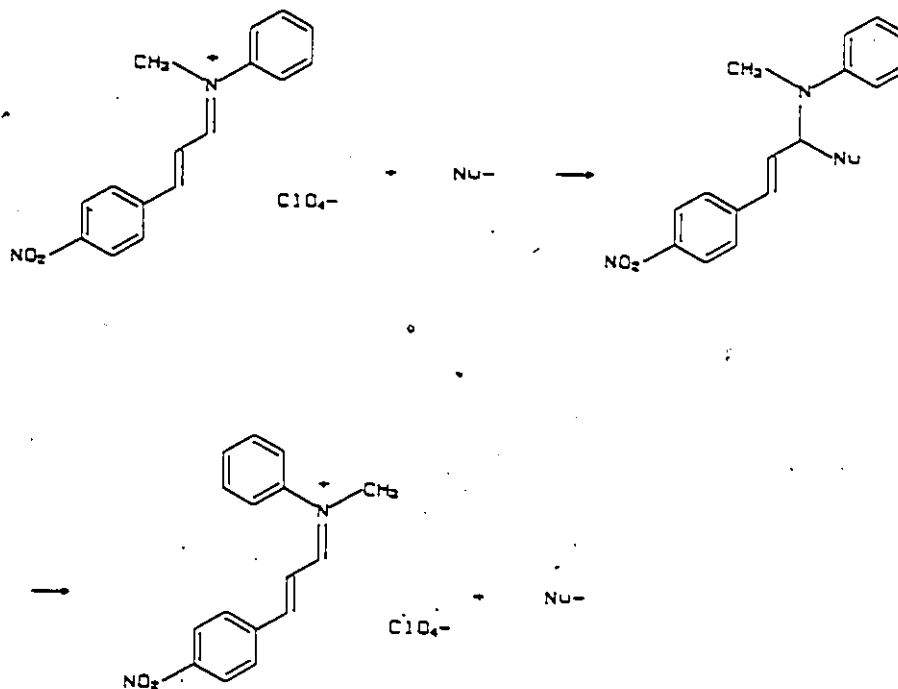


Figure 5-2 Hammett correlations for the rate constants of isomerization of iminium salts with substituents on the N-aryl ring, 57, 60 to 63, in TFA (—) and H₂SO₄/TFA (---). The latter values are plotted using $\log k(H)$ in TFA as the reference point.

isomerization are operative in these iminium salts, depending on the electronic nature of the phenyl substituents.

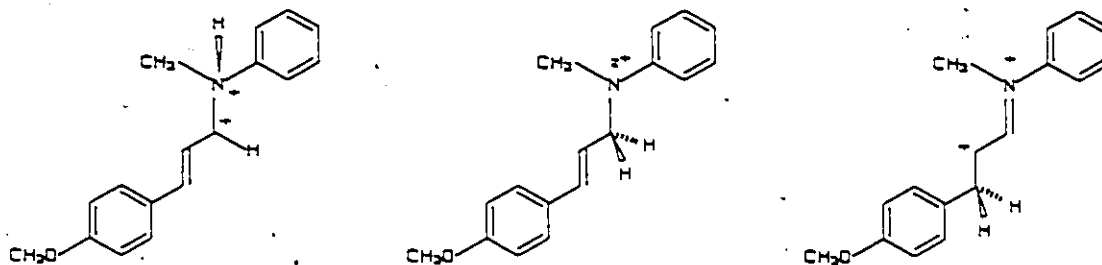
Electron-withdrawing substituents on either phenyl ring increase the rate of isomerization relative to that of the unsubstituted salt, 57. This supports a mechanism in which the addition of a nucleophile to the iminium salt leads to isomerization. In agreement with the prediction, as the acidity of the medium is increased, and its nucleophilicity decreased, the isomerization rates of salts 55-57, 60 and 61 decrease, Figures 5-1 and 5-2.



An alternative to nucleophile addition would be thermally-induced electron transfer.

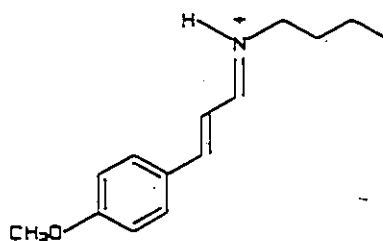
Electron-donating substituents on the C_3 phenyl ring also increase the rate of the reaction relative to that of

the unsubstituted ion, indicating that positive charge is delocalized towards the C₃ phenyl ring in the transition state. At higher acid concentrations the reaction rate increases, so the reaction must be acid catalysed. There are several possible protonation sites on the iminium salt that could lead to isomerization, but only protonation on the nitrogen generates an intermediate with positive charge in conjugation with the substituent on the C₃ phenyl ring.



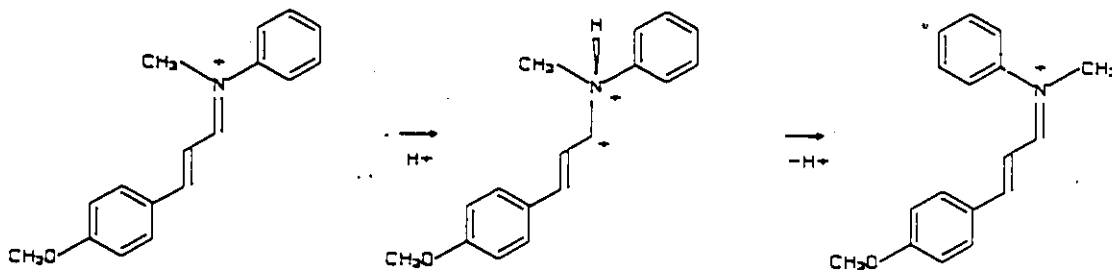
The isomerizations of 55-63 were followed in deuterated trifluoroacetic acid to see if any of the protons in the molecule exchanged with deuterons from the solvent. The samples were heated at 100°C for several half-lives, and only 59 showed evidence of deuterium incorporation. In this case, deuterium was found at C₂, C₆ and C₈, but equilibrium was reached in about one-sixth the time it took for exchange to be observed. Protonation at the C₂, C₆ or C₈ positions does not lead to C=N isomerization by any simple mechanism. The position on the molecule where proton addition could create an intermediate that can isomerize about the C=N bond, but not exchange an existing proton, is at the nitrogen.

Evidence for C=C bond isomerization catalyzed by protonation at this site has been observed previously in iminium ion 98. 150



98

The mechanism that best fits the data is protonation on the nitrogen to form a dication, in which rotation can take place about the C-N bond.



Iminium salt 63, with an electron-donating methoxy substituent on the N-phenyl ring, isomerizes faster than does the unsubstituted salt 57. The isomerization is not a first-order reaction, however the rate is increased and becomes first-order in the stronger acid medium. No deuterium incorporation is observed in the molecule. The evidence points to an isomerization mechanism by protonation on the nitrogen.

The methyl substituted salt, 62, isomerizes more

slowly than the unsubstituted salt, 57, in trifluoroacetic acid, but the rate is increased in the stronger acid medium, indicating that a protonation mechanism is possible in this case as well, at least in the more acidic solution. Salt 62 was heated in a solution of TFA-d/D₂SO₄ for several hours, until equilibrium was reached. The sample was then analyzed by 250 MHz ¹H and ²H NMR. No evidence of deuterium incorporation at any position in the molecule was found. Further analysis by ¹³C NMR confirmed these results.

The observation of a proton-catalyzed isomerization mechanism for salts 62 and 63 was somewhat unexpected since the positive charge of the dication intermediate cannot be delocalized onto the electron-donating N-phenyl ring in any simple manner.

An attempt was made to generate the dication under stabilizing conditions. A solution of iminium salt 59 was made in HF/SbF₅/SO₂ in a dry ice/acetone bath. A 250 MHz ¹H NMR spectrum of the solution at -60°C was identical to a spectrum of a mixture of the E,E and Z,E isomers, 59 and 68. Additional peaks are also present in the spectrum, but these do not correspond to the ¹H NMR signals observed for the phenyl allyl cation.²³⁹

III. Summary

Two mechanisms are responsible for C=N isomerization in these iminium salts, an acid catalysed and a nucleophile catalysed mechanism, depending on the electronic nature of

the substituent on either phenyl ring.

In trifluoroacetic acid, a weakly nucleophilic solvent, nucleophile addition is a viable isomerization mechanism. This suggests that under conditions of greater nucleophilicity, such as aprotic solvents, the predominant pathway for isomerization will be by nucleophile catalysis. A counterion that is a better nucleophile than perchlorate could also contribute to thermal isomerization. In view of these results, and previous similar conclusions about C=C isomerization mechanisms in iminium salts¹⁵⁰, the thermal isomerizations of the retinylidene iminium salts need to be examined. In addition, reaction conditions for photochemical isomerization experiments need to be checked to ensure that catalysed thermal isomerizations are not interfering.

EXPERIMENTAL METHODS

CHAPTER 6
EXPERIMENTAL METHODS

I. Materials and Syntheses

Trifluoroacetic acid (TFA) was distilled from concentrated H_2SO_4 and stored in a dry N_2 atmosphere. TFA-d was used as purchased from Aldrich. Acetonitrile was dried by distilling from CaH_2 and letting stand over activated molecular sieves for 24 hours. Fluorescent impurities in acetonitrile were minimized by using HPLC-grade solvent, and discarding the first 20 ml of distillate.

N-methyl, N-aryl, 3-aryl-2-propenylidene iminium perchlorate

The iminium salts 55-63 and 95 were prepared by the same procedure, outlined here for salt 57. Freshly distilled N-methyl aniline (1.26 mL, 0.012 mol) in 20 mL dry diethyl ether was cooled in an ice bath. A slight excess of perchloric acid (1.2 mL of 70% $HClO_4$, 0.014 mol) was added dropwise. A solution of cinnamaldehyde (1.9 mL, 0.015 mol) in ether (10 mL) was added, the mixture swirled and allowed to stand until the product precipitated from solution, within a few minutes. The product was filtered, washed with ether, recrystallized from acetonitrile/ether, and dried in vacuo overnight.

Physical data and elemental analyses for the salts 55-63 are reported in Tables 2-1 and 2-2. 1H NMR and ^{13}C NMR

data of TFA solutions of these salts are summarized in Tables 2-3 and 2-4 respectively. Some data for iminium salt 95 is given in Tables 6-1 and 6-2.

The reagents required for the syntheses were commercially available with the following exceptions: p-methoxy cinnamaldehyde, p-chlorocinnamaldehyde, p-methylcinnamaldehyde, m-methoxy cinnamaldehyde, and N-methyl-p-chloroaniline. p-methoxycinnamaldehyde, p-chlorocinnamaldehyde, p-methylcinnamaldehyde, m-methoxycinnamaldehyde

These cinnamaldehyde derivatives were synthesized from the corresponding benzaldehyde derivatives and acetaldehyde by aldol condensation reactions using literature procedures.^{240,241}

N-methyl-p-chloroaniline

N-methyl-p-chloroaniline was synthesized by a modified literature procedure.²⁴² Benzaldehyde (6 mL, 0.06 mol) and p-chloroaniline (5.6 g, 0.04 mol) were dissolved in ether (20 mL), and left standing at room temperature for several hours. The solution was dried with K_2CO_3 and the solvent was evaporated to give a pale yellow solid, which was dried in vacuo for three hours. The solid was dissolved in toluene (20 mL), and dimethylsulfate, $(CH_3O)_2SO_2$, (5 mL, 6.5 g, 0.05 mol) was added. The solution was refluxed for 1 hour, H_2O was added (20 mL) and the solution was refluxed again for twenty minutes. After cooling the solution to room temperature, the two layers were separated, and the aqueous

Table 6-1

Physical and Spectroscopic Data for N-methyl, N-phenyl-3-(m-methoxyphenyl)-2-propenylidene iminium perchlorate, 95

m.p. (°C)	$\nu_{\text{CN}} (\text{cm}^{-1})$	$\lambda_{\text{max}} (\text{nm})$	photostationary state			
			%EE	%ZE	%EZ	%ZZ
121-122	1611	346	44	28	20	8

Table 6-2

^1H NMR Data for Iminium Salt 95^{a,b}

	H ₁	H ₂	H ₃	Aryl H	CH ₃	OCH ₃	J _{1,2} (Hz)	J _{2,3} (Hz)
EE	8.43d	<u>c</u>	7.98d	7.46-7.32m, 7.16-7.14m	3.95s	3.86s	11	15
ZE	8.61d	6.60dd	7.91d	7.55-6.97m	3.91s	3.77s	11	15
EZ	8.48d	6.85dd	8.14d		3.97s	3.79s	11	11
ZZ	8.68d	6.12dd	7.80d		3.93s	<u>c</u>	11	11

^ain ppm, referenced to $\text{N}(\text{CH}_3)_4^+\text{BF}_4^-$ at 3.10 ppm, in trifluoroacetic acid

^bs = singlet, d = doublet, dd = doublet of doublets, m = multiplet(s)

^cpeaks hidden

layer extracted with ether. The aqueous fraction was made basic with KOH, and cooled to give two layers. After separation of the layers, the top layer, containing the amine, was dried over KOH, and distilled from KOH (bp 120°C/4 mm). The distilled product contained unreacted p-chloroaniline, N-methyl-p-chloroaniline, and N,N-dimethyl-p-chloroaniline. Separation was achieved by column chromatography (silica gel, eluted with pet. ether/ether (10:30)). Yield was 2.8 g (50%).

II. Crystallization of E,E and Z,E Isomers

A mixture of E,E and Z,E isomers (1:1.5 by ^1H NMR) of iminium salt 57 was generated by dissolving 57 in CD_3NO_2 . Dry diethyl ether was added dropwise to the sample to start crystallization. The crystals were filtered, washed with ether, dried and redissolved in TFA. No evidence of the Z,E isomer was seen in the TFA solution by ^1H NMR, and no precipitation occurred from the CD_3NO_2 solution on further ~~ether~~ addition.

III. Instrumental Techniques

NMR Spectra

^1H NMR spectra of the iminium salts 55-63 were recorded on a Bruker WM250 spectrometer. A spectrum of 95 was recorded on a Bruker AM500 spectrometer. The solvent used was trifluoroacetic acid, and the spectra are referenced to an internal standard, tetramethylammonium tetrafluoro-

borate, $(\text{CH}_3)_4\text{NBF}_4$, at 3.10 ppm. Data are given in Tables 2-3 and 6-2.

^{13}C NMR spectra were recorded on either a Bruker WP80 spectrometer at 20.1 MHz or a Bruker WM250 spectrometer at 62.9 MHz. The ^{13}C NMR spectra are referenced to the CF_3 quartet of the solvent, CF_3COOH , at 114.7 ppm. Solutions of the iminium salts contained TFA-d or D_2SO_4 as lock compounds for the spectra recorded on the WP80 spectrometer. Data are reported in Table 2-4.

Mixtures of the E,E and Z,E isomers of the iminium salts were generated by heating the iminium salt in TFA at 100°C in sealed NMR tubes for several days. The resonances of the Z,E isomers were obtained from ^1H NMR spectra of the mixtures, and were assigned by comparison to the spectra of the E,E isomers, and by selective decoupling experiments. Data are given in Tables 2-5 and 6-2.

Solutions of the iminium salts in TFA were irradiated in a Rayonet photoreactor with 350 nm lamps to generate mixtures of the E,E, Z,E, E,Z, and Z,Z isomers. ^1H NMR spectra of these mixtures were used to identify the resonances of the E,Z and Z,Z isomers. In each case, a spectrum of the mixture after a short irradiation period, corresponding to about ten percent conversion of the E,E isomer, was used to identify and assign the resonances of the E,Z isomer, and a mixture obtained after a longer irradiation time was used to assign the resonances of the Z,Z isomer.

Data are summarized in Tables 2-6 and 6-2.

A Varian EM390 spectrometer was used to record ^1H NMR spectra for kinetic measurements, and Bruker WM250 or AM500 spectrometers were used to record ^1H NMR spectra for quantum yield analyses.

The solid state ^{13}C NMR spectrum was obtained by B. Sayer at 75.5 MHz on a Bruker 300 MHz spectrometer. Data are given in Table 2-4.

Absorption Spectra

Absorption spectra were recorded on either a Pye Unicam SP8-100, a Hewlett Packard 8451A, or a Perkin-Elmer Lambda 9 spectrophotometer.

Solutions of iminium salts 55-63 and 95 (about 10^{-5} M) in TFA were placed in 1 cm quartz UV cells to record their absorption spectra. Data are summarized in Tables 2-2 and 3-5.

Fluorescence Spectra

Fluorescence spectra were recorded on a Perkin-Elmer LS-5 fluorescence spectrophotometer. Solutions of iminium salts 55-63 in acetonitrile at concentrations of about 10^{-4} M, in 1 cm quartz fluorescence cells, were used in attempts to obtain room temperature fluorescence spectra. Low temperature attempts were made on a solution of 57 (about 10^{-3} M) in $\text{H}_2\text{SO}_4/\text{TFA}/\text{acetic acid}$ (2:2:1), which forms a glass at 77K. The sample was placed in a quartz cell (3mm o.d.), and cooled quickly in a dewar containing liquid N_2 to form

the glass. The sample was then transferred into the sample compartment, which was also cooled by liquid N_2 .

Fluorescence spectra of benzil or 97 in acetonitrile were obtained on degassed solutions at room temperature. A stream of dry N_2 was bubbled through acetonitrile to saturate the gas, and then bubbled into the solution in a 1 cm fluorescence cuvette through a rubber septum. The septum was separated from the solvent by teflon tape. After twenty minutes, the bubbling was stopped, the cell was sealed with parafilm, and the spectrum recorded. Both excitation and emission spectra were recorded, to ensure that emission was arising from the desired species. The intensities of the emission peaks remained constant for at least fifteen minutes, after which some reduction in intensity caused by O_2 quenching of the excited state was observed.

Infrared Spectra

Infrared spectra were recorded on a Nicolet 7199 FTIR spectrometer. The samples were prepared as KBr discs, using KBr that had been dried at $80^\circ C$ for several days. The frequencies measured are accurate to within 0.01 cm^{-1} , referenced by an internal He-Ne laser.

Cyclic Voltammetry

The glassware, working and auxiliary electrodes used in the experiment were rinsed with solvent, and oven dried ($80^\circ C$, overnight). The supporting electrolyte, tetrabutylammonium perchlorate was dried in vacuo, and stored in a

dessicator. The reference electrode, a saturated calomel electrode (SCE), was separated from the bulk solution in the cell by a glass frit.

The reductions of 55-63, 16 and N,N-dimethyl retinylidene iminium perchlorate were observed by cyclic voltammetry by the following procedure. A solution of tetrabutylammonium perchlorate (150 mg, 0.1 M) in acetonitrile (3 mL) was degassed by bubbling argon through it for 5 minutes. The argon was previously saturated with acetonitrile to minimize evaporation of the solvent. The background was recorded from +0.3V to -1.5V. The iminium salt was added to this solution (3 mg, about 10^{-5} mol, 3×10^{-3} M), the degassing repeated, and the reduction wave recorded. The scan rate used in the measurements was 0.5 V/s. The data are given in Table 4-1. The reduction of 57 was also measured at various scan rates, from 0.1 V/s to 2.0 V/s. Data are presented in Table 4-2.

Miscellaneous

The melting points of iminium salts 55-63 and 95, given in Tables 2-1 and 6-1, were measured on a Kofler Hot Stage melting point apparatus, and are not corrected.

Elemental analyses were obtained at either the Guelph Chemical Laboratories, or Galbraith Laboratories, Inc. Data are summarized in Table 2-1.

IV. Triplet-Triplet Energy Transfer Experiment

A solution of benzil in acetonitrile (about 10^{-5} M) was degassed by the procedure outlined above, and emission spectra were recorded at excitation wavelengths of 520 and 570 nm. Iminium salt 60 was added to this solution, which was then degassed again. An absorption spectrum gave the approximate concentration of iminium salt, 3×10^{-3} M. At 370 nm, the iminium salt absorbs >95% of the light. Emission spectra of this solution were obtained at excitation wavelengths of 320 and 370 nm.

V. Quantum Yield Measurements

Optical Bench

The optical bench consisted of a high pressure 150 W Xenon lamp housed in a Photochemical Research Associates lamp housing (ALH 215), and powered by a PRA power supply (M303). A water-cooled IR filter containing distilled water removed infrared radiation. The lamp was focussed onto the entrance slit of the monochromator (Jobin Yvon H.10). The entrance and exit slits used allow a 16 nm bandpass. The wavelength isolated for the quantitative experiments was 366 nm. The light was further filtered to remove higher order wavelengths of light, and collimated by a lens. The beam was then split by a glass plate set at 45° to the beam. A fraction of light was directed to a detector at 90° to the main beam (the comparison detector), the remainder passed to the sample,

which was placed in front of a second detector (the main detector). All parts of the optical train were mounted on an aluminium rail, and the entire optical bench was contained in a light-tight box. The detectors were UV enhanced silicon photodiodes (EG & G Instruments, UV 040 BQ). The diode signals were converted to digital output by a two channel digital current integrator, built by C. Schonfeld (Chemistry Department, McMaster University).

Actinometry

Ferrioxalate actinometry, following literature methods,²⁴³⁻²⁴⁶ was used to quantitate the light absorbed by the sample. The 0.06 M ferrioxalate actinometry solution was placed in a cylindrical cell in the sample holder and irradiated for a short period of time (5-8 minutes). The solution was not stirred, but the irradiation was stopped and the solution shaken several times during the experiment. The current reaching the comparison detector was recorded, as a number of counts. The main detector, behind the sample, did not detect light since the solution absorbed all the incident light. The number of photons incident on the sample were determined from the absorbance of a solution prepared from the irradiated actinometry solution,²⁴³ and used to calibrate the detector, as photons/count. The spectrometer used for measuring absorbance was calibrated with FeSO_4 solutions similar to the actinometry solutions, of known concentration. The response was linear for the absorbance range 0.09

to 0.8.

The calibrations of the optical bench were performed in duplicate, and were reproducible within 1%. Calibrations were performed once for a series of experiments extending over a period of four or five days. The stability of the system was checked by measuring the ratio of light entering the two detectors in the absence of the sample.

Quantum Yields

The glassware used for the measurements consisted of two parts, a cylindrical, quartz cell of volume 0.5 mL for the irradiation, and a glass arm in which the samples were prepared and degassed. The iminium salt was weighed into the container, and 0.5 mL of trifluoroacetic acid was added, from a calibrated glass pipette. The container was attached to a vacuum line with adaptors that contained a teflon stopcock, and that allowed N₂ to be added after the degassing was complete. The solutions was degassed with three freeze (77K), pump, and thaw cycles. After the cell was evacuated for the third time, it was filled with dry N₂. The container was closed with the stopcock, the sample transferred into the quartz portion of the container, and placed in the optical bench. The samples were irradiated for periods of time corresponding to about 10% reaction, usually about two hours. The sample compartment remained at room temperature during this time. After irradiation, about 0.3 mL of the sample was transferred to an NMR tube for analysis.

It was necessary to protect the samples from room light during the manipulations to avoid unwanted photochemical reactions, and to store the solutions in the refrigerator until analysis to avoid thermal reactions.

The quantum yields were measured for solutions of iminium salts 55-63 in TFA of concentrations about 0.04 M, 0.07 M and 0.09 M. Iminium salt 60 was not soluble enough in TFA to allow a measurement at the highest concentration. The values were corrected for small amounts of isomers other than the E,E isomer present before irradiation. The quantum yields of salts 56, 57 and 62 are corrected for isomerization that occurred during the sample preparation. The quantum yields of salt 58 are corrected for an impurity present in the salt, whose ^1H NMR spectrum contains a resonance that overlaps the resonance of H_1 of the Z,E isomer, 67. The values are not corrected for back reactions of the isomers produced during the irradiation. Raw data for the quantum yield measurements are given in Tables 6-3 and 6-4.

Quantum yields of isomerization were also measured for iminium salt 60 in 0.01 M sodium trifluoroacetate in TFA, 0.1 M sodium trifluoroacetate in TFA, and 0.1 M tetramethyl ammonium chloride in TFA. Quantum yields for iminium salt 59 were measured in 0.01 M sodium trifluoroacetate in TFA and 0.03 M H_2SO_4 in TFA. These values are corrected for thermal isomerization that occurred during the manipulation of the samples. Raw data for these experiments are given in

Table 6-5.

The quantities of each isomer present in the irradiated mixture were determined from ^1H NMR spectra of the solutions, obtained at room temperature. The detection-limit was about 0.5% when 1200 scans were used for the spectra. The relative isomer amounts were measured as peak areas (by cut and weigh) of the H_1 and H_3 peaks, and in some cases, where these are not sufficiently resolved, the H_2 peaks were used as well. The total peak areas were assumed to equal the quantity of E,E isomer initially used in the experiment, the amounts of each isomer were then determined from the relative areas of their respective peaks. The results were generally reproducible within 10%.

The relative isomerization quantum yields for the iminium salt 95, Table 3-5, were obtained by the same procedure, however the lamp was not calibrated for the irradiation.

VI. Photostationary States

Solutions of the iminium salts 55-63 and 95 in TFA were placed in NMR tubes, and irradiated for 36 hours or more in a Rayonet photoreactor (350 nm lamps, 50 nm bandwidth). The resulting mixtures were analysed by ^1H NMR. Relative isomer concentrations were determined from the peak areas of the resonances of H_1 , H_2 , and H_3 , as outlined for the quantum yield measurements. Data are given in Tables 3-4 and 6-1.

Table 6-3
Raw Quantum Yield Data for the Iminium Salts 55 - 59 in Trifluoroacetic Acid

Reaction	% Corr.	Wgt(g) x 10 ²	Moles x 10 ⁵	% Conv.	Corrected % Conv.	Moles Conv. x 10 ⁶	Einsteins of Light x 10 ⁶	ϕ
55 → 64	1.50	1.980	5.399	5.23	3.73	2.01	6.84	0.295
"	"	1.400	3.817	5.50	4.00	1.53	5.15	0.297
"	"	0.825	2.249	8.70	7.20	1.62	4.33	0.374
"	"	1.880	5.126	2.83	1.33	0.682	2.27	0.301
"	"	1.400	3.817	3.19	1.69	0.645	1.96	0.329
"	"	0.780	2.127	3.47	1.97	0.419	1.61	0.260
56 → 65	5.97	1.560	4.380	8.31	2.34	1.02	5.45	0.187
"	"	1.175	3.299	8.70	2.73	0.901	5.11	0.176
"	"	0.790	2.218	9.55	3.58	0.794	3.81	0.208
56 → 74	0.84	1.560	4.380	3.14	2.30	1.01	5.45	0.185
"	"	1.175	3.299	3.66	2.82	0.930	5.11	0.182
"	"	0.790	2.218	3.92	3.08	0.683	3.81	0.179
57 → 66	2.10	1.615	5.019	5.12	3.02	1.516	8.10	0.187
"	"	1.170	3.636	5.71	3.61	1.313	6.54	0.200
"	"	0.790	2.455	5.85	3.75	0.921	4.42	0.208
57 → 75	-	1.615	5.019	4.03	4.03	2.02	8.10	0.249
"	"	1.170	3.636	5.14	5.14	1.87	6.54	0.286
"	"	0.790	2.455	4.26	4.26	1.05	4.42	0.237
58 → 67	3.40	1.750	5.212	6.91	3.51	1.83	12.96	0.141
"	"	1.190	3.544	7.87	4.47	1.58	9.77	0.162
"	"	0.795	2.368	6.46	3.06	0.725	5.73	0.127
58 → 76	-	1.750	5.212	4.46	4.46	2.32	12.96	0.179
"	"	1.190	3.594	4.58	4.58	1.62	9.77	0.166
"	"	0.795	2.368	3.81	3.81	0.902	5.73	0.157
59 → 68	-	1.450	4.122	7.64	7.64	3.15	12.63	0.249
"	"	1.040	2.956	8.84	8.84	2.61	9.42	0.277
"	"	0.750	2.132	7.25	7.25	1.55	7.12	0.218
59 → 77	-	1.450	4.122	3.42	3.42	1.41	12.63	0.112
"	"	1.040	2.956	3.68	3.68	1.09	9.42	0.116
"	"	0.750	2.132	3.85	3.85	0.821	7.12	0.115

Table 6-4
Raw Quantum Yield Data for Iminium Salts 60 - 63 in Trifluoroacetic Acid

Reaction	% Corr.	Wgt(g) $\times 10^2$	Moles $\times 10^5$	% Conv.	Corrected & Conv.	Moles Conv. $\times 10^6$	Einsteins of Light $\times 10^6$	ϕ
60 → 69	-	1.175	3.204	5.18	5.18	1.66	7.88	0.211
"	-	0.950	2.590	4.75	4.75	1.23	6.57	0.187
"	-	0.825	2.249	4.49	4.49	1.01	5.43	0.186
60 → 78	-	1.175	3.204	6.49	6.49	2.08	7.88	0.264
"	-	0.950	2.590	5.21	5.21	1.35	6.57	0.205
"	-	0.825	2.249	4.98	4.98	1.12	5.43	0.206
60 → 87	-	1.175	3.240	4.40	4.40	1.41	7.88	0.179
"	-	0.950	2.590	2.28	2.28	0.59	6.57	0.090
"	-	0.825	2.249	2.62	2.62	0.59	5.43	0.108
61 → 70	1.50	1.940	5.446	4.38	2.88	1.57	11.31	0.139
"	"	1.210	3.397	5.18	3.68	1.25	8.85	0.141
"	"	0.825	2.316	5.62	4.12	0.954	5.40	0.177
61 → 79	-	1.940	5.446	2.86	2.86	1.56	11.31	0.138
"	-	1.210	3.397	4.30	4.30	1.46	8.85	0.165
"	-	0.825	2.316	4.32	4.32	1.00	5.40	0.185
62 → 80	5.20	1.570	4.676	8.83	3.63	1.70	9.29	0.183
"	"	1.140	3.395	9.11	3.91	1.33	5.91	0.225
"	"	0.790	2.353	10.89	5.69	1.34	4.76	0.282
62 → 80	0.59	1.570	4.676	3.50	2.91	1.36	9.29	0.146
"	"	1.140	3.395	3.85	3.26	1.11	5.91	0.188
"	"	0.790	2.353	4.69	4.10	0.965	4.76	0.203
63 → 72	1.50	1.515	4.307	6.52	5.02	2.16	11.61	0.186
"	"	0.995	2.828	6.02	4.52	1.28	7.70	0.166
"	"	0.750	2.132	5.86	4.36	0.930	5.39	0.173
63 → 81	-	1.515	4.307	2.68	2.68	1.15	11.61	0.099
"	-	0.995	2.828	3.54	3.54	1.00	7.70	0.130
"	-	0.750	2.132	3.22	3.22	0.687	5.39	0.127

Table 6-5
Raw Quantum Yield Data for Iminium Salts 59 and 60 in Various Solutions

Reaction	% Corr.	Wgt(g) x 10 ²	Moles x 10 ⁵	% Conv.	Corrected % Conv.	Moles Conv. x 10 ⁶	Einsteins of Light x 10 ⁶	ϕ
55 → 64 ^a	1.9	1.865	5.085	3.27	1.37	0.697	1.94	0.36
"	"	1.300	3.545	3.02	1.12	0.396	1.45	0.27
"	"	0.810	2.209	3.40	1.50	0.331	1.04	0.32
"	2.2	1.030	2.808	6.27	4.06	1.14	4.56	0.25
55 → 64 ^b	1.85	0.980	2.672	4.68	2.83	0.756	2.20	0.344
55 → 64 ^c	1.93	0.955	2.604	5.34	3.41	0.890	3.15	0.282
59 → 68 ^a	-	0.840	2.388	4.85	4.85	1.16	8.84	0.131
59 → 77 ^a	-	"	"	4.95	4.95	1.18	"	0.133
59 → 68 ^d	1.66	0.805	2.280	5.62	3.96	0.906	6.22	0.146
59 → 77 ^d	-	"	"	3.35	3.35	0.766	"	0.123

^a 0.01 M Na⁺CF₃COO⁻/TFA

^b 0.1 M Na⁺CF₃COO⁻/TFA

^c 0.1 M (CH₃)₄N⁺Cl⁻/TFA

^d 0.03 M H₂SO₄/TFA

VII. Electron Transfer Experiments

Luminescence Quenching Experiments

The electron donor tris(2,2'-bipyridine)ruthenium(II) dichloride, 97, was synthesized by a literature procedure.²⁴⁷ Quenching experiments were performed using iminium salts 55-60, as follows. Solutions of about 10^{-6} to 10^{-5} M 97 in acetonitrile were degassed and an absorption spectrum was recorded to estimate the concentration of 97. An emission spectrum of the solution was obtained at excitation wavelengths ≥ 520 nm. An excess of iminium salt was then added (about 100-fold excess), and the solution was degassed again. The absorption spectrum of the solution was used to estimate the concentration of iminium salt in the solution, and to determine the extent of iminium salt absorption at the wavelength of irradiation in the luminescence experiment. The solution was then irradiated at a wavelength that allowed absorption by 97, but minimized absorption by the iminium salt, and the emission spectrum recorded. The decrease in the emission peak, at the maximum, was compared to the increase in absorption at the irradiating wavelength to determine whether quenching had occurred. Data for the experiments are given in Table 4-3.

NMR Experiments

Solutions of iminium salts 57 or 60 and 97 in TFA were irradiated to examine electron transfer by product analyses. In the absence of light, at room temperature, 97

did not decompose in TFA. The rate of thermal isomerization of 60 in TFA was not enhanced by 97.

Iminium salt 60 (5 mg, 4.5×10^{-2} M) and 97 (5 mg, 2.6×10^{-2} M) were dissolved in 0.3 mL TFA in an NMR tube, and irradiated with light of wavelength >425 nm. The light source used was a 150 W Xenon lamp. The desired range of wavelengths was achieved by placing two cut-off filters in the light path. The reaction was monitored by ^1H NMR (EM 390). The peak height of the N-methyl signal of the E,E isomer of 60 relative to the sum of the peak heights of the E,E and Z,E isomers was used to determine percent composition of the mixture.

A similar experiment was performed for iminium salt 57. In addition, a photomixture of the four isomers of 57 was generated by irradiating a TFA solution of the salt in an NMR tube in a Rayonet photoreactor for >12 hours. Salt 97 was added to this mixture and the solution was irradiated and monitored as outlined above.

VIII. Thermal Experiments

The 0.01 M H_2SO_4 /trifluoroacetic acid mixture was made by diluting 0.04 mL of 100% H_2SO_4 to 50.00 mL with TFA.

H_O Measurements

The acidity of the solvents used in these experiments was determined by the Hammett indicator method, using 2,4-dinitroaniline.²⁴⁸ The values found were TFA, -4.3; TFA-d, -4.0; 0.01 M H_2SO_4 /TFA, -5.4.

Kinetic Measurements

The iminium salt (about 25 mg, 7×10^{-5} mol, 0.2 M) and an internal standard, tetramethylammonium tetrafluoroborate (about 3 mg) were dissolved in TFA (about 0.3 mL) in a medium-walled NMR tube. The tube was then sealed, and a ^1H NMR spectrum obtained. The concentration measure used in the experiments was the peak height of the N-CH_3 peak relative to the peak height of the signal of the internal standard. The widths at half height of these peaks were similar. The reaction did not take place at room temperature, or at the probe temperature of the NMR instrument (34°C) at an appreciable rate. The sample tube was placed in a constant temperature bath (refluxing water, $100 \pm 1^\circ\text{C}$). At regular intervals, the reaction was stopped by cooling the tube quickly to room temperature. ^1H NMR spectra of the mixture were used to monitor the change in the sample. The decrease in the height of the NCH_3 peak of the E,E isomer (relative to the internal standard) was monitored in all cases except 59, where the increase of the peak height of the NCH_3 signal of the product isomer, the Z,E isomer, was followed.

The reactions were monitored until two-thirds complete. The samples were then heated until a constant EE/ZE ratio was maintained. The relative isomer ratio was determined by measuring the relative peak heights of the NCH_3 peaks whenever possible. For 59 and 63, other peaks in the

spectrum were used.

At longer heating times for iminium salts 56, 57, 58 and 62 in TFA, and also 61 in H_2SO_4/TFA , an additional product was observed in the solutions by 1H NMR, but this product(s) was not present during the kinetic measurements in amounts detectable by the NMR technique used (about 10% detection limit).

The rates of isomerization were determined using equation 21.²⁴⁹

$$\ln (A_0 - A_e / A - A_e) = (k_f + k_r)t \quad [21]$$

A = concentration of E,E isomer at time t

A_0 = initial concentration of E,E isomer

A_e = equilibrium concentration of E,E isomer

k_f , k_r = rate constants for the forward and back reactions, respectively

A graph of $\ln (A_0 - A_e / A - A_e)$ versus time gave the sum of the forward and reverse rate constants as the slope of the graph. The rate constants can be separated using equation 22.

$$A_e / B_e = k_r / k_f \quad [22]$$

B_e = equilibrium concentration of the Z,E isomer

As an example, raw data for the isomerization of iminium salt 58 is shown in Table 6-6.

For the analysis of the reaction of 59, equation 23 was used.

$$\ln (B_e / B_e - B) = (k_f + k_r)t \quad [23]$$

B = concentration of Z,E isomer at time t

Each rate constant reported is the average of the results of at least two experiments. The rate constant for the isomerization of 63 in TFA is estimated from the half reaction time.

Deuterium Incorporation

The isomerizations of the iminium salts 55-63 were followed in TFA-d. Estimates of the reaction rate at 100°C were obtained from one-point kinetics, and are given in Table 6-7. The samples were heated in sealed tubes as described above. The samples were cooled once during the isomerization, to determine the concentrations of the two isomers by ^1H NMR. The height of the NCH_3 signal of the Z,E isomer relative to the total peak heights of the NCH_3 peaks of the Z,E and E,E isomers was used to estimate the concentration of the Z,E isomer. The samples were allowed to equilibrate for >5 half-lives, and as many as 20 half lives for 58, 59, 62 and 63. Evidence for deuterium incorporation was sought in the ^1H NMR spectra (EM390), and for 63 at 250 MHz (Bruker WM250).

Deuterium incorporation in salt 62 was further investigated in the stronger acid made by combining TFA-d (0.3 mL) and D_2SO_4 (10^{-3} mL). The sample was heated to equilibrium, about 3 hours at 100°C. Spectral techniques used to examine the mixture were ^1H NMR (WM 250), ^2H NMR (WM 250) and ^{13}C NMR (WP 80). For the latter two spectra, the sample was diluted to about 2 mL with TFA.

Table 6-6

Raw Rate Data for the Isomerization of
Iminium Salt 58 to 67 in TFA at 100°C^a

time (min.)	A ₀	A _e	A	X = A ₀ -A _e /A-A _e	ln X
0	1.46	0.67	1.46	1	0
1090			1.36	1.14	0.13
2540			1.20	1.49	0.40
4190			1.09	1.88	0.63
5565			1.01	2.32	0.84
6870			0.98	2.55	0.94
8110			0.92	3.16	1.15
9725			0.86	4.16	1.43

^aestimated error in concentration measurements is ±10%

Table 6-7

Approximate Rate Constants for the Isomerizations of
Iminium Salts 55-63 in TFA-d at 100°C^a

Reaction	$k_f(s^{-1})$ $\times 10^6$	$k_r(s^{-1})$ $\times 10^6$	# half lives	D incorp.
55 → 64	28	20	7	no
56 → 65	14	11	12	no
57 → 66	3.3	2.7	5	no
57 → 66	2.6	2.1	6	no
58 → 67	2.6	2.4	5	no
59 → 68	>500	>500	20	H ₂ , H _{6,8}
60 → 69	83	97	110	no
61 → 70	17	16	12	no
61 → 70	4.1	3.7	4	no
62 → 71	5	4	30	no
63 → 72	>180	>150	30	no

^aestimated error +30%

Super-Acid Solution of Iminium Salt 57

The sample was prepared by transferring about 0.05 mL HF/SbF₅ into an NMR tube in a N₂-filled glove bag, and cooling the tube in a dry ice/acetone bath. SO₂ was condensed into the tube until a volume of 0.3 mL was obtained. The mixture was stirred with a glass rod. The iminium salt, 57 (about 20 mg), and a reference compound, tetramethylammonium tetrafluoroborate (about 3 mg), were added so that they remained on the inner walls of the tube, and the solution stirred to mix the salts in slowly. The sample was kept cold. ¹H NMR spectra were recorded at -60°C, -35°C, and -20°C. At the highest temperature, the sample began to decompose.

REFERENCES

REFERENCES

1. R. Uhl, E.W. Abrahamson, *Chem. Rev.*, 81, 291-312 (1981).
2. V. Balogh-Nair, K. Nakanishi in "New Comprehensive Biochemistry", Ch. Tamm, Ed., Elsevier Biomedical Press: Amsterdam, Vol. 3, 1982, pp. 283-334.
3. K. Nakanishi, *Pure and Appl. Chem.*, 57, 769-776 (1985).
4. P.S. Zurer, *Chem. Eng. News*, 61, Nov. 28, 24-35 (1983).
5. N.A. Dencher, *Photochem. Photobiol.*, 38, 753-767 (1983).
6. H.J.A. Dartnall in "The Eye", H. Dawson, Ed., Academic Press: New York, Vol. 2, 1962, pp. 523-533.
7. A. Cooper, *Nature (London)*, 282, 531-533 (1979).
8. T. Seki, R. Hara, T. Hara, *Photochem. Photobiol.*, 32, 469-479 (1980).
9. J. Schwemer, *J. Comp. Physiol. A*, 154, 535-547 (1984).
10. G. Eyring, B. Curry, A. Broek, J. Lugtenburg, R. Mathies, *Biochemistry*, 21, 384-393 (1982).
11. K.J. Rothschild, W.A. Cantore, H. Marrero, *Science*, 219, 1333-1335 (1983).
12. K.A. Bagley, V. Balogh-Nair, A.A. Croteau, G. Dollinger, T.G. Ebrey, L. Eisenstein, M.K. Hong, K. Nakanishi, J. Vittitow, *Biochemistry*, 24, 6055-6071 (1985).
13. K.A. Bagley, L. Eisenstein, T.G. Ebrey, M. Tsuda, *Biophys. J.*, 47, 234A (1985).

14. I. Palings, R.A. Mathies, J.A. Pardoen, C. Winkel, J. Lugtenburg, *Biophys. J.*, 47, 358A (1985).
15. J. Shriver, G. Mateescu, R. Fager, D. Torchia, *Nature (London)*, 270, 271-273 (1977).
16. B. Honig, U. Dinur, K. Nakanishi, V. Balogh-Nair, M.A. Gawinowicz, M. Arnaboldi, M.G. Motto, *J. Am. Chem. Soc.*, 101, 7084-7086 (1979).
17. C. Longstaff, R.R. Rando, *Biochemistry*, 24, 8137-8145 (1985).
18. S.O. Smith, J. Lugtenburg, R.A. Mathies, *J. Membr. Biol.*, 85, 95-109 (1985).
19. W.H. Waddell, J. Lecomte, J.L. West, U.E. Younes, *Photochem. Photobiol.*, 39, 213-219 (1984).
20. N. Sasaki, F. Tokunaga, T. Ogurusu, T. Yoshizawa, *Photobiochem. Photobiophys.*, 7, 341-347 (1984).
21. A. Cooper, *Chem. Phys. Lett.*, 99, 305 (1983).
22. K. Peters, M.L. Applebury, P.M. Rentzepis, *Proc. Natl. Acad. Sci. U.S.A.*, 74, 3119-3123 (1977).
23. M. Tsuda, F. Tokunaga, T.G. Ebrey, K.T. Yue, J. Marque, L. Eisenstein, *Nature (London)*, 287, 461-462 (1980).
24. T.G. Monger, R.R. Alfano, R.H. Callender, *Biophys. J.*, 27, 105-115 (1979).
25. T. Kobayashi, *FEBS Lett.*, 106, 313-316 (1979).
26. A.J. Pande, R.H. Callender, T.G. Ebrey, M. Tsuda, *Biophys. J.*, 45, 573-576 (1984).

27. N. Wada, T. Ura, H. Suzuki, *J. Phys. Soc. Japan*, 53, 3717-3727 (1984).
28. R.H. Callender, T. Suzuki, *Biophys. J.*, 34, 261-270 (1981).
29. A.G. Doukas, M.R. Junnarkar, R.R. Alfano, R.H. Callender, T. Kakitani, B. Honig, *Proc. Natl. Acad. Sci. U.S.A.*, 81, 4790-4794 (1984).
30. A.G. Doukas, M.R. Junnarkar, R.R. Alfano, R.H. Callender, V. Balogh-Nair, *Biophys. J.*, 47, 795-798 (1985).
31. S.J. Milder, D.S. Kliger, *Biophys. J.*, 49, 567-570 (1986).
32. R.S.H. Liu, A.E. Asato, *Proc. Natl. Acad. Sci. U.S.A.*, 82, 259-263 (1985).
33. H. Akita, S.P. Tanis, M. Adams, V. Balogh-Nair, K. Nakanishi, *J. Am. Chem. Soc.*, 102, 6370-6372 (1980).
34. J. Buchert, V. Stefancic, A.G. Doukas, R.R. Alfano, R.H. Callender, J. Pande, H. Akita, V. Balogh-Nair, K. Nakanishi, *Biophys. J.*, 43, 279-283 (1983).
35. R.D. Calhoon, R.R. Rando, *Biochemistry*, 24, 3029-3034 (1985).
36. R.D. Calhoon, R.R. Rando, *Biochemistry*, 24, 6446-6452 (1985).
37. C. Longstaff, R.D. Calhoon, R.R. Rando, *Biophys. J.*, 49, 32A (1986).

38. G. Wald, J. Durell, R.C.C. St. George, *Science*, 111, 179-181 (1950).
39. A. Kropf, R. Hubbard, *Ann. N.Y. Acad. Sci.*, 74, 266-280 (1958).
40. K. Azuma, M. Azuma, W. Sickel, *J. Physiol.*, 271, 747-759 (1977).
41. C.D.B. Bridges, *Exp. Eye Res.*, 22, 435-455 (1976).
42. R.A. Henselman, M.A. Cusanovich, *Biochemistry*, 15, 5321-5325 (1976).
43. T. Kouyama, R.A. Bogomolni, W. Stoeckenius, *Biophys. J.*, 48, 201-208 (1985).
44. D. Oesterhelt, N. Meentzen, L. Schuhmann, *Eur. J. Biochem.*, 40, 453-463 (1973).
45. M.J. Pettei, A.P. Yudd, K. Nakanishi, R. Henselman, W. Stoeckenius, *Biochemistry*, 16, 1955-1959 (1977).
46. A. Lewis, J. Spoonhower, R.A. Bogomolni, R.H. Lozier, W. Stoeckenius, *Proc. Natl. Acad. Sci. U.S.A.*, 71, 4462-4466 (1974).
47. A. Yamaguchi, T. Unemoto, A. Ikegami, *Photochem. Photobiol.*, 33, 511-516 (1981).
48. H.S. Rodman, B.A. Wallace, A. Croteau, B.H. Honig, *Biophys. J.*, 47, 92A (1985).
49. G.S. Harbison, J. Herzfeld, R.G. Griffin, *Biochemistry*, 22, 1-5 (1983).

50. G.S. Harbison, S.O. Smith, J.A. Pardoën, C. Winkel, J. Lugtenburg, J. Herzfeld, R. Mathies, R.G. Griffin, Proc. Natl. Acad. Sci. U.S.A., 81, 1706-1709 (1984).
51. K.J. Rothschild, H. Marrero, Proc. Natl. Acad. Sci. U.S.A., 79, 4045-4049 (1982).
52. K. Bagley, G. Dollinger, L. Eisenstein, A.K. Singh, L. Zimanyi, Proc. Natl. Acad. Sci. U.S.A., 79, 4972-4976 (1982).
53. S.O. Smith, A.B. Myers, J.A. Pardoën, C. Winkel, P.P.J. Mulder, J. Lugtenburg, R. Mathies, Proc. Natl. Acad. Sci. U.S.A., 81, 2055-2059 (1984).
54. K. Ohno, Y. Takeuchi, M. Yoshida, Biochim. Biophys. Acta, 462, 575-582 (1977).
55. M.A. Marcus, A. Lewis, Biochemistry, 17, 4722-4735 (1978).
56. S. Seltzer, R. Zuckermann, J. Amer. Chem. Soc., 107, 5523-5525 (1985).
57. T. Rosenfeld, B. Honig, M. Ottolenghi, J. Hurley, T.G. Ebrey, Pure Appl. Chem., 49, 341-351 (1977).
58. E. Koelling, W. Gaertner, D. Oesterhelt, L. Ernst, Angew. Chem., Int. Ed. Engl., 23, 81-82 (1984).
59. M. Sheves, N. Friedman, A. Albeck, M. Ottolenghi, Biochemistry, 24, 1260-1265 (1985).

60. C.H. Chang, R. Govindjee, T. Ebrey, K.A. Bagley,
G. Dollinger, L. Eisenstein, J. Marque, H. Roder,
J. Vittitow, J.-M. Fang, K. Nakanishi, *Biophys. J.*, 47,
509-512 (1985).
61. H.-J. Polland, W. Zinth, M.A. Franz, W. Kaiser,
E. Koelling, D. Oesterhelt, *Biophys. J.*, 323A (1985).
62. H.-J. Polland, M.A. Franz, W. Zinth, W. Kaiser,
E. Koelling, D. Oesterhelt, *Biophys. J.*, 49, 651-662
(1986).
63. J.B. Hurley, T.G. Ebrey, *Biophys. J.*, 22, 49-66 (1978).
64. R.R. Birge, T.M. Cooper, *Biophys. J.*, 42, 61-69 (1983).
65. T. Kouyama, K. Kinoshita, Jr., A. Ikegami, *Biophys. J.*,
47, 43-54 (1985).
66. J. Pande, R.H. Callender, T.G. Ebrey, *Proc. Natl. Acad.
Sci. U.S.A.*, 78, 7379-7382 (1981).
67. M. Braiman, R. Mathies, *Proc. Natl. Acad. Sci. U.S.A.*,
79, 403-407 (1982).
68. F. Siebert, W. Maentele, *Eur. J. Biochem.*, 130, 565-573
(1983).
69. K.J. Rothschild, J. Lugtenburg, *Biophys. J.*, 45, 209A,
(1984).
70. K.J. Rothschild, E. Marrero, M. Braiman, R. Mathies,
Photochem. Photobiol., 40, 675-679 (1984).
71. J. Turner, C.-L. Hsieh, A.R. Burns, M.A. El-Sayed, *Proc.
Natl. Acad. Sci. U.S.A.*, 76, 3046-3050 (1979).

72. C.-L. Hsieh, M. Nagumo, M. Nicol, M.A. El-Sayed, J. Phys. Chem. 85, 2714-2717 (1981).
73. S.O. Smith, M. Braiman, R. Mathies in "Time-Resolved Vibrational Spectroscopy", G.H. Atkinson, Ed., Academic Press: New York, 1983, pp. 219-230.
74. A. Lewis in "Time-Resolved Vibrational Spectroscopy", G.H. Atkinson, Ed., Academic Press: New York, 1983, pp. 239-249.
75. M.A. El-Sayed, C.-L. Hsieh, M. Nicol in "Time-Resolved Vibrational Spectroscopy", G.H. Atkinson, Ed., Academic Press: New York, 1983, pp. 251-262.
76. C.-L. Hsieh, M.A. El-Sayed, M. Nicol, M. Nagumo, J.-H. Lee, Photochem. Photobiol., 38, 83-94 (1983).
77. K.J. Rothschild, P. Roepe, J. Lugtenburg, J.A. Pardoen, Biochemistry, 23, 6103-6109 (1984).
78. K.J. Rothschild, P. Roepe, J. Gillespie, Biochim. Biophys. Acta, 808, 140-148 (1985).
79. E.P. Ippen, C.V. Shank, A. Lewis, M.A. Marcus, Science, 200, 1279-1281 (1978).
80. M.C. Downer, M. Islam, C.V. Shank, A. Lewis, A. Harootunian, S. Tan, Biophys. J., 47, 98A (1985).
81. M.L. Applebury, K.S. Peters, P.M. Rentzepis, Biophys. J., 23, 375-382 (1978).
82. Y.A. Matveetz, S.V. Chekalin, A.V. Sharkov, J. Opt. Soc. Am. B: Opt. Phys., 2, 634-639 (1985).

83. A.V. Sharkov, A.V. Pakulev, S.V. Chekalin,
Y.A. Matveetz, *Biochim. Biophys. Acta*, 808, 94-102
(1985).
84. A.V. Sharkov, Y.A. Matveetz, S.V. Chekalin,
A.V. Pakulev, *Dokl. Biophysics*, 281, 65-68 (1985).
85. R.H. Lozier, R.A. Bogomolni, W. Stoeckenius, *Biophys. J.*
15, 955-962 (1975).
86. M.C. Kung, D. Devault, B. Hess, D. Oesterhelt, *Biophys.*
J., 15, 907-911 (1975).
87. J.F. Nagle, L.A. Parodi, R.H. Lozier, *Biophys. J.*, 38,
161-174 (1982).
88. M. Tsuda, M. Glaccum, B. Nelson, T.G. Ebrey, *Nature*
(London), 287, 351-353 (1980).
89. S.O. Smith, J.A. Pardoen, P.P.J. Mulder, B. Curry,
J. Lugtenburg, R. Mathies, *Biochemistry*, 22, 6141-6148
(1983).
90. P.A. Hargrave, J.A. McDowell, D.R. Curtis, J.K. Wang,
E. Juszczak, S.L. Fong, J.K.M. Rao, P. Argos, *Biophys.*
Struct. Mech., 9, 235-244 (1983).
91. Y.A. Orchinnikov, N.G. Abdulaev, M.Y. Feigina,
I.D. Artamonov, A.S. Bogachuk, A.S. Zolotarev,
E.R. Eganyan, P.V. Kostetskii, *Bioorg. Khim.*, 9, 1331-
1340 (1983).
92. J. Nathaus, D.S. Hogness, *Cell*, 34, 807-814 (1983).

93. H.G. Khorana, G.E. Gerber, W.C. Herlihy, C.P. Gray, R.J. Anderegg, K. Nihei, K. Biemann, Proc. Natl. Acad. Sci. U.S.A., 76, 5046-5050 (1979).
94. T. Ebrey, R. Govindjee, B. Honig, E. Pollock, W. Chan, R. Crouch, A. Yudd, K. Nakanishi, Biochemistry, 14, 3933-3941 (1975).
95. R.H. Callender, A. Doukas, R. Crouch, K. Nakanishi, Biochemistry, 15, 1621-1629 (1976).
96. L. Salem, P. Bruckmann, Nature (London), 258, 526-528 (1975).
97. R.R. Birge, L.M. Hubbard, J. Am. Chem. Soc., 102, 2195-2205 (1980).
98. A.R. Oseroff, R.H. Callender, Biochemistry, 13, 4243-4248 (1974).
99. I. Palings, R.A. Mathies, J. Pardoën, C. Winkel, J. Courtin, P. Mulder, J. Lugtenburg, Biophys. J., 49, 276A (1986).
100. M.E. Heyde, D. Gill, R.G. Kilponen, L. Rimai, J. Am. Chem. Soc., 93, 6776-6780 (1971).
101. S.O. Smith, A.B. Myers, R.A. Mathies, J.A. Pardoën, C. Winkel, E.M.M. van den Berg, J. Lugtenburg, Biophys. J., 47, 653-664 (1985).
102. J. Shriver, E.W. Abrahamson, G.D. Mateescu, J. Am. Chem. Soc., 98, 2407-2409 (1976).
103. Y. Inoue, Y. Tokito, R. Chujo, Y. Miyoshi, J. Am. Chem. Soc., 99, 5592-5596 (1977).

104. C. Pattaroni, J. Lauterwein, *Helv. Chem. Acta*, 64, 1969-1985 (1981).
105. G.D. Mateescu, E.W. Abrahamson, J.W. Shriver, W. Copan, D. Muccio, M. Iqbal, V. Waterhous in "Spectroscopy of Biological Molecules", C. Sandorfy, T. Theophanides, Eds., Reidel Pub. Co.: Boston, 1983, pp. 257-290.
106. G.S. Harbison, S.O. Smith, J.A. Pardoen, J.M.L. Courtin, J. Lugtenburg, J. Herzfeld, R.A. Mathies, R.G. Griffin, *Biochemistry*, 24, 6955-6962 (1985).
107. G.S. Harbison, P.P.J. Mulder, H. Pardoen, J. Lugtenburg, J. Herzfeld, R.G. Griffin, *J. Am. Chem. Soc.*, 107, 4809-4816 (1985).
108. B. Honig, A.D. Greenberg, U. Dinur, T.G. Ebrey, *Biochemistry*, 15, 4593-4599 (1976).
109. J. Lugtenburg, M. Muradin-Szweykowska, R. van der Steen, C. Heeremans, G.S. Harbison, J. Herzfeld, R.G. Griffin, S.O. Smith, R.A. Mathies, *Biophys. J.*, 49, 210A (1986).
110. P. Tavan, K. Schulten, D. Oesterhelt, *Biophys. J.*, 47, 415-430 (1985).
111. H. Kakitani, T. Kakitani, E. Rodman, B. Honig, *Photochem. Photobiol.*, 41, 471-479 (1985).
112. P.E. Blatz, J.H. Mohler, E.V. Navangul, *Biochemistry*, 11, 848-855 (1972).

113. P.E. Blatz, J.H. Mohler, *Biochemistry*, 11, 3240-3243 (1972).
114. P.E. Blatz, J.H. Mohler, *Biochemistry*, 14, 2304-2309 (1975).
115. P.E. Blatz, L. Lane, J.C. Aumiller, *Photochem. Photobiol.*, 22, 261-263 (1975).
116. R. Mathies, L. Stryer, *Proc. Natl. Acad. Sci. U.S.A.*, 73, 2169-2173 (1976).
117. J.R. Corsetti, B.E. Kohler, *J. Chem. Phys.*, 67, 5237-5243 (1977).
118. K. Nakanishi, V. Balogh-Nair, M. Arnaboldi, K. Tsujimoto, B. Honig, *J. Am. Chem. Soc.*, 102, 7945-7947 (1980).
119. W.H. Waddell, A.M. Schaffer, R.S. Becker, *J. Am. Chem. Soc.*, 99, 8456-8460 (1977).
120. M.A. Gawinowicz, V. Balogh-Nair, J.S. Sabol, K. Nakanishi, *J. Am. Chem. Soc.*, 99, 7720-7721 (1977).
121. M. Arnaboldi, M.G. Motto, K. Tsujimoto, V. Balogh-Nair, K. Nakanishi, *J. Am. Chem. Soc.*, 101, 7082-7084 (1979).
122. J.L. Spudich, D.A. McCain, K. Nakanishi, M. Okabe, N. Shimizu, H. Rodman, B. Honig, R.O. Bogomolni, *Biophys. J.*, 49, 479-483 (1986).
123. M. Sheves, K. Nakanishi, B. Honig, *J. Am. Chem. Soc.*, 101, 7086-7088 (1979).
124. M.G. Motto, M. Sheves, K. Tsujimoto, V. Balogh-Nair, K. Nakanishi, *J. Am. Chem. Soc.*, 102, 7947-7949 (1980).

125. M. Sheves, K. Nakanishi, J. Am. Chem. Soc., 105, 4033-4039 (1983).
126. V. Balogh-Nair, J.D. Carriker, B. Honig, V. Kamat, M.G. Motto, K. Nakanishi, R. Sen, M. Sheves, M.A. Tanis, K. Tsujimoto, Photochem. Photobiol., 33, 483-488 (1981).
127. F. Derguini, C.F. Bigge, A.A. Croteau, V. Balogh-Nair, K. Nakanishi, Photochem. Photobiol., 39, 661-665 (1984).
128. F. Derguini, C.G. Caldwell, M.G. Motto, V. Balogh-Nair, K. Nakanishi, J. Am. Chem. Soc., 105, 646-648 (1983).
129. T. Kakitani, H. Kakitani, B. Honig, K. Nakanishi, J. Am. Chem. Soc., 105, 648-650 (1983).
130. M. Sheves, T. Baasov, N. Friedman, J. Chem. Soc., Chem. Commun., 77-79 (1983).
131. M. Sheves, T. Baasov, Tetrahedron Lett., 1745-1748 (1983).
132. M. Sheves, V. Rosenbach, Chem. Lett., 525-528 (1984).
133. M. Sheves, T. Baasov, N. Friedman, M. Ottolenghi, R. Feinmann-Weinberg, V. Rosenbach, B. Ehrenberg, J. Am. Chem. Soc., 106, 2435-2437 (1984).
134. M. Sheves, B. Kohne, Y. Mazur, J. Chem. Soc., Chem. Commun., 1232-1234 (1983).
135. T. Baasov, M. Sheves, J. Am. Chem. Soc., 107, 7524-7533 (1985).

136. I. Tabushi, Y. Kuroda, K. Shimokawa, J. Am. Chem. Soc., 101, 4759-4760 (1979).
137. M. Sheves, T. Baasov, J. Am. Chem. Soc., 106, 6840-6841 (1984).
138. D. Lukton, R.R. Rando, J. Am. Chem. Soc., 106, 4525-4531 (1984).
139. R.S. Becker, K. Freedman, J. Am. Chem. Soc., 107, 1477-1485 (1985).
140. K.A. Freedman, R.S. Becker, J. Am. Chem. Soc., 108, 1245-1251 (1986).
141. J.M. Donahue, W.H. Waddell, Photochem. Photobiol., 40, 399-401 (1984).
142. M.M. Fischer, K. Weiss, Photochem. Photobiol., 20, 423-432 (1974).
143. A. Alchalel, B. Honig, M. Ottolenghi, T. Rosenfeld, J. Am. Chem. Soc., 97, 2161-2166 (1975).
144. P.K. Das, G. Kogan, R.S. Becker, Photochem. Photobiol., 30, 689-695 (1979).
145. D. Huppert, P.M. Rentzepis, D.S. Kliger, Photochem. Photobiol., 25, 193-197 (1977).
146. R.S. Becker, K. Freedman, J.A. Hutchinson, L.J. Noe, J. Am. Chem. Soc., 107, 3942-3944 (1985).
147. P.S. Mariano, Tetrahedron, 39, 3845-3879 (1983).
148. R.F. Childs, B.D. Dickie, J. Chem. Soc., Chem. Commun., 1268-1269 (1981).

149. B.D. Dickie, Ph.D. Thesis, McMaster University, 1982.
150. R.F. Childs, B.D. Dickie, J. Am. Chem. Soc., 105, 5041-5046 (1983).
151. P.A. Kollman in Adv. Org. Chem., H. Boehme, H.G. Viehe, Eds., Vol. 9, Part 1, 1976, pp. 1-21.
152. M.C. Bruni, J.P. Daudey, J. Langlet, J.P. Malrieu, F. Momicchioli, J. Am. Chem. Soc., 99, 3587-3596 (1977).
153. R.J. Abraham, P. Loftus, "Proton and Carbon-13 NMR Spectroscopy", Heyden: London, 1979, pp. 24-29.
154. L.M. Trefonas, R.L. Flurry, Jr., R. Majeste, E.A. Myers, R.F. Copeland, J. Amer. Chem. Soc., 88, 2145-2149 (1966).
155. F.J. Chentli-Benchikha, J.-P. Declercq, G. Germain, M. Van Meerssche, T. Debaerdemaeker, O. Dideberg, A. Michel, J.P. Putzeys, Acta Cryst., B33, 3428-3437, (1977).
156. B.W. Matthews, R.E. Stenkamp, P.M. Colman, Acta Cryst., B29, 449-454 (1973).
157. A. Zedler, S. Kulpe, Z. Chem., 10, 267-268 (1970).
158. F.J. Chentli-Benchikha, J.-P. Declercq, G. Germain, M. Van Meerssche, Cryst. Struct. Commun., 6, 421-424 (1977).
159. J. Kroon, H. Krabbendam, Acta Cryst., B30, 1463-1465 (1974).

160. D.J. Haas, D.R. Harris, H.H. Mills, *Acta Cryst.*, 19, 676-679 (1965).
161. G.F. Baumgartner, E. Gunther, G. Scheibe, *Z. Electrochem.*, 60, 570-572 (1956).
162. G. Scheibe, *Chimia*, 15, 10-20 (1961).
163. F. Dorr, J. Kotschy, H. Hansen, *Ber. Buns. Ges. Physik. Chem.*, 69, 11-16 (1965).
164. G. Scheibe, J. Heiss, K. Feldmann, *Angew. Chem., Int. Ed. Engl.*, 4, 525 (1965).
165. A.R. Gutierrez, D.G. Whitten, *J. Am. Chem. Soc.*, 98, 6233-6236 (1976).
166. H. Goerner, D. Schulte-Frohlinde, *Chem. Phys. Lett.*, 101, 79-85 (1983).
167. H. Goerner, H. Gruen, *J. Photochem.*, 28, 329-350 (1985).
168. H. Goerner, A. Fojtik, J. Wroblewski, L.J. Currell, *Z. Naturforsch.*, 40A, 525-537 (1985).
169. H. Goerner, D. Schulte-Frohlinde, *J. Phys. Chem.*, 89, 4105-4112 (1985).
170. H. Goerner, *J. Phys. Chem.*, 89, 4112-4119 (1985).
171. H.H. Perkampus, B. Behjati, *J. Heterocycl. Chem.*, 11, 511-514 (1974).
172. B. Behjati, T. Bluhm, *J. Heterocycl. Chem.*, 16, 1639-1640 (1979).
173. P.S. Mariano, J.L. Stavinoha, G. Pepe, E.F. Meyer, Jr., *J. Am. Chem. Soc.*, 100, 7114-7116 (1978).

174. P.S. Mariano, A. Leone-Bay, *Tetrahedron Lett.*, 4581-4584 (1980).
175. E.C. Taylor, R.O. Kan, W.W. Paudler, *J. Am. Chem. Soc.*, 83, 4484-4485 (1961).
176. E.C. Taylor, R.O. Kan, *J. Am. Chem. Soc.*, 85, 776-784 (1963).
177. C.K. Bradsher, L.E. Beavers, *J. Org. Chem.*, 22, 1740-1741 (1957).
178. J. Bendig, B. Gepert, D. Kreysig, *J. Prakt. Chem.*, 320, 739-748 (1978).
179. L. Kaplan, J.W. Pavlik, K.E. Wilzbach, *J. Am. Chem. Soc.*, 94, 3283-3284 (1972).
180. D. Rehm, A. Weller, *Isr. J. Chem.*, 8, 259-271 (1970).
181. F.D. Lewis, J.R. Petisce, J.D. Oxman, M.J. Nepras, *J. Am. Chem. Soc.*, 107, 203-207 (1985).
182. R. Merenyi in Reference 151, pp. 78-86.
M.-L. Filleux-Blanchard, D. le Botlan, *Org. Mag. Res.*, 9, 618-620 (1977).
C. Rabiller, J.P. Renou, G.J. Martin, *J. Chem. Soc., Perkin Trans. 2*, 536-541 (1977).
H. Kessler, D. Leibfritz, *Chem. Ber.*, 104, 2158-2169 (1971).
J.E. Johnson, N.M. Silk, M. Arfan, *J. Org. Chem.*, 47, 1958-1961 (1982).
K.J. Dignam, A.F. Hegarty, *J. Chem. Soc., Perkin Trans. 2*, 1437-1443 (1979).

- G.M. Sharma, O.A. Roels, *J. Org. Chem.*, 38, 3648-3651 (1973).
183. A. Krebs, J. Breckwoldt, *Tetrahedron Lett.*, 3797-3802 (1969).
A. Krebs, *Tetrahedron Lett.*, 1901-1904 (1971).
184. M.P. Sammes, *J. Chem. Soc., Perkin Trans. 2*, 1501-1507 (1981).*
185. J.E. Johnson, N.M. Silk, E.A. Nalley, M. Arfan, *J. Org. Chem.*, 46, 546-552 (1981).
also suggested for: W.B. Jennings, S. Al-Showiman, M.S. Tolley, D.R. Boyd, *J. Chem. Soc., Perkin Trans. 2*; 1535-1539 (1975).
G.J. Martin, S. Poignant, *J. Chem. Soc., Perkin Trans. 2*, 642-646 (1974).
186. G. Scheibe, C. Jutz, W. Seiffert, D. Grosse, *Angew. Chem., Int. Ed. Engl.*, 3, 306 (1964).
187. G.S. Hammond, R.C. Neuman, Jr., *J. Phys. Chem.*, 67, 1655-1659, 1659-1665 (1963).
188. H. Guesten, D. Schulte-Frohlinde, *Z. Naturforsch.*, 34B, 1556-1566 (1979).
189. R.J. Abraham, P. Loftus, "Proton and Carbon-13 NMR Spectroscopy", Heyden: London, 1979, p. 28.
190. D.J. Pasto, C.R. Johnson, "Organic Structure Determination", Prentice-Hall: Toronto, 1969, p. 183.
191. R.F. Childs, G.S. Shaw, C.J.L. Lock, R. Faggiani, to be published.

192. J.H. Pinckard, B. Wille, L. Zechmeister, J. Am. Chem. Soc., 70, 1938-1944 (1948).
193. E. Carlson, R.B. Jones, Jr., M. Raban, J. Chem. Soc., Chem. Commun., 1235-1237 (1969).
194. E.B. Agracheva, L.Ya. Krasnikova, V.F. Gachkovskii, Zh. Obs. Khim., 50, 2307-2313 (1980).
195. N.J. Turro, "Modern Molecular Photochemistry", Benjamin/Cummings Pub. Co.: Don Mills, 1978, p. 106.
196. In reference 195, p. 114.
197. W.J. Leigh, D.R. Arnold, Can. J. Chem., 59, 3061-3075 (1981).
198. J.B. Birks, G.N.R. Tripathi, M.D. Lumb, Chem. Phys., 33, 185-194 (1978).
199. In reference 195, pp. 87, 88.
200. R.R. Birge, in "The Proceedings of the NATO Advanced Studies Institute on the Spectroscopy of Biological Molecules", C. Sandorfy, T. Theophanides, Eds., Reidel Pub. Co.: Boston, 1983, pp. 457-471.
201. B. Palmer, B. Jumper, W. Hagan, J.C. Baum, R.L. Christensen, J. Am. Chem. Soc., 104, 6907-6913 (1982).
202. R.R. Birge, B.M. Pierce, L.P. Murray in reference 200, pp. 473-486.
203. R.R. Birge, L.P. Murray, B.M. Pierce, H. Akita, V. Balogh-Nair, L.A. Findsen, K. Nakanishi, Proc. Natl. Acad. Sci. U.S.A., 82, 4117-4121 (1985).

204. L. Salem, *Accts. Chem. Research*, 12, 87-92 (1979).
205. F. Dietz, A. Tadjer, N. Tyutyulkov, *Chem. Phys. Lett.*, 99, 120-121 (1983).
206. J. Michl, *Mol. Photochem.*, 4, 243-255 (1972).
207. V. Bonacic-Koutecky, J. Michl, *Theor. Chim. Acta*, 68, 45-55 (1985).
208. D. Gegiou, K.A. Muszkat, E. Fischer, *J. Am. Chem. Soc.*, 90, 12-18 (1968).
209. R.M. Weiss, A. Warshel, *J. Am. Chem. Soc.*, 101, 6131-6133 (1979).
210. V. Sundstrom, T. Gillbro, *Ber. Buns. Ges.*, 89, 222-226 (1985).
211. V. Sundstrom, T. Gillbro, *Chem. Phys. Lett.*, 109, 538-543 (1984).
212. S.P. Velsko, G.R. Fleming, *J. Chem. Phys.*, 76, 3553-3562 (1982).
213. J.P. Malrieu, I. Nebot-Gil, J. Sanchez-Marin, *Pure Appl. Chem.*, 56, 1241-1254 (1984).
214. H. Suzuki, O. Yoshida, Y. Koseko, *J. Phys. Soc. Japan*, 53, 2411-2420 (1984).
215. P. Bruckmann, L. Salem, *J. Am. Chem. Soc.*, 98, 5037-5038 (1976).
216. R.S.H. Liu, Y. Butt, *J. Am. Chem. Soc.*, 93, 1532-1534 (1971).
217. P. Courtot, R. Rumin, J.-Y. Salaun, *Pure Appl. Chem.*, 49, 317-331 (1977).

218. B.H. Baretz, A.K. Singh, R.S.H. Liu, *Nuov. J. Chim.*, 5, 297-303 (1981).
219. V.J. Rao, R.J. Fenstermacher, R.S.H. Liu, *Tetrahedron Lett.*, 1115-1118 (1984).
220. Y. Ito, T. Dote, Y. Uozu, T. Matsuura, *J. Am. Chem. Soc.*, 108, 841-842 (1986).
221. In reference 195, p. 113.
222. L.R. Eastman, Jr., B.M. Zarnegar, J.M. Butler, D.G. Whitten, *J. Am. Chem. Soc.*, 96, 2281-2283 (1974).
223. R.S.H. Liu, A.E. Asato, M. Denny, *J. Am. Chem. Soc.*, 105, 4829-4830 (1983).
224. A.F. Kluge, C.P. Lillya, *J. Am. Chem. Soc.*, 93, 4458-4463 (1971).
225. A.B. Ellis, R. Schreiner, R.A. Ulkus, *Proc. Natl. Acad. Sci. U.S.A.*, 78, 3993-3997 (1981).
226. M.E. Zawadzki, A.B. Ellis, *J. Org. Chem.*, 48, 3156-3161 (1983).
227. H.E. Zimmerman, V.R. Sandel, *J. Am. Chem. Soc.*, 85, 915-922 (1963).
228. N.J. Turro, P. Wan, *J. Photochem.*, 28, 93-102 (1985).
229. P. Wan, *J. Org. Chem.*, 50, 2583-2586 (1985).
230. In reference 195, p. 183.
231. M.J. de Nie-Sarink, U.K. Pandit, *Tetrahedron Lett.*, 2449-2452 (1979).
232. D.H. Evans, K.M. O'Connell, R.A. Petersen, M.J. Kelly, *J. Chem. Education*, 60, 290-293 (1983).

233. C.P. Andrieux, J.M. Saveant, *J. Electroanal. Chem.*, 26, 223-235 (1970).
234. M. Julliard, M. Chanon, *Chem. Rev.*, 83, 425-506 (1983).
235. G. Jones, II, V. Malba, *J. Org. Chem.*, 50, 5776-5782 (1985).
236. T. Kennelly, H.D. Gafney, M. Braun, *J. Am. Chem. Soc.*, 107, 4431-4440 (1985).
237. M. Pankratz, R.F. Childs, *J. Org. Chem.*, 50, 4553-4558 (1985).
238. J.B. Milne, in "The Chemistry of Non-Aqueous Solvents", J.J. Lagowski, Ed., Academic Press: New York, 1978, Vol VB, pp. 1-52.
239. G.A. Olah, R.J. Spear, *J. Am. Chem. Soc.*, 97, 1539-1546 (1975).
240. H. Pauly, K. Feuerstein, *Chem. Ber.*, 62, 297-311 (1929).
241. M. Scholtz, A. Wiedemann, *Chem. Ber.*, 36, 845-854 (1903).
242. *Org. Syn.*, 44, 72-74 (1964).
243. C.G. Hatcher, C.A. Parker, *Proc. Roy. Soc.*, A235, 518-536 (1956).
244. W.D. Bowman, J.N. Demas, *J. Phys. Chem.*, 80, 2434-2435 (1976).
245. D.E. Nicodem, M.L.P.F. Cabral, J.C.N. Ferreira, *Mol. Photochem.*, 8, 213-238 (1977).

246. D.E. Nicodem, O.M.V. Aquilera, J. Photochem., 21, 189-193 (1983).
247. Inorg. Syn., 21, 127-128 (1982).
248. L.P. Hammett, "Physical Organic Chemistry", McGraw-Hill: New York, 1970, pp. 263-313.
249. J.W. Moore, R.G. Pearson, "Kinetics and Mechanism", 3rd ed., Wiley: New York, 1981, p. 304.